DEMONSTRATION OF A MOLECULAR INTERACTION BETWEEN THIOREDOXIN AND THE PRO-FS GENE PRODUCT OF HIV-1, A MIMIC OF NF KAPPA B

by

GUOPING SU

(Under the Direction of Ethan Will Taylor)

ABSTRACT

A programmed –1 frameshift in the HIV-1 protease gene has been previously demonstrated. The sequence encoded in the overlapping –1 reading frame, named *pro-fs*, has significant similarity to the DNA binding loop of NF-κB, which is also the peptide known to bind thioredoxin (Trx) as part of the process of NF-κB activation. The hypothesis that the putative HIV-1 *pro-fs* gene product functions by mimicry of NF-κB via interacting with Trx was tested by co-immunoprecipitation and GST-pull down assay in vitro. Both experiments consistently showed that *pro-fs* binds human Trx in vitro; and the binding affinity is apparently stronger with Trx-wt than with Trx-CS, in which the two Cys residues in the active center of Trx were mutated to Ser. The fact that *pro-fs* interacts with Trx-CS rules out the possibility that the interaction between *pro-fs* and Trx is just due to cross-linkage via formation of an intermolecular disulfide bond between the Cys residues of *pro-fs* (the Sec residues in *pro-fs* sequence are mutated to Cys for bacterial expression) and the Cys residues in the active site of Trx. Due to the nature of the –1

frameshift mechanism, *pro-fs* and the HIV-1 protease share the first 20 amino acid residues at the N-terminus. Since both the retroviral protease and NF-κB function as dimers, we investigated whether *pro-fs* also dimerizes in living mammalian cells by fluorescent resonance energy transfer (FRET) analysis using confocal microscopy. Fluorescence microscopy was utilized to investigate the hypothesis that *pro-fs* is a nuclear protein, based upon its high pI and mimicry of NF-κB. The results demonstrated that *pro-fs* localizes in cell nuclei and forms oligomers. FRET analysis was also used to study the interaction between *pro-fs* and Trx in living cells. The results showed that phorbol 12-myristate 13-acetate (PMA) treatment of the 293T cells induces the nuclear translocation of Trx, and *pro-fs* binds to both Trx-wt and Trx-CS in PMA-stimulated cells. Together with the results of co-immunoprecipitation and GST-pull down assay, it suggests that Trx-*pro-fs* binding is a structurally specific interaction that involves multiple amino acid residues in the interactive region.

INDEX WORDS: Frameshift; retrovirus; HIV-1; protease; *pro-fs*; NF kappa B; thioredoxin; PMA; FRET; confocal microscopy; cysteine; dimer; oligomer; GST-pull down; co-immunoprecipitation.

DEMONSTRATION OF A MOLECULAR INTERACTION BETWEEN THIOREDOXIN AND THE PRO-FS GENE PRODUCT OF HIV-1, A MIMIC OF NF KAPPA B

by

GUOPING SU

B.S., China Agricultural University, P. R. China, 1995

M.S., Louisiana State University, U.S.A. 1998

A Dissertation Submitted to the Graduate Faculty of The University of Georgia in Partial Fulfillment of the Requirements for the Degree

DOCTOR OF PHILOSOPHY

ATHENS, GEORGIA

2003

DEMONSTRATION OF A MOLECULAR INTERACTION BETWEEN THIOREDOXIN AND THE PRO-FS GENE PRODUCT OF HIV-1, A MIMIC OF NF KAPPA B

by

GUOPING SU

Major Professor: Ethan Will Taylor

Committee: Diane Hartle
Phillip Greenspan
James Hargrove
Arthur Grider

Electronic Version Approved:

Maureen Grasso
Dean of the Graduate School
The University of Georgia
December 2003

DEDICATION

TO

MY DEAREAST DAD, MOM

AND

SISTERS, BROTHER-IN-LAWS, NIECES

WITH LOVE

ACKNOWLEDGEMENTS

I would like to express my most sincere thanks and gratitude to my major professor Dr. Will Taylor for his guidance, support, patience and encouragement during my graduate studies. He has been a great mentor and led me to see the beauty in science.

I also want to express my appreciation towards all of the professors in my advisory committee, Dr. Diane Hartle, Dr. Phillip Greenspan, Dr. James Hargrove and Dr. Arthur Grider, for their continuous support and help. Especially, I would like to thank Dr. Hartle and Dr. Greenspan for always being there for me. Their support made my doctoral research a more pleasant journey. I also sincerely thank Dr. Hargrove for his guidance in my dissertation writing.

I would like to dedicate this thesis to my dearest parents, my sisters and their families, who gave me unconditional love and care, and always had faith in me. Unfortunately, my dear father is deceased before I started my doctoral study. But I believe he must be very proud of me now, as he has always been.

Last, but definitely not least, I would also like to express my deep appreciation to my friends for their love, support and encouragements throughout my school years. It meant a lot to me.

TABLE OF CONTENTS

Page

LIST OF FIGURES

Page

CHAPTER 1

INTRODUCTION AND LITERATURE REVIEW

1.1. NF-κB: a linker of HIV and immune activation

The rate of replication of a virus in lymphoid tissues is important for disease progression, which requires the reactivation of the proviral genome in the infected cells [1, 2]. The regulation of HIV transcription is dependent on the functions of both the viral Tat protein (*trans*-activator of transcription) as well as the activities of a number of cellular transcriptional factors [3, 4]. These transcription factors interact with viral promoter and enhancer elements, located predominantly within the viral long terminal repeat (LTR), such as binding sites for nuclear factor kappa B (NF-κB), Sp1, USF, NFAT-1, and activator protein 1 (AP-1) [5]. A variety of stimuli, including cytokines, phorbol esters, tumor promoters, protein kinase inhibitors [6], heat shock [7] and oxidative conditions [8-12], regulate the transcription of the HIV-1 provirus through the modulation of the complex eukaryotic promoter localized in the LTR. Although a large number of different cellular transcription factors have been suggested to participate in the regulation of HIV transcription, either through direct interactions with HIV DNA or RNA, or through modulating the effects of Tat protein, only a few of them have been clearly shown to have important effects on viral replication, among which NF-κB plays a critical role in HIV disease [13].

NF-κB is a ubiquitous and well-known transcription factor in cell nuclei that binds to a specific DNA consensus sequence. It regulates hundreds of genes involved in immune activation and cellular responses to stress, including cytokine genes associated with T cell activation and inflammation responses (for example, GM-CSF, IL-6, IL-8, IL-2, etc.), adhesion molecules (for example, VCAM-1 and E-selectin), and genes that regulate cell proliferation and apoptosis [14-17]. In addition to a wide variety of cellular genes, it also regulates gene expression of viruses including HIV-1, cytomegalovirus (CMV), and simian virus 40 (SV40) [17-19]. NF-κB belongs

to a family of inducible mammalian transcription factors, the Rel/NF-κB family, which are encoded by five genes p50/p105, p65/RelA, c-Rel, RelB, and p52/p100 [20, 21]. The Rel homology domain (RHD) contains conserved amino acid sequences in all NF-κB/Rel proteins (Fig. 1.1) involved in important functions including DNA binding, dimerization, nuclear localization, and interaction with IκB molecules [22]. Many homo- and heterodimeric forms have been described, which may account for their distinct transcriptional regulation properties [23, 24]. Among these the NF-κB heterodimer consisting of the p65/RelA and p50 subunits is the classic form. NF-κB dimers exist in most cell types in an inactive cytoplasmic form associating with inhibitory molecule IκB [25]. Initial activation of NF-κB in the cytosol occurs as a result of specific phosphorylation of IκB, followed by ubiquitination of IκB and proteolytic degradation of IκB by the 26S proteasome, which results in unmasking of the nuclear translocation signal on NF-κB. Then the active NF-κB dimers can enter the nucleus and bind to their cognate DNA binding sites to activate gene transcription (Fig.1.2) [26-32].

The presence of NF-κB binding sites in the enhancer sequences in the U3 region of the viral LTR is a fundamental characteristic of all the primate immunodeficiency lentiviruses. There are two functional NF-κB sites located in LTR of HIV-1, which lie directly upstream to the Sp1 tandem binding sites. The mechanisms by which NF-κB activates HIV transcription are fundamentally the same as those by which NF-κB activates transcription of the multitude of normal cellular targets. Active NF-κB dimers, particularly the p50/p65 or p52/p65, bind to the κB motifs in the LTR, through which the potent transcriptional activation domain of p65 RelA is brought to the LTR promoter and activate HIV transcription [21, 33-36]. The transcriptional activation of HIV-1 LTR was clearly shown to depend on NF-κB when exposed to oxidative

stress mediated by either hydrogen peroxide or tumor necrosis factor-α (TNF-α) [11, 12, 37, 38]. Thus, by incorporating two NF-κB binding sites in LTR, HIV has cleverly co-opted this fundamental cellular regulatory pathway to support its own intimate interactions with the resting and activated host immune system.

Moreover, it is also important to note that NF-κB also works in a synergic manner with several other transcription factors, such as the Ets family of transcription factors and C/EBP transcription factors, in the activation of HIV transcription [39, 40]. Other transcription factors besides NF-κB have been reported to also interact with the HIV enhancer κB motifs. PU.1, a member of the Ets family of transcription factors, has been reported to play a role with NF-κB in activating HIV LTR transcription induced by lipopolysaccharide (LPS) in macrophages by binding to an additional Ets motif located within the upstream NF-κB binding site, whereas NF-κB binds to the downstream site [41]. NFAT-1, a T-cell transcription factor distantly related to the NF-κB/Rel family protein, can also bind to the HIV LTR NF-κB sites and negatively regulate the NF-κB activation of LTR transcription, whereas NFAT-2 positively regulates HIV-1 LTR through NF-κB binding sites [42]. These studies illustrate the complexity of NF-κB regulation of the HIV LTR and suggest the importance of cellular transcription activators in altering viral replication and perhaps pathogenesis.

Not only can NF-κB activate HIV transcription, it also plays a number of different roles in HIV-cell interactions that could affect HIV replication. NF-κB can be activated by many viral infections, including infections by human leukemia virus, human herpes virus, other human retroviruses [43]. A hypothesis of an autocrine stimulatory loop, which HIV infection activates NF-κB to further enhance HIV gene replication, was made to illustrate the mechanism [21]. The binding of HIV to CD4 on cell surface, HIV Tat protein, and HIV protease were reported to

account for this autocrine stimulatory loop of NF-κB activation by either inducing IκB phosphorylation and degradation or increasing proteolytic processing of the inhibitory p105 NF-κB-1 precursor to generate more p50 (Fig.1.3) [28, 44-47]. It is probably noteworthy that HIV infection may suppress HIV-induced apoptosis in infected myeloid cells by inducing activation of NF-κB [48].

NF-κB is susceptible to regulation by the intracellular reduction-oxidation (redox) state [14-17, 49, 50]. A large variety of stimuli are now known to induce the activation of NF-κB, including phorbol ester (such as PMA), phytohaemmaglutinin (PHA), TNF-α, LPS, HIV-1 protease, calcium ionophores and H_2O_2. These stimuli function at least in part by a common pathway involving reactive oxygen intermediates (ROI) [11, 51-55]. Antioxidants such as N-acetylcysteine (NAC) or lipoic acid were shown to efficiently block NF-κB activation in the signaling pathway in the cells [11, 56]. Furthermore, even fully activated NF-κB was found to be blocked by gold ion via a redox mechanism in vitro, during which the reduced Cys residues in the active center of NF-κB was oxidized [57]. Other studies also reported that treatment with some antioxidants or the overexpression of the detoxifying enzyme glutathione peroxidase (GPx), a selenoprotein, were able to abolish the activation of NF-κB [58-60]. Therefore, in general, antioxidants are now considered to be effective NF-κB inhibitors. The importance of cellular redox status and antioxidant defense will be discussed in more detail in the following section.

1.2. Selenium (Se) and selenoproteins: important factors in regulation of cellular redox milieu

One of the principal classes of chemical reactions for life on this planet is oxidoreduction. There is strong chemical reactivity of the thiols on protein molecules. However, oxygen plays pleiotropic roles in the life of modern living organisms. While oxygen is indispensable for the cell to obtain the essential chemical energy in the form of adenosine triphosphate (ATP), oxygen is also often transformed into highly reactive forms, ROI, which can be toxic to the cell and play critical roles in a number of diseases such as inflammatory disease, atherosclerosis, cataractogenesis, Alzheimer disease, cardiovascular disease [61-63]. The role of oxidants in the inactivation of viruses was described as early as 1970 [64]. Over the decades, accumulating evidence illustrates the involvement of oxidants in viral infection and disease progression, such as infection by influenza virus, hepatitis-causing viruses, and most importantly HIV [65-67]. Humans infected with HIV have been shown to be under chronic oxidative stress caused by perturbations of the host antioxidant defense system, including changes in ascorbic acid, tocopherol, carotenoids, Se, superoxide dismutase and glutathione (GSH). In addition, elevated levels of hydroperoxides and malondialdehyde are found in plasma of HIV-infected individuals (reviewed by [68]). The complex role of oxidants in viral infection has led us to realize the importance of antioxidants in immune defense.

The relationship between low intake of the antioxidant nutrients, such as Se, Zinc, Vitamin E, lipoic acid, and Vitamin A, with a high disease incidence has been demonstrated in numerous studies [69-71]. Se is an essential trace mineral in various aspects of human health. The past three decades have revealed the important roles of Se in prevention of cancers,

cardiovascular disease, and viral infection, as well as regulating thyroid function, immune function, mood and reproduction, and especially its critical role for host antioxidant defense [72-74]. Growing evidence links Se deficiency to the occurrence, virulence, or disease progression of several viral infections. Starting from 1979, a relationship between low Se status and Keshan disease, a nonobstructive cardiomyopathy endemic to parts of China, was documented [75]. Later it was shown that Se-deficiency could trigger non-virulent coxsackie virus to become virulent, a situation that is likely to be relevant to the development of Keshan disease [76]. These observations in regard to coxsackie virus may also explain the steady emergence of new strains of influenza virus in China within its Se-deficient belt [76]. Both experimental data and epidemiological surveys demonstrated the association between low dietary Se intake and increased hepatitis virus (B or C) infection as well as the resulted increase of liver cancer incidence; and a continuous intake of Se is essential to sustain the chemopreventive effect against the progression of the condition to liver cancer [77, 78].

Se seems also to be a crucial nutrient for HIV-infected individuals. A correlation between HIV disease outcome and patient's Se status has been widely documented suggesting that Se deficiency exposes the host to a more significant risk than deficiency of any other nutrient. Plasma Se is not only correlated with various indicators of disease progression, but is also an independent predictor of mortality in HIV infection, being a significantly greater risk factor for mortality than low helper-T-cell count in some studies [79-82]. In fact, there are more than 20 papers reported a progressive decline in plasma Se in parallel with the on-going loss of CD4 T cells in HIV-1 infection [83]. Se-deficient HIV patients showed a mortality risk from HIV-related causes nearly 20 times that of those with adequate levels [80].

There is evidence showing that Se is a potent inhibitor of HIV replication in vitro [84]. Se supplementation suppressed HIV replication induced by TNF-α in acute infected monocytes via increasing concentration of selenoproteins GPx and thioredoxin reductase (TR), which inhibit NF-κB activation [14, 84, 85]. Therefore, adequate concentrations of Se are essential to maintain a reductive cytoplasmic milieu in HIV-infected cells to suppress the rate of HIV replication.

The influence of Se on the immune system is multifactorial. Most of its important functions are associated with specific selenoproteins in the form of selenocysteine (Sec), a rare amino acid encoded by the opal stop codon UGA in bacteria, archea, and eukaryotic organisms [86, 87]. Sec is a Se analog of the sulfur amino acid, cysteine (Cys), and acts as an integral constituent of the selenoproteins. Thus, via the selenoproteins, Se can influence broad areas of cell function through regulation of the activity of redox-active proteins [88]. Most of the identified selenoproteins play a role in antioxidant defense and are important for the involvement of Se in the immune system. There are 4 classes of GPx enzymes (cellular or classical [89], plasma or extracellular [90], phospholipid hydroperoxide [91], and gastrointestinal [92]), which all detoxify hydrogen peroxide and organic lipid peroxides at the expense of reduced GSH, thereby preventing the formation of the highly toxic hydroxyl radical, which causes cellular damage [93]. Like GPx, selenoenzymes families of thioredoxin reductase (TR) [94] and iodothyronine deiodinases [95-97] also have essential functions in redox regulation of many metabolic functions in cells (in particular transcription factors) as well as in thyroid hormone metabolism. Selenoprotein P is an extracellular, monomeric glycoprotein containing up to 10 selenocysteine residues in the polypeptide chain and was proposed to exert extracellular oxidant defense as GSH-dependent peroxidase for phospholipid hydroperoxides in extracellular fluid [98]. Selenoprotein W reduced the sensitivity of both cell lines to H_2O_2 cytotoxicity and was

suggested to have antioxidant functions in a GSH dependent manner [99]. Selenophosphate synthetase 2 catalyzes the production of selenophosphate, which is an essential inorganic precursor for the synthesis of selenocysteine from serine during selenoprotein synthesis [100]. Recently, 25 genes that code for selenoproteins have been detected in the human genome using bioinformatics tools and more than 20 selenoproteins have been characterized by purification, cloning, recombinant expression and prediction of function using bioinformatic techniques [101, 102].

Since Se status plays an important role in viral infection and disease progression, it is not surprising to find out that viruses have acquired homologues of selenoproteins during the course of evolution to hijack the Se supply of the host, thereby reducing the ability of the host to produce enough mammalian selenoproteins and to generate an effective immune response. The first confirmed examples of a virally encoded selenoprotein, a functional GPx enzyme encoded by *Molluscum contagiosum*, a poxvirus that causes persistent skin neoplasms in children and acquired immunodeficiency syndrome (AIDS) patients, has now been firmly substantiated by both theoretical [103] and experimental evidence [104]. It has a high degree of homology with the known mammalian selenoprotein GPx-1 (76%) at the amino acid level, with an identically in-frame UGA codon. This viral selenoprotein was shown to protect human keratinocytes against cytotoxic effects of ultraviolet irradiation and hydrogen peroxide, which provides a mechanism for a virus to defend itself against environmental stress [104]. Similarly, studies of the genome sequence of the pathogenic Fowlpox virus, the poxvirus that infects chickens and turkeys, revealed a GPx homologue with 44% identity to human GPx [105]. In addition to the presence of GPx-homologues in the poxviruses, Taylor and his colleagues have presented theoretical evidence based on molecular modeling that suggested the capability of making viral

selenoproteins, such as GPx, by many human viral pathogens such as HIV-1 and 2, coxsackie virus B3, hepatitis B and C viruses, and the measles virus [106, 107]. This hypothesis was supported by findings from the experimental data, in which the viral GPx module, when expressed in mammalian cells, showed measurable GPx activity [107]. Taylor et al. suggested that sufficient dietary Se intake may maintain host cellular immunity and appropriate redox control, thus protects host against HIV progression. While under low Se conditions, increased oxidative stress induces cell apoptosis and activates viral replication, thus leading to increased pathogenic effects [71].

1.3. Thioredoxin: a complex factor in regulating NF-κB activation

The selenoprotein TR and its substrate thioredoxin (Trx) have been shown to regulate NF-κB activation through oxidoreduction. TR is a member of the Type-I pyridine nucleotide-disulfide oxidoreductase enzyme family that includes glutathione reductase, lipoamide dehydrogenase, and mercuric ion reductase, with a conserved -Cys-Val-Asn-Val-Gly-Cys- redox catalytic site in the N-terminal region [108]. These enzymes catalyze the NADPH-dependent reduction of their substrates (Fig. 1.4), including lipoic acid, vitamin K-3, 5, 5'-dithiobis (2-nitrobenzoic acid), dehydroascorbic acid, the tumour-suppressor protein p53 and Trx [93, 109, 110]. Both mammalian [94] and *Caenorhabditis elegans* [111, 112] encoded TR contain a Sec residue in an additional redox center at their C-terminus formed by Cys495 and Sec496, which is strikingly different from the *Escherichia coli* enzyme. It has been confirmed that the Sec center plays a key role in the novel, wide ranging functions as an oxidant sensor controlling cell signaling pathways [108, 113, 114]. The role of the Se atom in Sec during catalysis of Trx by TR

is to transfer electrons to oxidized Trx, with the reduced Trx subsequently serving as an important source of reducing power for thioredoxin peroxidase, ribonucleotide reductase and other proteins and enzymes containing redox-active disulfide groups, such as NF-κB [71] (Fig. 1.4). Since TR is a selenoprotein, its activity is tightly regulated by Se status. It was reported that both TR activity and its mRNA level were greatly down-regulated in Se-deficient rat liver comparing to that in Se-adequate rat liver, similar to the fall in Se-dependent GPx-1 activity [115]; as a result, it may increase the risk of cancer [116]. In vivo experiment showed that adding Se at 1μM to the medium of cultured cells gave about 11-23 fold increase and adding Se at 10 μM a 40-65 fold increase in activity via increasing Se incorporation into the enzyme without an significant increase in protein synthesis of TR [116].

Trx, a small ubiquitous protein with two redox-active cysteine residues in its catalytic center, with the consensus amino acid sequence -Trp-Cys-Gly-Pro-Cys-Lys-, is known to be an important endogenous redox-regulating molecule due to its thiol reducing activity [50, 117, 118]. It exists either in a reduced form with a dithiol or in an oxidized form, in which the cysteine residues form an intra-molecular disulfide bridge. Trx participates in redox reactions by reversible oxidation of the two Cys residues and catalyzes dithiol-disulfide exchange reactions involving many thio-dependent cellular processes, including a variety of biological functions related to intracellular signaling, gene regulation, resistance to oxidant stress, and control of apoptosis [118-120].

Trx was initially identified as a hydrogen donor from *E. coli* [121], and later was recognized for its role in induction of the α subunit of the IL-2 receptor in human, which is now known to be under the regulation of NF-κB [122-124]. Trx regulates the DNA binding ability of a number of cellular transcription factors, either directly, as in the case of NF-κB (by reducing a

disulfide bond involving Cys62 of the p50 subunit) [16, 50, 122, 125, 126] and the glucocorticoid receptor {Makino, 1996 #60}, or indirectly, as in the case of AP-1 via Ref-1 [127]. Hirota and his colleagues demonstrated that Trx associates directly with NF-κB and plays dual and opposing roles in the regulation of NF-κB activation. Overexpression of wild-type Trx suppressed NF-κB activation in the cytoplasm while overexpression of nuclear-targeted Trx potentiated NF-κB-dependent transcription in the nucleus [50]. Structure analysis has elucidated the mechanism for the redox regulation of NF-κB by Trx. First, the crystal structures of the NF-κB subunit p50 with its target DNA revealed the novel DNA-binding β barrel structure of NF-κB and confirmed the prediction that the DNA-binding loop contains the Cys62 residue [128, 129]. Then, NMR studies by a group in National Institutes of Health determined that a boot-shaped hollow on the surface of Trx containing the redox-active Cys residues (Cys32 and Cys35) can recognize the DNA-binding loop of p50 of NF-κB and is likely to reduce the oxidized Cys62 of NF-κB [126]. The NMR structure also indicates that the reduction of NF-κB by Trx involves a structurally specific interaction because in addition to the intermolecular disulfide bridge between Cys32 of human Trx and Cys62 of NF-κB. The Trx - NF-κB complex was stabilized by numerous hydrogen-bonding, electrostatic and hydrophobic interactions involving multiple amino acid residues [126].

Several lines of evidence indicate an important role for Trx in HIV-1 replication and disease. In addition to the essential role of Trx in the cell nucleus for reductive activation of NF-κB [16, 50, 122], and thus for activation of HIV transcription, Trx is a key participant in a mechanism whereby HIV-infected cells resist apoptosis while simultaneously inducing apoptosis of bystander cells via upregulation of FasL. It was shown that Trx directly associates with the N-terminal portion of apoptosis signaling kinase 1 (ASK1), a key component of TNFα-induced

apoptosis [130], promoting the ubiquitination and degradation of ASK1, removing the pro-apoptotic signal to downstream kinases [117, 130]. Mutagenesis studies showed that the presence of at least one of the two active site Cys residues (C32 or C35) is required for Trx to inhibit ASK1-dependent apoptosis [117]. There is evidence indicates that the pleiotropic HIV-1 nef protein participates in the process of inhibiting ASK1-dependent apoptosis by preventing stimulus-coupled release of Trx from ASK1 in HIV infected cells [131]. More generally, because of its role as a hydrogen donor for ribonucleotide reductase, essential for DNA synthesis [132], Trx is required by retroviruses for formation of their DNA provirus. Clinical data has shown that there is an increase in plasma Trx levels in HIV disease, particularly in the later stages [133].

1.4. HIV-1 encoded selenoproteins: predictions and hypotheses

Previously, Taylor et al. predicted several selenoprotein modules encoded by HIV-1 based on theoretical evidence, including an *env* variant associated with a predicted –1 frameshift site, which was named *env-fs* and was subsequently identified as a virally-encoded homologue of GPx. The viral GPx (vGPx) module contains a single opal stop codon (UGA), encodes for Sec. The putative vGPx showed functional GPx activity when cloned and expressed as a selenoprotein in mammalian cells [107]. Another predicted selenoprotein is potentially expressed by a –1 frameshift from the HIV-1 protease coding region [134], and was later named *pro-fs* [135]. The frameshift site in HIV-1 protease gene was established experimentally using a standard in vitro assay [71]. The *pro-fs* sequence contains two in-frame UGA codons, potentially enabling the incorporation of Sec to form a selenoprotein [71, 135].

Programmed –1 translational frameshifting happens when the ribosome shifts upstream by one nucleotide during the course of reading an mRNA. As a consequence, the protein product is encoded in two overlapping reading frames [136, 137]. Thus, there are two primary products translated from a single mRNA that share the N-sequence encoded upstream of the shift, and differ in the sequence encoded downstream of the shift, possibly having very different functions or enzymatic activities [136, 137]. Due to this nature of –1 frameshifting, *pro-fs* would first be expressed as a *gag-pol-pro-fs* double frameshift fusion protein because the pol gene itself reguires a –1 frameshifting to be expressed. After processing by the viral protease, the first 20 N-terminal residues of *pro-fs* would be identical to the protease sequence. This shared module is fused to a C-terminal domain of 49 residues encoded in the –1 reading frame to form the *pro-fs* protein. The amino acid sequence of *pro-fs* is highly conserved in HIV-1 sequences, especially the sequence spanning its first UGA codon, which overlaps the HIV protease active site in the zero frame [71]. Based on the protein sequence, the computed pI of *pro-fs* is 11; thus, *pro-fs* was predicted to be a very basic, positively charged protein, which suggests that it may be a nuclear protein.

Sequence analysis suggested a match to the NF-κB family of transcription factors, which contains a conserved Cys that aligns with the highly conserved UGA codon of *pro-fs*. The homology between *pro-fs* and the DNA binding loop of NF-κB, which is also the peptide interacting with Trx, is highly significant, with a similarity score 4.5 standard deviations better than that expected for random sequences of identical composition. The sequence alignment suggests that the protease-processed form of *pro-fs* could be at the least a minimal mimic of an NF-κB-like DNA-binding domain, or Trx-binding domain. Mammalian cells co-expressing *pro-fs* and a HIV-1 LTR driven lacZ reporter gene construct showed increased β-gal activity in

response to TNF-α treatment, and deletion of the NF-κB binding sites located in HIV-1 LTR abolished the effect, which suggests that *pro-fs* is a potent bioactivator of HIV-1 LTR, exerting its effects via NF-κB (Taylor et al, unpublished data). The existing NMR structure of Trx-NF-κB enabled the construction of a homology model of *pro-fs* peptide binding Trx. The minimized energy of the *pro-fs*-Trx complex showed a lower value than that of Trx-NF-κB complex, indicating *pro-fs*, like NF-κB, is a target of Trx (Taylor et al, unpublished data).

It may be also significant that both retroviral proteases and NF-κB function as dimers. The arrangement of the *pro-fs* gene in HIV-1 suggests that perhaps the protease N-terminal region (the first 20 amino acid residues) functions as a common dimerization motif that can be attached to protease and *pro-fs*, which are encoded by the same nucleic acid sequence in two different reading frames. Thus, it was previously suggested that *pro-fs* itself might exist as a dimer [134].

The functional role of *pro-fs* is far from clear. Does it function by direct binding to NF-κB site in the HIV LTR in a homodimeric form, or by forming heterodimer with NF-κB subunits? Does it function as a mimic of the nuclear TR to maintain nuclear Trx in a reduced state, or as a substrate of Trx? Is it produced by HIV-1 at early stage of infection to promote HIV-1 replication, or at latent stage to prevent apoptosis of the infected cells? Obviously, we cannot draw any conclusion based on the evidence that already exists. More investigation needs to be taken place to solve the puzzle. The most immediate hypotheses derived from the known facts are: (1) *Pro-fs* functions by mimicry of NF-κB by interacting with Trx; (2) *Pro-fs* is a nuclear protein, and forms a dimer. The main purpose of this dissertation is to test these hypotheses, and thus clarify the role of *pro-fs* in this network and build the foundation for future research.

References

1. Embretson, J., et al., *Massive covert infection of helper T lymphocytes and macrophages by HIV during the incubation period of AIDS.* Nature, 1993. **362**(6418): p. 359-62.
2. Pantaleo, G., et al., *HIV infection is active and progressive in lymphoid tissue during the clinically latent stage of disease.* Nature, 1993. **362**(6418): p. 355-358.
3. Berkhout, B., R.H. Silverman, and K.T. Jeang, *Tat trans-activates the human immunodeficiency virus through a nascent RNA target.* Cell, 1989. **59**(2): p. 273-282.
4. Dingwall, C., et al., *Human immunodeficiency virus 1 tat protein binds trans-activation-responsive region (TAR) RNA in vitro.* PNAS, 1989. **86**(18): p. 6925-6929.
5. Luciw, P.A. and B.L. Shacklett, *Molecular biology of the human and simian immunodeficiency viruses.*, in *HIV Molecular Organization, Pathogenicity and Treatment.*, W.J.W. Morrow and N.L. Haigwood, Editors. 1993, Elsevier Science Publishers. p. 123-219.
6. Brown, F.L., et al., *Inducible transcriptional activation of the human immunodeficiency virus long terminal repeat by protein kinase inhibitors.* Mol. Cell. Biol., 1993. **13**: p. 5245-5254.
7. Kretz-Remy, C., E.E.M. Bates, and A.-P. Arrigo, *Amino Acid Analogs Activate NF-kappa B through Redox-dependent Ikappa B-alpha Degradation by the Proteasome without Apparent Ikappa B-alpha Phosphorylation. CONSEQUENCE ON HIV-1 LONG TERMINAL REPEAT ACTIVATION.* J. Biol. Chem., 1998. **273**(6): p. 3180-3191.
8. Allard, J., et al., *Oxidative stress and plasma antioxidant micronutrients in humans with HIV infection.* Am J Clin Nutr, 1998. **67**(1): p. 143-147.

9. Israel, N., et al., *Redox status of cells influences constitutive or induced NF-kappa B translocation and HIV long terminal repeat activity in human T and monocytic cell lines.* J Immunol, 1992. **149**(10): p. 3386-3393.

10. Israel, N. and M.A. Gougerot-Pocidalo, *Oxidative stress in human immunodeficiency virus infection.* Cell Mol Life Sci, 1997. **53**(11-12): p. 864-870.

11. Schreck, R., P. Rieber, and P.A. Baeuerle, *Reactive oxygen intermediates as apparently widely used messengers in the activation of the NF-kappa B transcription factor and HIV-1.* The EMBO Journal, 1991. **10**(8): p. 2247-2258.

12. Schulze-Osthoff, K., et al., *Depletion of the mitochondrial electron transport abrogates the cytotoxic and gene-inductive effects of TNF*. EMBO J., 1993. **12**(8): p. 3095-3104.

13. Nabel, G. and D. Baltimore, *An inducible transcription factor activates expression of human immunodeficiency virus in T cells.* Nature, 1987. **326**(6114): p. 711-713.

14. Brigelius-Flohe, R., et al., *Interleukin-1-induced nuclear factor kappa B activation is inhibited by overexpression of phospholipid hydroperoxide glutathione peroxidase in a human endothelial cell line.* Biochemical Journal, 1997. **328**: p. 199-203.

15. Kim, I.Y. and T.C. Stadtman, *Inhibition of NF-kappaB DNa binding and nitric oxide induction in human T cells and lung adenocarcinoma cellsby selenite treatment.* Proc Natl Acad Sci, 1997. **94**: p. 12904-12907.

16. Mitomo, K., et al., *Two different cellular redox systems regulate the DNA-binding activity of the p50 subunit of NF-kappa B in vitro.* Gene, 1994. **145**: p. 197-203.

17. Kawakami, K., C. Scheidereit, and R.G. Roeder, *Identification and purification of a human immunoglobulin-enhancer-binding protein (NF-kappa B) that activates*

transcription from a human immunodeficiency virus type 1 promoter in vitro. PNAS, 1988. **85**(13): p. 4700-4704.

18. Phares, W., B.R.J. Franza, and W. Herr, *The kappa B enhancer motifs in human immunodeficiency virus type 1 and simian virus 40 recognize different binding activities in human Jurkat and H9 T cells: evidence for NF-kappa B-independent activation of the kappa B motif.* J Virol., 1992. **66**(12): p. 7490-7498.

19. Sambucetti, L.C., et al., *NF-kappa B activation of the cytomegalovirus enhancer is mediated by a viral transactivator and by T cell stimulation.* EMBO J., 1989. **8**(13): p. 4251-4258.

20. Baldwin, A.S., Jr., *Series Introduction: The transcription factor NF-{{kappa}}B and human disease.* J. Clin. Invest., 2001. **107**(1): p. 3-6.

21. Rabson, A.B. and H.-C. Lin, *NF-κB and HIV: Linking Viral and Immune Activation*, in *HIV-1: Molecular Biology and Pathogenesis - Viral Mechanisms*, K.-T. Jeang, Editor. 2000, Academic Press. p. 161-207.

22. Baldwin, A.S., *THE NF-κB AND IκB PROTEINS: New Discoveries and Insights.* Annual Review of Immunology, 1996. **14**(1): p. 649-681.

23. Lin, R., D. Gewert, and J. Hiscott, *Differential Transcriptional Activation in Vitro by NF-kappaB/Rel Proteins.* J. Biol. Chem., 1995. **270**(7): p. 3123-3131.

24. Schmid, R.M., et al., *Cloning of an NF-kappa B subunit which stimulates HIV transcription in synergy with p65.* Nature, 1991. **352**(6337): p. 733-736.

25. Baeuerle, P.A. and A.S. Baldwin, *I kappa B: a specific inhibitor of the NF-kappa B transcription factor.* Science, 1988. **242**(4878): p. 540-546.

26. Baeuerle, P.A. and D. Baltimore, *NF-κB: Ten Years After.* Cell, 1996. **87**(1): p. 13-20.

27. Biswas, G., et al., *Mitochondria to nucleus stress signaling: a distinctive mechanism of NF{kappa}B/Rel activation through calcineurin-mediated inactivation of I{kappa}B{beta}.* J. Cell Biol., 2003. **161**(3): p. 507-519.

28. Hiscott, J., H. Kwon, and P. Genin, *Hostile takeovers: viral appropriation of the NF-kB pathway.* J. Clin. Invest., 2001. **107**(2): p. 143-151.

29. Siebenlist, U., G. Fransozo, and K. Brown, *Structure, regulation and function of NF-κB.* Annu. Rev. Cell Biol., 1994. **10**: p. 405-430.

30. Stancovski, I. and D. Baltimore, *NF-κB Activation: The IκB Kinase Revealed?* Cell, 1997. **91**: p. 299-302.

31. Tian, B. and A.R. Brasier, *Identification of a Nuclear Factor Kappa B-dependent Gene Network.* Recent Prog Horm Res, 2003. **58**(1): p. 95-130.

32. Waris, G., et al., *Hepatitis C virus NS5A and subgeomic replicons activate NF-kB via tyrosine phosphorylation of IkBa and its degradation by calpain protease.* J. Biol. Chem., 2003: p. M303248200.

33. Antoni, B.A., S.B. Stein, and A.B. Rabson, *Regulation of human immunodeficiency virus infection: implications for pathogenesis.* Adv Virus Res, 1994. **43**: p. 53-145.

34. Baeuerle, P. and D. Baltimore, *A 65-kappaD subunit of active NF-kappaB is required for inhibition of NF-kappaB by I kappaB.* Genes Dev., 1989. **3**(11): p. 1689-1698.

35. Bednarik, D.P. and T.M. Folks, *Mechanisms of HIV-1 latency.* AIDS, 1992. **6**(1): p. 3-16.

36. Doerre, S., et al., *The c-rel Protooncogene Product Represses NF-{kappa}B p65-Mediated Transcriptional Activation of the Long Terminal Repeat of Type 1 Human Immunodeficiency Virus.* PNAS, 1993. **90**(3): p. 1023-1027.

37. Griffin, G.E., et al., *Activation of HIV gene expression during monocyte differentiation by induction of NF-kappa B.* Nature, 1989. **339**(6219): p. 70-73.

38. Schreck, R., K. Albermann, and P. Bauerle, *Nuclear factor κB: An oxidative stress-response transcription factor of eukaryotic cells.* Free Rad. Res. Comm., 1992. **17**: p. 221-237.

39. Bassuk, A., R. Anandappa, and J. Leiden, *Physical interactions between Ets and NF-kappaB/NFAT proteins play an important role in their cooperative activation of the human immunodeficiency virus enhancer in T cells.* J. Virol., 1997. **71**(5): p. 3563-3573.

40. Ruocco, M.R., et al., *Regulation of HIV-1 Long Terminal Repeats by Interaction of C/EBP(NF-IL6) and NF-kappa B/Rel Transcription Factors.* J. Biol. Chem., 1996. **271**(37): p. 22479-22486.

41. Lodie, T.A., et al., *Both PU.1 and Nuclear Factor-{kappa}B Mediate Lipopolysaccharide-Induced HIV-1 Long Terminal Repeat Transcription in Macrophages.* J Immunol, 1998. **161**(1): p. 268-276.

42. Macian, F. and A. Rao, *Reciprocal Modulatory Interaction between Human Immunodeficiency Virus Type 1 Tat and Transcription Factor NFAT1.* Mol. Cell. Biol., 1999. **19**(5): p. 3645-3653.

43. Mosialos, G., *The role of Rel/NF-B proteins in viral oncogenesis and the regulation of viral transcription.* Semin Cancer Biol, 1997. **8**(2): p. 121-129.

44. Benkirane, M., K.-T. Jeang, and C. Devaux, *The cytoplasmic domain of CD4 plays a critical role during the early stages of HIV infection in T-cells.* EMBO J., 1994. **13**(23): p. 5559-5569.

45. Demarchi, F., M.I. Gutierrez, and M. Giacca, *Human Immunodeficiency Virus Type 1 Tat Protein Activates Transcription Factor NF-kappa B through the Cellular Interferon-Inducible, Double-Stranded RNA-Dependent Protein Kinase, PKR.* J. Virol., 1999. **73**(8): p. 7080-7086.

46. Riviere, Y., et al., *Processing of the precursor of NF-kappa B by the HIV-1 protease during acute infection.* Nature, 1991. **350**(6319): p. 625-626.

47. Westendorp, M.O., et al., *HIV-1 Tat potentiates TNF-induced NF-kappa B activation and cytotoxicity by altering the cellular redox state.* EMBO J., 1995. **14**(3): p. 546-554.

48. DeLuca, C., et al., *Nuclear Ikappa Bbeta Maintains Persistent NF-kappa B Activation in HIV-1-infected Myeloid Cells.* J. Biol. Chem., 1999. **274**(19): p. 13010-13016.

49. Baeuerle, P.A. and T. Henkel, *Function and Activation of NF-kappaB in the Immune System.* Annual Review of Immunology, 1994. **12**(1): p. 141-179.

50. Hirota, K., et al., *Distinct Roles of Thioredoxin in the Cytoplasm and in the Nucleus. A TWO-STEP MECHANISM OF REDOX REGULATION OF TRANSCRIPTION FACTOR NF-kappa B.* J. Biol. Chem., 1999. **274**(39): p. 27891-27897.

51. Brown, K., et al., *Mutual regulation of the transcriptional activator NF-kappa B and its inhibitor, I kappa B-alpha.* Proceedings Of The National Academy Of Sciences Of The United States Of America, 1993. **90**(6): p. 2532-2536.

52. Ginn-Pease, M.E. and R.L. Whisler, *Optimal NF[kappa]B Mediated Transcriptional Responses in Jurkat T Cells Exposed to Oxidative Stress Are Dependent on Intracellular Glutathione and Costimulatory Signals.* Biochemical and Biophysical Research Communications, 1996. **226**(3): p. 695-702.

53. Menon, S.D., G.R. Guy, and Y.H. Tan, *Involvement of a putative protein-tyrosine phosphatase and I kappa B-alpha serine phosphorylation in nuclear factor kappa B activation by tumor necrosis factor.* The Journal Of Biological Chemistry, 1995. **270**(32): p. 18881-18887.

54. Sen, R. and D. Baltimore, *Inducibility of kappa immunoglobulin enhancer-binding protein Nf-kappa B by a posttranslational mechanism.* Cell, 1986. **47**(6): p. 921-928.

55. Zhang, D., et al., *HIV type 1 protease activation of NF-kappa B within T lymphoid cells.* AIDS Research And Human Retroviruses, 1995. **11**(2): p. 223-230.

56. Suzuki, Y.J., B.B. Aggarwal, and L. Packer, *Alpha-lipoic acid is a potent inhibitor of NF-kappa B activation in human T cells.* Biochem Biophys Res Commun, 1992. **189**(3): p. 1709-1715.

57. Yang, J.-P., et al., *Inhibition of the DNA-binding activity of NF-kappa B by gold compounds in vitro.* FEBS Lett, 1995. **361**(1): p. 89-96.

58. Beg, A., et al., *Tumor necrosis factor and interleukin-1 lead to phosphorylation and loss of I kappa B alpha: a mechanism for NF-kappa B activation.* Mol. Cell. Biol., 1993. **13**(6): p. 3301-3310.

59. Henkel, T., et al., *Rapid proteolysis of I kappa B-alpha is necessary for activation of transcription factor NF-kappa B.* Nature, 1993. **365**(6442): p. 182-185.

60. Kretz-Remy, C., et al., *Inhibition of I kappa B-alpha phosphorylation and degradation and subsequent NF-kappa B activation by glutathione peroxidase overexpression.* J. Cell Biol., 1996. **133**(5): p. 1083-1093.

61. Butterfield, D.A. and A. Castegna, *Proteomic analysis of oxidatively modified proteins in Alzheimer's disease brain: insights into neurodegeneration.* Cell Mol Biol, 2003. **49**(5): p. 747-751.

62. Brennan, M.L. and S.L. Hazen, *Emerging role of myeloperoxidase and oxidant stress markers in cardiovascular risk assessment.* Curr Opin Lipidol, 2003. **14**(4): p. 353-359.

63. Stadtman, E. and C. Oliver, *Metal-catalyzed oxidation of proteins. Physiological consequences.* J. Biol. Chem., 1991. **266**(4): p. 2005-2008.

64. Belding, M.E., S.J. Klebanoff, and C.G. Ray, *Peroxidase-mediated virucidal systems.* Science, 1970. **167**(3915): p. 195-196.

65. Legrand-Poels, S., et al., *Activation of human immunodeficiency virus type 1 by oxidative stress.* AIDS Res Hum Retroviruses, 1990. **6**(12): p. 1389-1397.

66. Oda, T., et al., *Oxygen radicals in influenza-induced pathogenesis and treatment with pyran polymer-conjugated SOD.* Science, 1989. **244**(4907): p. 974-976.

67. Ohshima, H. and H. Bartsch, *Chronic infections and inflammatory processes as cancer risk factors: possible role of nitric oxide in carcinogenesis.* Mutat Res, 1994. **305**(2): p. 253-264.

68. Droge, W., H.P. Eck, and S. Mihm, *Oxidant-antioxidant status in human immunodeficiency virus infection.* Methods Enzymol, 1994. **233**: p. 594-601.

69. Diplock, A.T., *Antioxidant nutrients and disease prevention: an overview.* Am J Clin Nutr, 1991. **53**(1 Suppl): p. 189S-193S.

70. Oteiza, P.I., et al., *Zinc deficiency induces oxidative stress and AP-1 activation in 3T3 cells.* Free Radic Biol Med, 2000. **28**(7): p. 1091-1099.

71. Taylor, E.W., et al., *Nutrition, HIV, and drug abuse: the molecular basis of a unique role for selenium.* J Acquir Immune Defic Syndr, 2000. **25 Suppl 1**: p. S53-61.

72. Sunde, R.A., *Selenium*, in *Handbook of Nutritionally Essential Minerals*, B.L. O'Dell and R.A. Sunde, Editors. 1997, Marcel Dekker: New York. p. 493-556.

73. Taylor, E.W., *Selenium and viral disease: facts and hypotheses.* J. Orthomol. Med., 1997. **12**: p. 227-239.

74. Turner, R.J. and J.M. Finch, *Selenium and the immune response.* Proc. Nutr. Soc., 1991. **50**: p. 275-285.

75. Group, K.D.R., *Observations on effect of sodium selenite in prevention of Keshan disease.* Chinese Med J., 1979. **92**: p. 471-476.

76. Beck, M.A., et al., *Rapid genomic evolution of a non-virulent coxsackievirus B3 in selenium-deficient mice results in selection of identical virulent isolates.* Nature Medicine, 1995. **1**(5): p. 433-436.

77. Yu, S.Y., Y.J. Zhu, and W.G. Li, *Protective role of selenium against hepatitis B virus and primary liver cancer in Qidong.* Biological Trace Element Research, 1997. **56**(1): p. 117-124.

78. Yu, M.W., et al., *Plasma selenium levels and risk of hepatocellular carcinoma among men with chronic hepatitis virus infection.* American Journal Of Epidemiology, 1999. **150**(4): p. 367-374.

79. Allavena, C., et al., *Relationship of trace-element, immunological markers, and HIV infection progression.* Biol. Trace Elem. Res., 1995. **47**(133-138).

80. Baum, M.K., et al., *High risk of HIV-related mortality is associated with selenium deficiency.* J Acquir Immune Defic Syndr Hum Retrovirol, 1997. **15**: p. 370-376.

81. Constans, J., et al., *Serum selenium predicts outcome in HIV infection.* J. Acquir. Immune. Defic. Syndr. Hum. Retrovirol., 1995. **10**(3): p. 392.

82. Dworkin, B.M., *Selenium deficiency in HIV infection and the acquired immunodeficiency syndrome (AIDS).* Chem. Biol. Interact., 1994. **91**: p. 181-186.

83. Look, M.P., et al., *Serum selenium versus lymphocyte subsets and markers of disease progression and inflammatory response in human immunodeficiency virus-1 infection.* Biological Trace Element Research, 1997. **56**(1): p. 31-41.

84. Sappey, C., et al., *Stimulation of glutathione peroxidase activity decreases HIV type 1 activation after oxidative stress.* AIDS. Res. Hum. Retroviruses., 1994. **10**(11): p. 1451-1461.

85. Hori, L., et al., *Selenium supplementation suppresses tumor necrosis factor α-induced human immunodeficiency virus type 1 replication in vitro.* AIDS Research And Human Retroviruses, 1997. **13**: p. 1325-1332.

86. Bock, A., et al., *Selenocysteine: the 21st amino acid.* Mol. Microbiol., 1991. **5**: p. 515-520.

87. Cone, J.E., et al., *Chemical characterization of the selenoprotein component of clostridial glycine reductase: identification of selenocysteine as the organoselenium moiety.* Proc. Natl. Acad. Sci. U. S. A., 1976. **73**(8): p. 2659-2663.

88. McKenzie, R.C., J.R. Arthur, and G.J. Beckett, *Selenium and the regulation of cell signaling, growth, and survival: molecular and mechanistic aspects.* Antioxid Redox Signal, 2002. **4**(2): p. 339-351.

89. Rotruck, J.T., et al., *Selenium: biochemical role as a component of glutathione peroxidase.* Science, 1973. **179**(4073): p. 588-590.

90. Takahashi, K., J.W. Avissar, and H. Cohen, *Purification and characterization of human plasma glutathione peroxidase: a selenoglycoprotein distinct from the known cellular enzyme.* Arch. Biochem. Biophys, 1987. **256**(677-686).

91. Ursini, F., M. Maiorino, and C. Gregolin, *The selenoenzyme phospholipid hydroperoxide glutathione peroxidase.* Biochim. Biophys. Acta., 1985. **839**: p. 62-70.

92. Chu, F.-F., J.H. Doroshow, and R.S. Esworthy, *Expression, characterization, and tissue distribution of a new cellular selenium-dependent glutathione peroxidase. GSHPx-GI.* J. Biol. Chem., 1993. **268**: p. 2571-2576.

93. Holben, D.H. and A.M. Smith, *The Diverse Role of Selenium within Selenoproteins--A Review.* Journal of the American Dietetic Association, 1999. **99**(7): p. 836-843.

94. Gladyshev, V.N., K.-T. Jeang, and T.C. Stadtman, *Selenocysteine, identified as the penultimate C-terminal residue in human T-cell thioredoxin reductase, corresponds to TGA in the human placental gene.* PNAS, 1996. **93**(12): p. 6146-6151.

95. Berry, M.J., L. Banu, and P.R. Larsen, *Type I iodothyrine deiodinase is a selenocysteine-containing enzyme.* Nature, 1991. **349**(6308): p. 438-440.

96. Davey, J.C., et al., *Cloning of a cDNA for the Type II Iodothyronine Deiodinase.* J. Biol. Chem., 1995. **270**(45): p. 26786-26789.

97. Germain, D., et al., *Correction: A Thyroid Hormoneregulated Gene in Xenopus laevis Encodes a type III Iodothyronien 5-Deiodinase.* PNAS, 1994. **91**(23): p. 11282-.

98. Moschos, M.P., *Selenoprotein P.* Cell. Mol. Life. Sci., 2000. **57**(13-14): p. 1836-1845.

99. Jeong, D.-w., et al., *Selenoprotein W is a glutathione-dependent antioxidant in vivo.* FEBS Letters, 2002. **517**(1-3): p. 225-228.

100. Guimaraes, M.J., et al., *Identification of a novel selD homolog from Eukaryotes, Bacteria, and Archaea: Is there an autoregulatory mechanism in selenocysteine metabolism?* PNAS, 1996. **93**(26): p. 15086-15091.

101. Kryukov, G.V., Gladyshev, V. N., *Mammalian selenoprotein gene signature: identification and functional analysis of selenoprotein genes using bioinformatics methods,* in *Methods in Enzymology,* H. Sies and L. Packer, Editors. 2002, Academic Press: San Diego, CA. p. 84-100.

102. Lescure, A., D. Gautheret, and A. Krol, *Novel selenoproteins identified from genomic sequence data,* in *Methods in Enzymology,* H. Sies and L. Packer, Editors. 2002, Academic Press: San Diego, CA. p. 57-70.

103. Senkevich, T.G., et al., *Genome sequence of a human tumorigenic poxvirus: prediction of specific host response-evasion genes.* Science, 1996. **273**(5276): p. 813-816.

104. Shisler, J.L., et al., *Ultraviolet-induced cell death blocked by a selenoprotein from a human dermatotropic poxvirus.* Science, 1998. **279**(5347): p. 102-105.

105. Afonso, C.L., et al., *The Genome of Fowlpox Virus.* J. Virol., 2000. **74**(8): p. 3815-3831.

106. Zhang, W., et al., *Selenium-dependent glutathione peroxidase modules encoded by RNA viruses.* Biol. Trace. Elem. Res., 1999. **70**(2): p. 97-116.

107. Zhao, L., et al., *Molecular modeling and in vitro activity of an HIV-1-encoded glutathione peroxidase.* Proc. Natl. Acad. Sci. U.S.A., 2000. **97**(12): p. 6356-6361.

108. Mustacich, D. and G. Powis, *Thioredoxin reductase.* Biochem J., 2000. **346**(Pt 1): p. 1-8.

109. Casso, D. and D. Beach, *A mutation in a thioredoxin reductase homolog suppresses p53-induced growth inhibition in the fission yeast Schizosaccharomyces pombe.* Mol Gen Genet, 1996. **252**(5): p. 518-529.

110. Zhong, L., E.S.J. Arner, and A. Holmgren, *Structure and mechanism of mammalian thioredoxin reductase: The active site is a redox-active selenolthiol/selenenylsulfide formed from the conserved cysteine-selenocysteine sequence.* PNAS, 2000. **97**(11): p. 5854-5859.

111. Buettner, C., J.W. Harney, and M.J. Berry, *The Caenorhabditis elegans homologue of thioredoxin reductase contains a selenocysteine insertion sequence (SECIS) element that differs from mammalian SECIS elements but directs selenocysteine incorporation.* The Journal Of Biological Chemistry, 1999. **274**(31): p. 21598-21602.

112. Gladyshev, V.N., et al., *Selenocysteine-Containing Thioredoxin Reductase in C. elegans.* Biochemical and Biophysical Research Communications, 1999. **259**(2): p. 244-249.

113. Berggren, M., et al., *Cellular thioredoxin reductase activity is regulated by selenium.* Anticancer Res., 1997. **17**(5A): p. 3377-3380.

114. Ganther, H.E., *Selenium metabolism, selenoproteins and mechanisms of cancer prevention: complexities with thioredoxin reductase.* Carcinogenesis, 1999. **20**(9): p. 1657-1666.

115. Hadley, K.B. and R.A. Sunde, *Selenium regulation of thioredoxin reductase activity and mRNA levels in rat liver.* The Journal of Nutritional Biochemistry, 2001. **12**(12): p. 693-702.

116. Gallegos, A., et al., *Mechanisms of the regulation of thioredoxin reductase activity in cancer cells by the chemopreventive agent selenium.* Cancer Res, 1997. **57**(21): p. 4965-4970.

117. Liu, Y. and W. Min, *Thioredoxin Promotes ASK1 Ubiquitination and Degradation to Inhibit ASK1-Mediated Apoptosis in a Redox Activity-Independent Manner.* Circ Res, 2002. **90**(12): p. 1259-1266.

118. Tanaka, T., et al., *Redox regulation by thioredoxin superfamily; protection against oxidative stress and aging.* Free Radic Res, 2000. **33**(6): p. 851-855.

119. Arner, E.S.J. and A. Holmgren, *Physiological functions of thioredoxin and thioredoxin reductase.* Eur J Biochem, 2000. **267**(20): p. 6102-6109.

120. Powis, G., D. Mustacich, and A. Coon, *The role of the redox protein thioredoxin in cell growth and cancer.* Free Radic Biol Med, 2000. **29**(3-4): p. 312-322.

121. Laurent, T.C., E.C. Moore, and P. Reichard, *Enzymatic Synthesis of Deoxyribonucleotides. IV. ISOLATION AND CHARACTERIZATION OF THIOREDOXIN, THE HYDROGEN DONOR FROM ESCHERICHIA COLI B.* J. Biol. Chem., 1964. **239**(10): p. 3436-3444.

122. Matthews, J.R., et al., *Thioredoxin regulates the DNA binding activity of NF-κB by reduction of a disulphide bond involving cysteine 62.* Nucleic Acids Research, 1992. **20**(15): p. 3821-3830.

123. Tagaya, Y., et al., *ATL-derived factor (ADF), an IL-2 receptor/Tac inducer homologous to thioredoxin; possible involvement of dithiol-reduction in the IL-2 receptor induction [published erratum appears in EMBO J 1994 May 1;13(9):2244].* EMBO J., 1989. **8**(3): p. 757-764.

124. Wakasugi, N., et al., *Adult T-Cell Leukemia-Derived Factor/Thioredoxin, Produced by Both Human T- Lymphotropic Virus Type I- and Epstein-Barr Virus-Transformed*

Lymphocytes, Acts as an Autocrine Growth Factor and Synergizes with Interleukin 1 and Interleukin 2. PNAS, 1990. **87**(21): p. 8282-8286.

125. Hayashi, T., Y. Ueno, and T. Okamoto, *Oxidoreductive regulation of nuclear factor kappa B. Involvement of a cellular reducing catalyst thioredoxin.* J. Biol. Chem., 1993. **268**(15): p. 11380-11388.

126. Qin, J., et al., *Solution structure of human thioredoxin in a mixed disulfide intermediate complex with its target peptide from the transcription factor NF-κB.* Structure, 1995. **3**: p. 289-297.

127. Hirota, K., et al., *AP-1 transcriptional activity is regulated by a direct association between thioredoxin and Ref-1*. PNAS, 1997. **94**(8): p. 3633-3638.

128. Ghosh, G., et al., *Structure of NF-kappa B p50 homodimer bound to a kappa B site.* Nature, 1995. **373**(6512): p. 303 - 310.

129. Müller, C.W., et al., *Structure of the NF-kappa B p50 homodimer bound to DNA.* Nature, 1995. **373**(6512): p. 311-317.

130. Saitoh, M., et al., *Mammalian thioredoxin is a direct inhibitor of apoptosis signal-regulating kinase (ASK) 1* . EMBO J., 1998. **17**(9): p. 2596-2606.

131. Geleziunas, R., et al., *HIV-1 Nef inhibits ASK1-dependent death signalling providing a potential mechanism for protecting the infected host cell.* Nature, 2001. **412**(6830): p. 834-838.

132. Bjornstedt, M., et al., *Selenium and the thioredoxin and glutaredoxin systems.* Biomed Environ Sci, 1997. **10**((2-3)): p. 271-279.

133. Nakamura, H., et al., *Elevation of plasma thioredoxin levels in HIV-infected individuals.* Int. Immunol., 1996. **8**(4): p. 603-611.

134. Taylor, E.W., et al., *A Basis for New Approaches to the Chemotherapy of AIDS: Novel Genes in HIV-1 Potentially Encode Selenoproteins Expressed by Ribosomal Frameshifting and Termination Suppression.* J. Med. Chem., 1994. **37**: p. 2637-2654.

135. Taylor, E.W., R.G. Nadimpalli, and C.S. Ramanathan, *Genomic structures of viral agents in relation to the biosynthesis of selenoproteins.* Biol. Trace. Elem. Res., 1997. **56**: p. 63-91.

136. Farabaugh, P.J., *Programmed Translational Frameshifting.* Annual Review of Genetics, 1996. **30**(1): p. 507-528.

137. Jacks, T., et al., *Characterization of ribosomal frameshifting in HIV-1 gag-pol gene expression.* Nature, 1988. **331**: p. 280-283.

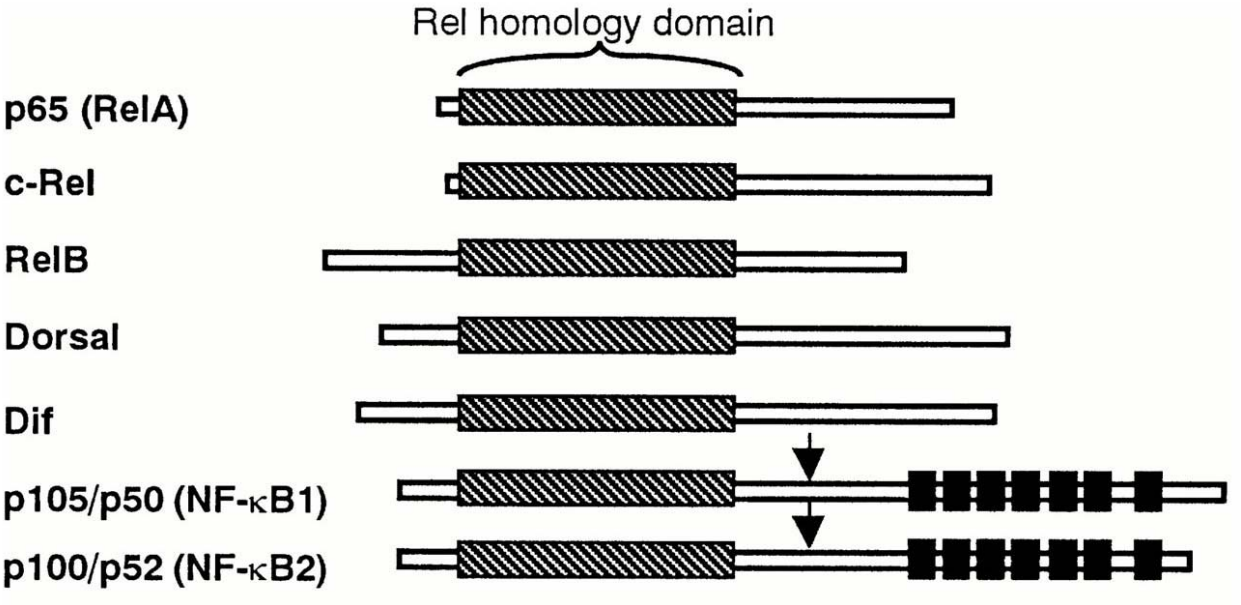

Figure 1.1. The NF-κB/Rel family of proteins. The NF-κB/Rel proteins form to a family of inducible transcription factors, which are encoded by five genes p105/p50 (NF-κB1), p65 (RelA), c-Rel, RelB, and p100/p52 (NF-κB2) [20]. The Rel homology domain (RHD) contains conserved amino acid sequences in all NF-κB/Rel proteins that are involved in important functions including DNA binding, dimerization, nuclear localization, and interaction with IκB molecules. Dorsal and Dif are Drosophila proteins, homologous to mammalian NF-κB/Rel family of proteins (adapted from Figure 1 in [22]).

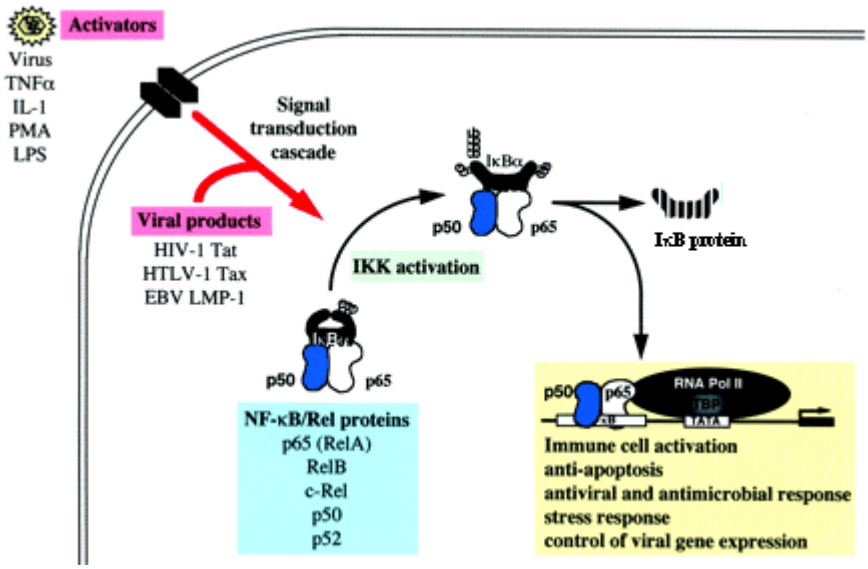

Figure 1.2. The NF-κB activation scheme. NF-κB localizes in the cytoplasm associating with the inhibitory IκB proteins. Upon stimulation by a large array of factors, such as viruses, cytokines, and stress-inducing agents, IκB undergoes phosphorylation, ubiquitination and degradation, leading to nuclear translocation of NF-κB DNA binding subunits, and thus transactivate NF-κB responsive genes containing the κB site sequence (5'-GGGRNNYYCC-3'). Target genes are selectively regulated by the distinct transcriptional activation potential of different NF-κB subunit combinations (adapted from Figure 1 in [28]).

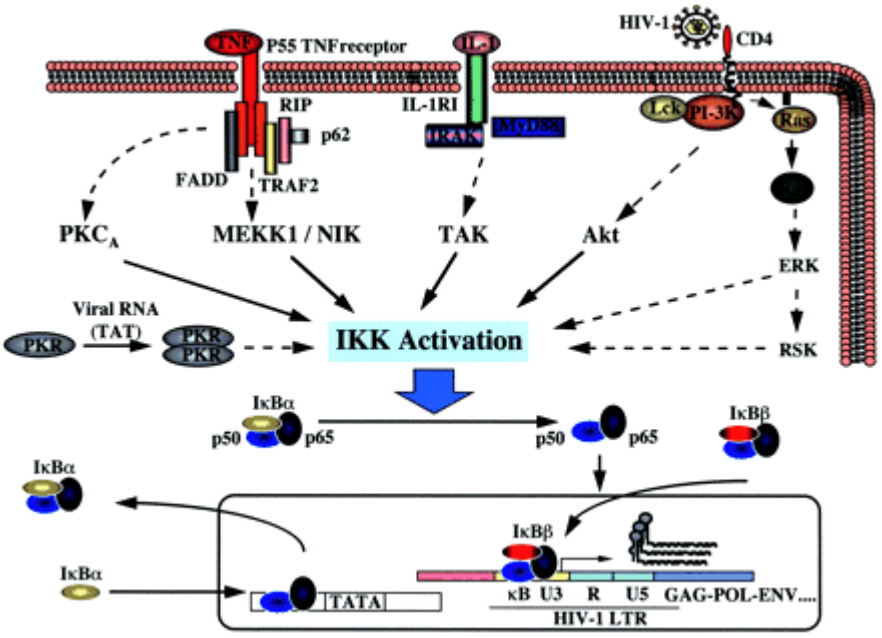

Figure 1.3. Proposed mechanisms of NF-κB activation in HIV-1-infected cells. Several mechanisms may regulate NF-κB activity in HIV-1–infected cells. Binding of HIV-1 to CD4 and CD4 crosslinking leads to NF-κB activation. Protein kinase R (PKR), induced by low level interferon (IFN) and HIV-1 transcripts, may induce IκB kinase (IKK) activation. Autocrine release of cytokines such as tumor necrosis factor -α (TNF-α) and interleukin -1 (IL-1) may constitutively stimulate the signaling pathways leading to NF-κB activation. Activation of the IKK complex either directly by HIV-1 regulatory proteins or by cytokine release leads to the phosphorylation, ubiquitination and degradation of IκB, thus releasing NF-κB to translocate to the nucleus and transactivate HIV gene transcription (adapted from Figure 2 in [28]).

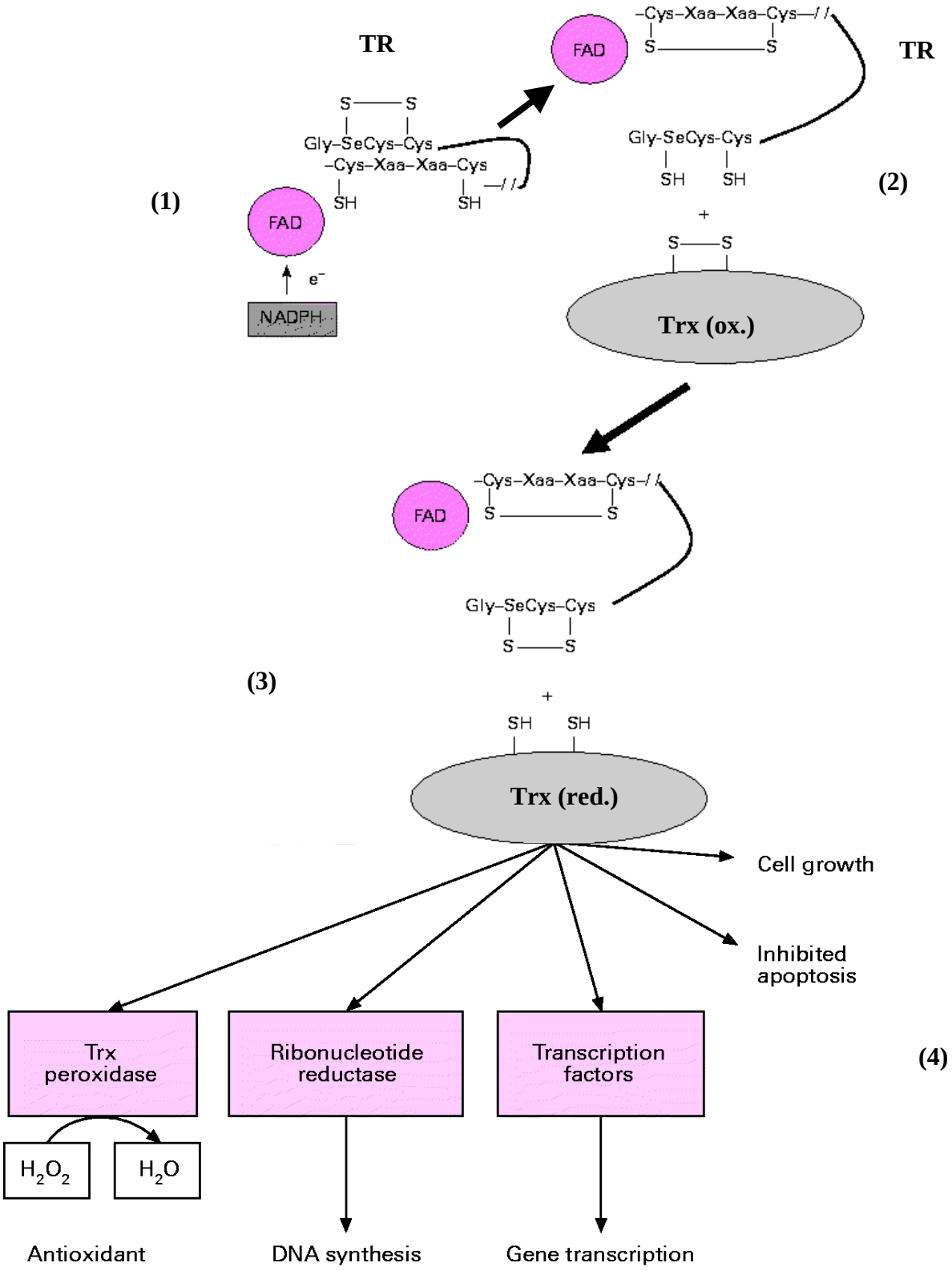
TR
FAD
–Cys–Xaa–Xaa–Cys–//
S——S
TR
S——S
Gly–SeCys–Cys
–Cys–Xaa–Xaa–Cys
SH
SH
–//
(1)
FAD
e⁻
NADPH
Gly-SeCys-Cys
SH
SH
(2)
+
S——S
Trx (ox.)
FAD
–Cys–Xaa–Xaa–Cys–//
S——S
Gly–SeCys–Cys
S——S
(3)
+
SH
SH
Trx (red.)
Cell growth
Inhibited apoptosis
Trx peroxidase
Ribonucleotide reductase
Transcription factors
(4)
H2O2
H2O
Antioxidant
DNA synthesis
Gene transcription

Figure 1.4. Mechanism of the reduction reaction of thioredoxin (Trx) catalyzed by the mammalian selenoprotein thioredoxin reductase (TR), and functions of Trx. (1) NADPH binds to the NADPH-binding domain of TR, and electrons (e^-) flow from NADPH through FAD to reduce the conserved catalytic-site -Cys-Xaa-Xaa-Cys- disulphide bond of TR. The C-terminal -Cys-SeCys- catalytic site is in the oxidized form at this time. (2) Thiol–disulphide exchange results in oxidation of the Cys-Xaa-Xaa-Cys- site and reduction of the C-terminal -Cys-SeCys- site. (3) The reduced Cys-SeCys moves away and transfers electrons to its substrate, oxidized Trx, to reduce its disulphide bond. (4) Reduced Trx provides reducing equivalents to Trx peroxidase, which breaks down H_2O_2 to water, ribonucleotide reductase, which reduces ribonucleotides to deoxyribonucleotides for DNA synthesis, and transcription factors, such as NF-κB, which leads to their increased binding to DNA and altered gene transcription. In addition, Trx increases cell growth and inhibits apoptosis (adapted from Figure 1 and Scheme 2 in [108]).

CHAPTER 2

A HIV-1 ENCODED PEPTIDE MIMICS THE DNA BINDING LOOP OF NF KAPPA B AND BINDS THIOREDOXIN WITH HIGH AFFINITY IN VITRO[1]

[1] Su, G., W. Min, and E. W. Taylor. To be submitted to Journal of Biological Chemistry.

ABSTRACT

It has previously been shown that the gene encoded in the overlapping –1 reading frame of the human immunodeficiency type 1 (HIV-1) protease, named *pro-fs*, has significant homology to the DNA binding loop of nuclear factor kappa B (NF-κB), which is known to bind thioredoxin (Trx). The hypothesis that the putative HIV-1 *pro-fs* gene product functions by mimicry of NF-κB via binding to Trx was tested by co-immunoprecipitation and GST-pull down assay. The UGA codons (coding for selenocysteine residues) in *pro-fs* sequence were mutated to Cys codons, and *pro-fs* was expressed in *E. coli* and purified by high performance liquid chromatography (HPLC). Both experiments consistently show that *pro-fs* binds to human Trx with high affinity in vitro. The mutation of the two conserved Cys residues in the redox center of Trx to Ser reduced the binding affinity but failed to abolish the interaction. These results ruled out the possibility that the interaction between *pro-fs* and Trx is merely due to the formation of an intermolecular disulfide bond between the Cys residues of *pro-fs* and the ones in the redox center of Trx, suggesting that Trx-*pro-fs* binding is a structurally specific interaction that involves multiple amino acid residues in the interactive region.

Keywords: Frameshift; HIV-1; Protease; NF kappa B; Thioredoxin; Selenocysteine; Cysteine; HPLC; Pro-fs; Co-immunoprecipitation; GST-pull down.

INTRODUCTION

Selenium (Se) is an essential trace element important for various aspects of human health (reviewed in [1]). Growing evidence links Se deficiency to the occurrence, virulence, or disease progression of several viral infections, such as Coxsackie virus, human immunodeficiency type 1 (HIV-1) virus, and hepatitis virus (B or C) [2-8]. A statistically significant correlation between HIV disease outcome and patient Se status has been widely documented. Se is not only correlated with various indicators of disease progression, but is also an independent predictor of mortality in HIV infection [2, 4, 6]. There is evidence showing that Se is a potent inhibitor of HIV replication in vitro [9]. Se supplementation was shown to suppress HIV replication induced by tumor necrosis factor-α (TNF-α) or interleukin-1 (IL-1) by increasing the concentration of cellular selenoproteins glutathione peroxidase (GPx) and thioredoxin reductase (TR) [9-12].

To activate its replication, HIV employs the cellular transcription factors that interact with its long terminal repeat (LTR), most importantly nuclear factor kappa B (NF-κB) [13-18]. NF-κB is composed of homo- or heterodimers of Rel family proteins (reviewed in [19]), which all share an N-terminal Rel homology domain (RHD) that is essential for DNA binding and dimerization. The classic NF-κB heterodimer (p50/p65) is sequestered in the cytoplasm by interaction with the inhibitory molecule IκB [19]. Initial activation of NF-κB in the cytosol occurs with phosphorylation and degradation of IκB, which results in unmasking of a nuclear translocation signal on NF-κB. Then the free NF-κB dimers can enter the nucleus and bind DNA to start gene transcription [20-25]. There are two conserved κB sites located in HIV LTR that are binding targets of NF-κB. Thus, the DNA-binding activity of NF-κB is a crucial factor in HIV replication. The transcriptional activation of HIV LTR via NF-κB can be stimulated by a

variety of proinflammatory or pathogenic stimuli including inflammatory cytokines, phorbol esters (PMA), T-cell mitogens, lipopolysaccharide (LPS), hydrogen peroxide (H_2O_2) and TNF-α [26-29], which function at least in part by forming radical oxygen intermediates (ROIs). NF-κB also regulates numerous cellular genes that relate to immune functions and host cellular defense against stress, including cytokine genes associated with T cell activation and inflammatory responses (for example, GM-CSF, IL-6, IL-8, IL-2, etc.), adhesion molecules (for example, VCAM-1 and E-selectin), and genes that regulate cell proliferation and apoptosis [10, 17, 30, 31].

NF-κB is susceptible to redox regulation by thioredoxin (Trx), which is known to be an important endogenous redox-regulating molecule with thiol reducing activity [32-34]. Trx plays a role in modulating various kinds of gene expression. It is a small ubiquitous protein with two Cys residues in its catalytic center with the consensus amino acid sequence Trp-Cys-Gly-Pro-Cys-Lys. Trx participates in redox reactions by reversible oxidation of the dithiol of the amino acid Cys32 and Cys35 residues to an intramolecular disulfide bond. It catalyzes dithiol-disulfide exchange reactions involving many thiol-dependent cellular processes, including intracellular signaling, gene regulation, resistance to oxidant stress, and control of apoptosis [34-36]. Hirota et al. demonstrated that Trx plays a dual and opposing role in the regulation of NF-κB. Overexpression of wild-type Trx suppressed NF-κB activation in the cytoplasm while overexpression of nuclear-targeted Trx enhanced NF-κB-dependent transcription in the nucleus [32]. A growing body of evidence shows that Trx serves as a reductive catalyst in the reduction reaction of the Cys62 residues of NF-κB [31, 32, 37], which is conserved in NF-κB RHD domain and needs to be maintained in a reduced (thiol) state in order for NF-κB to bind to DNA [31], e.g. κB sites in HIV LTR. It was demonstrated that the reduction of the Cys62 residue of

NF-κB requires direct association between the active center of Trx and the DNA binding loop of NF-κB [32, 38].

Previously, Taylor et al. predicted that HIV-1 may encode several selenoprotein modules, based on computational analysis of the viral genome [39]. One of these was potentially expressed by a –1 frameshift from the protease-coding region, and was later named *pro-fs* [39, 40]. *Pro-fs* contains two in-frame UGA codons. UGA codon is generally a stop codon, but now is well known for its role in coding for selenocysteine (Sec) in both eukaryotic and prokaryotic genomes, depending upon the presence of appropriate mRNA signals in the cell [41-43]. The amino acid sequence of *pro-fs* is highly conserved in HIV-1 sequences, especially at the UGA codons [44] [45]. Sequence analysis suggested a match to the NF-κB family of transcription factors, in which the conserved amino acid Cys62 residue aligns with the conserved UGA codon of *pro-fs* [45]. The frameshift site in HIV-1 protease gene occurs just upstream of the *pro-fs* sequence (RYRSRU) that matches the sequence of the NF-κB/Rel family DNA binding domain (RFRYXC) [45], which is also the peptide of NF-κB that interacts with Trx, as shown in the NMR structure [38].

The main aim of this paper is to clarify how *pro-fs* regulates HIV gene replication via NF-κB, and to elucidate a mechanistic role of *pro-fs* in cells, and its relationship with Trx. We hypothesized that Trx is a target of *pro-fs* because of the local sequence similarity mentioned above, between a central region of *pro-fs* and the DNA binding loop of NF-κB, which contains the critical Cys residue that must first be reduced by Trx in order for NF-κB to bind to DNA. A homology model of *pro-fs* peptide binding to Trx was constructed and the minimized energy of this complex was shown to be at least as favorable as that of the NMR structure of Trx-NF-κB complex (Taylor, et al., unpublished data). Therefore, we investigated the potential protein-

protein interaction between *pro-fs* and Trx in vitro. Our data indicate that there is a direct association between *pro-fs* and Trx.

MATERIAL AND METHODS

Construction of HIV-1 *pro-fs* bacterial expression vector. Because the hypothetical HIV-1 encoded peptide *pro-fs* was predicted to be expressed by a –1 frameshift in protease coding region [39], the primary gene product would be a gag-pol-*pro-fs* fusion protein of 557 amino acids (aa), with an expected molecular mass of about 62.3 kDa. However, a HIV-1 protease site was located immediately upstream of the protease coding region [39], so the *pro-fs* module, which is the C-terminal 69 aa of the predicted fusion product, may also cleaved and released as an independent small (about 8.3 kDa) protein, in which form it has great significant sequence similarity to NF-κB. It was this low molecular mass peptide that we have cloned. The above molecular mass was estimated using Protein Calculator (http://www.scripps.edu/~cdputnam/protcalc.html).

The full-length *pro-fs* gene was obtained by PCR from the constructs provided by Dr. Hondal (Vermont University). The stop codon TAA was mutated back from CAA in the original construct by amplifying the *pro-fs* coding region using sense primer PROFS-BAM, 5’ GAT ATC GGA TCC GTT CAA CTT CCC GC 3’, containing a *BamH*I site, and anti-sense primer PROFS-ECO, 5’ AGC TCG AAT TCT TAT GTC CAC AGA TTT CTA TGA G 3’, containing an *EcoR*I site. A protease site was constructed immediately before *pro-fs* coding region. The PCR product was then digested by *BamH*I and *EcoR*I and inserted into vector pET43.1b (Novagen), which contains a Nus·Tag and a hexahistidine (6x His) tag upstream of the cloning site (Fig. 2.1). The

pro-fs gene construct (Nus-*pro-fs*) was transformed into *Escherichia coli* (*E. coli*) strain BL21(DE3) from Stratagene (La Jolla, CA) using chemical transformation method followed by extraction and purification using QIAprep Miniprep Kits (Qiagen). Fidelity of the construct was verified by automated DNA sequencing (Molecular Genetics Instrumentation Facilities, University of Georgia).

Production of Nus-*pro-fs* and Nus proteins in bacteria. The transformed bacteria were cultured in 50ml of LB medium supplemented with 50 μg/ml of ampicillin for about 6 hrs at 37 °C with vigorous shaking until the optical density at 600 nm (OD_{600}) was 0.6-1.0. This was stored overnight at 4 °C and was then used to infect 1 L of the same medium as described above on the next day. Isopropyl-β-D-thiogalactopyranoside (IPTG) (Fisher Scientific) was added to the bacterial culture to a final concentration of 0.5 mM when the OD_{600} of culture reached 0.5 at 37 °C to induce protein production of Nus-*pro-fs*. The bacteria were continuously incubated with vigorous shaking at 30 °C for another 8 h before harvesting. The pET43.1b vector alone was transformed into *E. coli* BL21 (DE3) and Nus protein was produced using the protocol described above. Aliquots of cells were taken at 0, 2, 4, 6, 8, 16, 24 h post-induction for Nus-*pro-fs* and 0, 4, 8, 16 h for Nus to monitor the production of Nus-*pro-fs* and Nus by running the supernatants of cell lysates on SDS-PAGE (Fig. 2.2).

Protein purification using HPLC. Bacteria transformed with Nus-*pro-fs* construct or vector alone were harvested by centrifugation at 6,000 x g for 30 min at 4 C. Cell pellets were resuspended in buffer A (20 mM Sodium Phosphate, 0.5 M NaCl, pH 7.4) and cells were disrupted on ice by sonication using a model 550 Sonic Dismembrator (Fisher Scientific) in the

presence of protease inhibitor (Roche). Cell debris and a soluble fraction in buffer A were then separated by centrifugation at 10,000 x g for 30 min at 4 °C. The supernatant was immediately loaded into a Äkta Purifier (Pharmacia Biotech) to be fractionated on a HiTrap^{TM} metal chelating column (Amersham Biosciences) using high performance liquid chromatography (HPLC). Proteins were eluted from the column separately by application of a linear gradient of 0-0.5 M imidazole in Buffer B (0.5 M imidazole, 20 mM Sodium Phosphate, 0.5 M NaCl, pH 7.4), controlled by a program written to automatically increase buffer B intake.

Protein concentrations of each fraction were determined with Bio-Rad protein assay solution and aliquots were analyzed in Western blots to detect Nus-*pro-fs* or Nus protein with mouse anti-Nus tag monoclonal Ab (Novagen) and alkaline phosphatase (AP) conjugated goat anti-mouse-IgG. Signals were detected using Western Blue reagent (Promega) following the manufacture's instructions.

Immunoprecipitation and immunoblotting. For immunoprecipitation to analyze protein interaction in vitro, 3 μg of purified Nus-*pro-fs* and 5.5 μg of rabbit polyclonal anti-Trx antibody (Ab) (Sigma) were mixed without or with 2 μg of human Trx (Sigma) and incubated for overnight at 4 °C on a 3D rotor. The mixture was then added to the protein A magnetic beads (NEB) to incubate on 3D rotor for 2 h at 4 °C. Nus protein was used to incubate with Trx and Trx Ab for the same procedure as a negative control. The beads were separated from the supernatant by applying the mixture to the Dynal Magnetic Particle Concentrator (MPC, Dynal Biotech) for 2 min and followed with 4 washes with 1 ml of cold 0.1 M Sodium Phosphate buffer (pH 8.0). The immune complexes binding to the beads were eluted with 30 μl of cold 0.1 M glycine (pH 2.5) by gentle vortexing and inverting. Ten μl of the sample was analyzed in

Western blots with mouse anti-Nus tag monoclonal Ab (Novagen) and alkaline phosphatase (AP) conjugated goat anti-mouse-IgG secondary Ab. Signals were detected using Western Blue reagent (Promega) following manufacture's instructions.

GST-pull down assay. Two GST-Trx fusion proteins were used for a GST pull-down assay to study protein-protein interactions in vitro. Wild-type GST-Trx fusion protein (GST-Trx-wt) and a mutant GST-Trx fusion protein (GST-Trx-CS), were generously provided by Dr. W. Min (Center for Cardiovascular Research, University of Rochester Medical Center, Rochester, NY). In brief, GST-Trx fusion proteins expressed in *E. coli* XL-1 blue were affinity purified on glutathione-Sepharose (GSH) beads (Pharmacia) [33]. Three μg of Nus-*pro-fs* were added to 50 μl of glutathione-Sepharose beads alone or 50 μl beads bound with GST-Trx-wt or GST-Trx-CS, in which Trx residues Cys32 and Cys35 were mutated to Ser [33]. Fifty μl of cold 1X PBS buffer was added to each reaction to bring the final volume to 100 μl. Three μg of Nus protein was added to GST-Trx-wt or GST-Trx-CS as negative controls. After overnight incubation at 4 °C on 3D rotor, the beads were separated from supernatant by centrifugation at 14,000 rpm for 1 min. Beads were then washed 3 times with 1m cold 1X PBS buffer. The bound protein was then denatured by addition of 30 μl 2X protein sample buffer and boiling at 95 °C for 5 min. Ten μl of the sample was analyzed in Western blots with anti-Nus tag Ab as above.

RESULTS

Cloning and expression of Nus-*pro-fs* and Nus proteins. For the purpose of producing soluble pro-fs protein in bacteria, we inserted the *pro-fs* gene in vector pET43.1b (Fig. 2.1). The fusion

protein produced from this construct, Nus-*pro-fs*, therefore has Nus·Tag at the N-terminus and pro-fs at the C-terminus. His·Tag was located between these two domains for purification purposes. To purify the proteins using HPLC, Nus-*pro-fs* and Nus were expressed in bacteria by isopropyl-beta-D-thiogalactopyranoside (IPTG) induction. The time course aliquots of Nus-*pro-fs* and Nus expression were analyzed in 10% Tris-HCl SDS-PAGE gel (Bio-Rad). The protein was expressed in native form when induced at 30 °C (Fig. 2.2).

There were two successive peak fractions from HPLC purification (Fig. 2.3, panel A) containing Nus-*pro-fs* protein, as shown by Western blot analysis using Nus·Tag Ab (Fig. 2.3, panel C). One of the two peaks eluted on the HPLC chromatograph when the proportion of buffer B reached 16.1%, the other eluted when buffer B reached 23.9%. The first fraction of Nus-*pro-fs* had about 70% homogeneity and the second had about 90% or more homogeneity. The high purity of the protein allowed us to examine the interaction between *pro-fs* and Trx in vitro. There was one peak from HPLC purification that contained Nus protein as shown by Western blot analysis using Nus·Tag Ab (Fig. 2.3, panel C). This peak eluted when buffer B reached 31% (Fig. 2.3, panel B).

Co-immunoprecipitation of *pro-fs* and Trx demonstrated the interaction between the two proteins. Based upon the sequence similarity between *pro-fs* and the DNA binding loop of NF-κB, we hypothesize that *pro-fs* interacts with Trx. To assess this interaction in vitro, fusion protein Nus-*pro-fs* was co-immunoprecipated with human Trx protein using anti-Trx Ab via incubation with Protein A magnetic beads. Western blots of the elution products showed that Nus-*pro-fs* was not detected from incubation with beads and anti-Trx in the absence of Trx, and no Nus protein band was detected from incubation with Trx and anti-Trx. Only the combined Trx

+ Nus-*pro-fs* gave a strong positive band (Fig. 2.4), showing that Nus-*pro-fs* bound to the beads only in the presence of Trx, and that the pro-fs domain was required for that binding (Fig. 2.4).

***Pro-fs* binds to Trx-wt with a stronger affinity than to Trx-CS.** We then examined if the two Cys residues in the active center of Trx are essential for the interaction between Trx and *pro-fs*, by comparing interactions between Trx-wt + *pro-fs* and Trx-CS + *pro-fs*. When Nus-*pro-fs* was incubated with GSH beads alone, Nus-*pro-fs* was not detected on the Western blot (Fig. 2.5, lane 1), indicating that there is no unspecific binding of Nus-*pro-fs* to the GSH beads. Nus-*pro-fs* was detected in a Western blot with anti-Nus tag Ab from incubation with either GST-Trx-wt or GST-Trx-CS (Fig. 2.5, lane 2 and 3). However, a stronger signal of Nus-*pro-fs* was shown when the protein was incubated with GST-Trx-wt than with GST-Trx-CS. The control protein Nus was not detected in the Western blot from incubation with either GST-Trx-wt or GST-Trx-CS fusion proteins (Fig. 2.5, lane 4 and 5). This result concurred with that of co-immunoprecipitation as shown in Fig. 2.4.

DISCUSSION

The double Cys mutant of *pro-fs*, in which the two UGA codons were mutated to Cys, was successfully expressed in *E. coli* and purified as a soluble protein (Fig. 2.2 and Fig. 2.3 A and C). Since the amino acid Sec residue is a Se homologue of Cys, which has an S in the position of the Se, we assume the mutation does not alter the binding specificity of *pro-fs* to other proteins.

In this study, we demonstrate that the putative HIV-1 encoded peptide, *pro-fs*, is a target of the cellular antioxidative protein Trx. Both co-immunoprecipitation and GST-pull down results consistently show that *pro-fs* binds to human Trx in vitro (Fig. 2.4 and 2.5); and the binding affinity is apparently stronger with Trx-wt than with Trx-CS, in which the two Cys residues in the active center of Trx are mutated to Ser (Fig. 2.5). The fact that *pro-fs* interacts with Trx-CS rules out the possibility that the interaction between *pro-fs* and Trx is just due to cross-linkage via formation of an intermolecular disulfide bond between the Cys residues of *pro-fs* and the Cys residues in the active site of Trx. These results suggest that Trx-*pro-fs* binding is a structurally specific interaction that involves multiple amino acid residues in the interactive region. These results are consistent with the modeling results of Taylor et al. (unpublished data), which demonstrates that Trx binds *pro-fs* with a more favorable energy compared to Trx binding to its known ligand, the DNA binding loop of NF-κB, and that at least 8 amino acid residues are involved in the protein-protein interaction.

Trx participates in redox regulation in the cell by reversible oxidation of the free dithiol to an intramolecular disulfide bond between the two active center Cys residues. The reduction reaction of the Cys residues is known to be catalyzed only by the selenoprotein TR [46]. Mammalian TR has two redox active centers. The N-terminal center, conserved in bacteria, as well as *C. elegans* and mammals, is formed by two Cys residues. The one in the C-terminus is found only in TR expressed in mammals and *C. elegans*, and is formed by a conserved Sec residue and a conserved Cys residue. This Sec is required for catalytic activity of mammalian TR, whose activity is therefore tightly regulated by dietary Se status [47, 48]. Since there are two in-frame UGA codons in the *pro-fs* sequence, *pro-fs* can possibly incorporate one or two Sec residues, depending on the availability of Se. The direct and structural specific interaction

between Trx and *pro-fs* may enable *pro-fs* to store up and deliver the necessary reducing equivalents to Trx in the midst of the oxidizing environments. Thus, *pro-fs* may be a candidate to possess activity similar to the cellular enzyme TR to catalyze the reduction reaction of Trx, which in turn regulates the activation of NF-κB. Another important role of Trx is that it acts as a hydrogen donor for ribonucleotide reductase that is essential for DNA synthesis [46], thus, Trx is required by retroviruses for formation of their proviral DNA. By associating with and possibly reducing Trx, *pro-fs* might make contribution to viral DNA synthesis.

Viral replication is important for disease progression in AIDS patients throughout the latent stage [49, 50]. Not only does HIV employ the cellular transcriptional machinery, including various cellular transcriptional activators, such as NF-κB and activator protein-1 (AP-1), to produce new viruses, but also many HIV-encoded proteins directly participate and play major roles in the process of the viral reproduction. HIV tat protein is a well-known *trans*-activator that activates the transcription of LTR through a RNA dependent mechanism [51] and it was demonstrated that HIV-1 tat protein potentiates TNF-induced HIV-1 replication through activation of NF-κB by altering the cellular redox state [52]. The role of HIV-1 nef protein in regulating HIV transcription is controversial. It was initially thought that nef is a transcriptional repressor of HIV-1 LTR [53], but a recent report demonstrated that exogenous nef protein activates NF-κB and AP-1 and stimulates HIV-1 transcription in promonocytic cells [54]. Given the complexity of activation of HIV-1 transcription, it is reasonable for viruses to try to encode homologues of regulatory proteins involved in this process. Since *pro-fs* has high sequence similarity to the DNA binding loop of NF-κB, with a Se instead of S in the RHD, and has a computed pI of 11 (suggesting that it may be a nuclear protein), it is possible that *pro-fs* can bind to the HIV LTR in cell nucleus to activate HIV-1 replication. Because Trx is recognized as a

reducing agent of NF-κB by direct interaction, and modulates the DNA binding activity of NF-κB by dithiol-disulfide exchange reaction [32, 38], we argue that the structural specificity between Trx and *pro-fs* indicates that Trx may serves as a reducing agent to *pro-fs*. Taken together with experiments demonstrating that *pro-fs* is a potent activator of HIV-1 LTR and functions via NF-κB in a HIV-1 LTRlacZ reporter system (Taylor, et al., unpublished data), our results suggest that *pro-fs* may function as a mimic of NF-κB in activation of HIV-1 transcription. The existence of this protein might provide a way for virus to survive the battle against host antioxidative defense system and continue to replicate. Since NF-κB regulates hundreds of genes involved in host immune responses including cytokines, adhesion molecules and genes regulating apoptosis, as a mimic of NF-κB, it is possible for *pro-fs* to bind to other κB sites located in host DNA to activate cellular genes, enabling HIV to directly manipulate host cellular defenses.

AP-1 is a cellular transcription factor that regulates HIV transcription by binding to HIV LTR [55] [54]. It is a redox-responsive transcription factor, and was activated by transient expression of Trx in HeLa cells [56, 57]. It was shown that in HeLa and COS-7 cells, AP-1 is under redox regulation by Trx via redox factor 1 (Ref-1) [58], a DNA repair enzyme that restores AP-1-DNA binding activity [59, 60]. Hirota et al. showed that a direct active site-mediated association between Ref-1 and Trx is necessary for the redox regulation of AP-1 activation [58]. Thus, by directly interacting with Trx, *pro-fs* could possibly play a role in the redox regulation of AP-1 activated HIV-1 replication.

The involvement of Trx in HIV infection is not limited to that was described above. Trx plays a key role in inhibiting apoptosis of HIV-infected cells while simultaneously inducing apoptosis of bystander cells via upregulation of FasL. This mechanism requires the direct

association of Trx with the N-terminal portion of apoptosis signaling kinase 1 (ASK1), a key component of TNF-α-induced apoptosis [61]. By inhibiting ASK1 activity, Trx suppresses the subsequent ASK1-dependent apoptosis [33, 61]. Mutagenesis studies showed that the presence of at least one of the two conserved Cys residues in the redox center is required for Trx to inhibit ASK1-dependent apoptosis [33]. There is evidence indicates that HIV-1 nef protein participates in this process by preventing disassociation of Trx and ASK1 in HIV infected cells [62]. Thus, based on the interaction between Trx and *pro-fs*, there is a good chance that HIV-1 encoded *pro-fs* would also participate in the regulation of apoptosis process in infected cells.

The redox regulation in host cells is complicated. The role of reactive oxygen species and oxidative stress in HIV pathogenesis has received considerable attention in recent years due to their roles in inducing activation of HIV transcription. NF-κB plays a key role in regulating HIV-1 replication and was the first transcription factor found to response to oxidative stress mediated by prooxidants and pathogenic stimuli [26-29]. Conversely, this activation can be inhibited by antioxidants, including glutathione, N-acetyl-L-cysteine (NAC), and the cellular selenoprotein GPx [63-65]. It has been reported that low dose of Se supplementation can suppress NF-κB activation in response to TNF-α and H_2O_2 in vitro, via increased production of GPx [12]. It seems reasonable for the viruses to directly intervene in the biochemical pathways in host redox regulation to protect themselves against cellular antioxidative defense by encoding viral selenoproteins. Through this mechanism, virus can hijack the Se in host and cause a decline of cellular selenoprotein production. *Molluscum contagiosum*, a poxvirus that causes persistent skin neoplasms in children and acquired immunodeficiency syndrome (AIDS) patients, encodes a functional GPx enzyme [66, 67]. It was shown to protect human keratinocytes against cytotoxic effects of ultraviolet irradiation and hydrogen peroxide, which provides a mechanism for a virus

to defend itself against environmental stress [67]. It was reported that HIV-1 encodes a highly truncated GPx enzyme [39] that showed measurable GPx activity [68]. Thus, it is not unprecedented that HIV-1 would encode a selenoprotein to help escape from host antioxidant defense.

We should point out that, at this stage, *pro-fs* is still a hypothetical protein. *Pro-fs* is encoded in the overlapping –1 reading frame in HIV-1 protease-coding region. Ribosomal frameshifting is an inefficient process, which only happens by 1-10% of the time during transcription [39]. As part of the pol gene, HIV-1 protease is also encoded via a –1 frameshift from the gag coding region, thus, the chance for *pro-fs* to be expressed is about 1% or less than structural proteins. The low abundance of *pro-fs* might account for the fact that *pro-fs* has not been detected in HIV-infected cells. The other reason might be because *Pro-fs* has a low molecular weight of approximately either 7.2 or 8.3 kDa, depending on whether one or both in-frame UGA codons are decoded as Sec. However, it is noteworthy to point out that in a study of the effect of HIV-infection on selenoprotein expression in ^{75}Se-labeled human Jurkat T cells, low molecular mass Se-labeled compounds in HIV-infected cells were detected (Fig. 2.1 B in [69]). The position of this wide band partially overlaps the 6 kDa marker, and is thus in the correct size range to correspond to predicted isoforms of *pro-fs*. The GST-pull down assay used in this study provides a means to assess the expression of HIV-1 encoded *pro-fs*. It should not be very difficult to determine the existence of *pro-fs* by applying GST-pull down assay to the lysate of HIV-infected cells labeled with ^{75}Se and subsequent 2-D gel electrophoresis.

In conclusion, our results showed that a novel HIV-1 encoded peptide, *pro-fs*, is a mimic of NF-κB. It binds human Trx with high affinity in vitro, and the interaction is structurally

specific. A better understanding of the outcome of this interaction in HIV infection and disease progression is necessary due to the complexity of factors involved.

ACKNOWLEDGEMENTS

This work was supported by PHS Grant DA13561 from National Institute of Drug Abuse (NIDA).

REFERENCES

1. Sunde, R.A., *Selenium*, in *Handbook of Nutritionally Essential Minerals*, B.L. O'Dell and R.A. Sunde, Editors. 1997, Marcel Dekker: New York. p. 493-556.
2. Allavena, C., et al., *Relationship of trace-element, immunological markers, and HIV infection progression.* Biol. Trace Elem. Res., 1995. **47**(133-138).
3. Beck, M.A., et al., *Rapid genomic evolution of a non-virulent coxsackievirus B3 in selenium-deficient mice results in selection of identical virulent isolates.* Nature Medicine, 1995. **1**(5): p. 433-436.
4. Baum, M.K., et al., *High risk of HIV-related mortality is associated with selenium deficiency.* J Acquir Immune Defic Syndr Hum Retrovirol, 1997. **15**: p. 370-376.
5. Constans, J., et al., *Serum selenium predicts outcome in HIV infection.* J. Acquir. Immune. Defic. Syndr. Hum. Retrovirol., 1995. **10**(3): p. 392.
6. Dworkin, B.M., *Selenium deficiency in HIV infection and the acquired immunodeficiency syndrome (AIDS).* Chem. Biol. Interact., 1994. **91**: p. 181-186.

7. Yu, S.Y., Y.J. Zhu, and W.G. Li, *Protective role of selenium against hepatitis B virus and primary liver cancer in Qidong.* Biological Trace Element Research, 1997. **56**(1): p. 117-124.

8. Yu, M.W., et al., *Plasma selenium levels and risk of hepatocellular carcinoma among men with chronic hepatitis virus infection.* American Journal Of Epidemiology, 1999. **150**(4): p. 367-374.

9. Sappey, C., et al., *Stimulation of glutathione peroxidase activity decreases HIV type 1 activation after oxidative stress.* AIDS. Res. Hum. Retroviruses., 1994. **10**(11): p. 1451-1461.

10. Brigelius-Flohe, R., et al., *Interleukin-1-induced nuclear factor kappa B activation is inhibited by overexpression of phospholipid hydroperoxide glutathione peroxidase in a human endothelial cell line.* Biochemical Journal, 1997. **328**: p. 199-203.

11. Hori, L., et al., *Selenium supplementation suppresses tumor necrosis factor α-induced human immunodeficiency virus type 1 replication in vitro.* AIDS Research And Human Retroviruses, 1997. **13**: p. 1325-1332.

12. Makropoulos, V., T. Brüning, and K. Schulze-Osthoff, *Selenium-mediated inhibition of transcription factor NF kappa B and HIV-1 LTR promoter activity.* Archives of Toxicology, 1996. **70**(5): p. 277 - 283.

13. Antoni, B.A., S.B. Stein, and A.B. Rabson, *Regulation of human immunodeficiency virus infection: implications for pathogenesis.* Adv Virus Res, 1994. **43**: p. 53-145.

14. Baeuerle, P. and D. Baltimore, *A 65-kappaD subunit of active NF-kappaB is required for inhibition of NF-kappaB by I kappaB.* Genes Dev., 1989. **3**(11): p. 1689-1698.

15. Bednarik, D.P. and T.M. Folks, *Mechanisms of HIV-1 latency.* AIDS, 1992. **6**(1): p. 3-16.

16. Doerre, S., et al., *The c-rel Protooncogene Product Represses NF-{kappa}B p65-Mediated Transcriptional Activation of the Long Terminal Repeat of Type 1 Human Immunodeficiency Virus.* PNAS, 1993. **90**(3): p. 1023-1027.

17. Kawakami, K., C. Scheidereit, and R.G. Roeder, *Identification and purification of a human immunoglobulin-enhancer-binding protein (NF-kappa B) that activates transcription from a human immunodeficiency virus type 1 promoter in vitro.* PNAS, 1988. **85**(13): p. 4700-4704.

18. Rabson, A.B. and H.-C. Lin, *NF-κB and HIV: Linking Viral and Immune Activation*, in *HIV-1: Molecular Biology and Pathogenesis - Viral Mechanisms*, K.-T. Jeang, Editor. 2000, Academic Press. p. 161-207.

19. Baldwin, A.S., *THE NF-κB AND IκB PROTEINS: New Discoveries and Insights.* Annual Review of Immunology, 1996. **14**(1): p. 649-681.

20. Baeuerle, P.A. and D. Baltimore, *NF-κB: Ten Years After.* Cell, 1996. **87**(1): p. 13-20.

21. Biswas, G., et al., *Mitochondria to nucleus stress signaling: a distinctive mechanism of NF{kappa}B/Rel activation through calcineurin-mediated inactivation of I{kappa}B{beta}.* J. Cell Biol., 2003. **161**(3): p. 507-519.

22. Siebenlist, U., G. Fransozo, and K. Brown, *Structure, regulation and function of NF-κB.* Annu. Rev. Cell Biol., 1994. **10**: p. 405-430.

23. Stancovski, I. and D. Baltimore, *NF-κB Activation: The IκB Kinase Revealed?* Cell, 1997. **91**: p. 299-302.

24. Tian, B. and A.R. Brasier, *Identification of a Nuclear Factor Kappa B-dependent Gene Network.* Recent Prog Horm Res, 2003. **58**(1): p. 95-130.

25. Waris, G., et al., *Hepatitis °C virus NS5A and subgeomic replicons activate NF-kB via tyrosine phosphorylation of IkBa and its degradation by calpain protease.* J. Biol. Chem., 2003: p. M303248200.

26. Griffin, G.E., et al., *Activation of HIV gene expression during monocyte differentiation by induction of NF-kappa B.* Nature, 1989. **339**(6219): p. 70-73.

27. Schreck, R., P. Rieber, and P.A. Baeuerle, *Reactive oxygen intermediates as apparently widely used messengers in the activation of the NF-kappa B transcription factor and HIV-1.* The EMBO Journal, 1991. **10**(8): p. 2247-2258.

28. Schreck, R., K. Albermann, and P. Bauerle, *Nuclear factor κB: An oxidative stress-response transcription factor of eukaryotic cells.* Free Rad. Res. Comm., 1992. **17**: p. 221-237.

29. Schulze-Osthoff, K., et al., *Depletion of the mitochondrial electron transport abrogates the cytotoxic and gene-inductive effects of TNF.* EMBO J., 1993. **12**(8): p. 3095-3104.

30. Kim, I.Y. and T.C. Stadtman, *Inhibition of NF-kappaB DNa binding and nitric oxide induction in human T cells and lung adenocarcinoma cellsby selenite treatment.* Proc Natl Acad Sci, 1997. **94**: p. 12904-12907.

31. Mitomo, K., et al., *Two different cellular redox systems regulate the DNA-binding activity of the p50 subunit of NF-kappa B in vitro.* Gene, 1994. **145**: p. 197-203.

32. Hirota, K., et al., *Distinct Roles of Thioredoxin in the Cytoplasm and in the Nucleus. A TWO-STEP MECHANISM OF REDOX REGULATION OF TRANSCRIPTION FACTOR NF-kappa B.* J. Biol. Chem., 1999. **274**(39): p. 27891-27897.

33. Liu, Y. and W. Min, *Thioredoxin Promotes ASK1 Ubiquitination and Degradation to Inhibit ASK1-Mediated Apoptosis in a Redox Activity-Independent Manner.* Circ Res, 2002. **90**(12): p. 1259-1266.

34. Tanaka, T., et al., *Redox regulation by thioredoxin superfamily; protection against oxidative stress and aging.* Free Radic Res, 2000. **33**(6): p. 851-855.

35. Arner, E.S.J. and A. Holmgren, *Physiological functions of thioredoxin and thioredoxin reductase.* Eur J Biochem, 2000. **267**(20): p. 6102-6109.

36. Powis, G., D. Mustacich, and A. Coon, *The role of the redox protein thioredoxin in cell growth and cancer.* Free Radic Biol Med, 2000. **29**(3-4): p. 312-322.

37. Matthews, J.R., et al., *Thioredoxin regulates the DNA binding activity of NF-κB by reduction of a disulphide bond involving cysteine 62.* Nucleic Acids Research, 1992. **20**(15): p. 3821-3830.

38. Qin, J., et al., *Solution structure of human thioredoxin in a mixed disulfide intermediate complex with its target peptide from the transcription factor NF-κB.* Structure, 1995. **3**: p. 289-297.

39. Taylor, E.W., et al., *A Basis for New Approaches to the Chemotherapy of AIDS: Novel Genes in HIV-1 Potentially Encode Selenoproteins Expressed by Ribosomal Frameshifting and Termination Suppression.* J. Med. Chem., 1994. **37**: p. 2637-2654.

40. Taylor, E.W., R.G. Nadimpalli, and C.S. Ramanathan, *Genomic structures of viral agents in relation to the biosynthesis of selenoproteins.* Biol. Trace. Elem. Res., 1997. **56**: p. 63-91.

41. Berry, M.J., et al., *Functional characterization of the eukaryotic SECIS elements which direct selenocysteine insertion at UGA codons.* EMBO J., 1993. **12**: p. 3315-3322.

42. Bock, A., et al., *Selenocysteine: the 21st amino acid.* Mol. Microbiol., 1991. **5**: p. 515-520.

43. Shen, Q., F.F. Chu, and P.E. Newburger, *Sequences in the 3'-untranslated region of the human cellular glutathione peroxidase gene are necessary and sufficient for selenocysteine incorporation at the UGA codon.* J. Biol. Chem., 1993. **268**: p. 11463-11469.

44. Taylor, E.W., et al., *HIV-1 encodes a sequence overlapping env gp41 with highly significant similarity to selenium-dependent glutathione peroxidases.* J. Acquir. Immune. Defic. Syndr. Hum. Retrovirol., 1997. **15**(5): p. 393-394.

45. Taylor, E.W., et al., *Nutrition, HIV, and drug abuse: the molecular basis of a unique role for selenium.* J Acquir Immune Defic Syndr, 2000. **25 Suppl 1**: p. S53-61.

46. Bjornstedt, M., et al., *Selenium and the thioredoxin and glutaredoxin systems.* Biomed Environ Sci, 1997. **10**((2-3)): p. 271-279.

47. Gallegos, A., et al., *Mechanisms of the regulation of thioredoxin reductase activity in cancer cells by the chemopreventive agent selenium.* Cancer Res, 1997. **57**(21): p. 4965-4970.

48. Hadley, K.B. and R.A. Sunde, *Selenium regulation of thioredoxin reductase activity and mRNA levels in rat liver.* The Journal of Nutritional Biochemistry, 2001. **12**(12): p. 693-702.

49. Embretson, J., et al., *Massive covert infection of helper T lymphocytes and macrophages by HIV during the incubation period of AIDS.* Nature, 1993. **362**(6418): p. 359-62.

50. Pantaleo, G., et al., *HIV infection is active and progressive in lymphoid tissue during the clinically latent stage of disease.* Nature, 1993. **362**(6418): p. 355-358.

51. Gentz, R., C.H. Chen, and C.A. Rosen, *Bioassay for trans-activation using purified human immunodeficiency virus tat-encoded protein: trans-activation requires mRNA synthesis.* PNAS, 1989. **86**(3): p. 821-824.

52. Westendorp, M.O., et al., *HIV-1 Tat potentiates TNF-induced NF-kappa B activation and cytotoxicity by altering the cellular redox state.* EMBO J., 1995. **14**(3): p. 546-554.

53. Ahmad, N. and S. Venkatesan, *Nef protein of HIV-1 is a transcriptional repressor of HIV-1 LTR.* Science, 1988. **241**(4872): p. 1481-1485.

54. Varin, A., et al., *Exogenous Nef Protein Activates NF-kappa B, AP-1, and c-Jun N-Terminal Kinase and Stimulates HIV Transcription in Promonocytic Cells. ROLE IN AIDS PATHOGENESIS.* J. Biol. Chem., 2003. **278**(4): p. 2219-2227.

55. Li, Y., G. Mak, and B. Franza, Jr, *In vitro study of functional involvement of Sp1, NF-kappa B/Rel, and AP1 in phorbol 12-myristate 13-acetate-mediated HIV-1 long terminal repeat activation.* J. Biol. Chem., 1994. **269**(48): p. 30616-30619.

56. Meyer, M., R. Schreck, and P. Baeuerle, *H2O2 and antioxidants have opposite effects on activation of NF-kappa B and AP-1 in intact cells: AP-1 as secondary antioxidant-responsive factor.* EMBO J., 1993. **12**(5): p. 2005-2015.

57. Schenk, H., et al., *Distinct Effects of Thioredoxin and Antioxidants on the Activation of Transcription Factors NF-{kappa}B and AP-1.* PNAS, 1994. **91**(5): p. 1672-1676.

58. Hirota, K., et al., *AP-1 transcriptional activity is regulated by a direct association between thioredoxin and Ref-1.* PNAS, 1997. **94**(8): p. 3633-3638.

59. Xanthoudakis, S. and T. Curran, *Identification and characterization of Ref-1, a nuclear protein that facilitates AP-1 DNA-binding activity.* EMBO J., 1992. **11**(2): p. 653-665.

60. Xanthoudakis, S., et al., *Redox activation of Fos-Jun DNA binding activity is mediated by a DNA repair enzyme.* EMBO J., 1992. **11**(9): p. 3323-3335.

61. Saitoh, M., et al., *Mammalian thioredoxin is a direct inhibitor of apoptosis signal-regulating kinase (ASK) 1* . EMBO J., 1998. **17**(9): p. 2596-2606.

62. Geleziunas, R., et al., *HIV-1 Nef inhibits ASK1-dependent death signalling providing a potential mechanism for protecting the infected host cell.* Nature, 2001. **412**(6830): p. 834-838.

63. Beg, A., et al., *Tumor necrosis factor and interleukin-1 lead to phosphorylation and loss of I kappa B alpha: a mechanism for NF-kappa B activation.* Mol. Cell. Biol., 1993. **13**(6): p. 3301-3310.

64. Henkel, T., et al., *Rapid proteolysis of I kappa B-alpha is necessary for activation of transcription factor NF-kappa B.* Nature, 1993. **365**(6442): p. 182-185.

65. Kretz-Remy, C., et al., *Inhibition of I kappa B-alpha phosphorylation and degradation and subsequent NF-kappa B activation by glutathione peroxidase overexpression.* J. Cell Biol., 1996. **133**(5): p. 1083-1093.

66. Senkevich, T.G., et al., *Genome sequence of a human tumorigenic poxvirus: prediction of specific host response-evasion genes.* Science, 1996. **273**(5276): p. 813-816.

67. Shisler, J.L., et al., *Ultraviolet-induced cell death blocked by a selenoprotein from a human dermatotropic poxvirus.* Science, 1998. **279**(5347): p. 102-105.

68. Zhao, L., et al., *Molecular modeling and in vitro activity of an HIV-1-encoded glutathione peroxidase.* Proc. Natl. Acad. Sci. U.S.A., 2000. **97**(12): p. 6356-6361.

69. Gladyshev, V.N., et al., *Levels of major selenoproteins in T cells decrease during HIV infection and low molecular mass selenium compounds increase.* PNAS, 1999. **96**(3): p. 835-839.

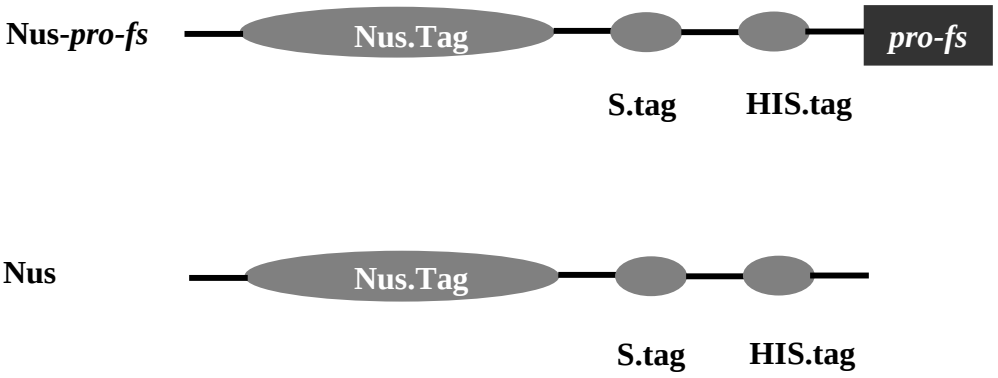

Figure 2.1. Schematic structures of Nus-*pro-fs* and Nus proteins. *Pro-fs* was fused to the C-terminus of Nus·Tag as Nus-*pro-fs*. The vector alone expressed in *Escherichia coli* BL21 (DE3), Nus protein, was used as negative control through out the studies. His·Tag in the fusion protein binds to HiTrap metal chelating column loaded with Ni_2SO_4 to enable purification using HPLC.

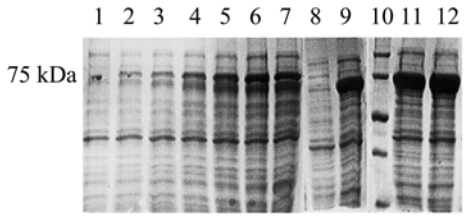

Figure 2.2. SDS-PAGE analysis of the expression of Nus-*pro-fs* and Nus proteins in *Escherichia coli* (*E. coli*) BL21 (DE3). Aliquots of cells were taken at 0, 2, 4, 6, 8, 16, 24 h post-induction and supernatants of cell lysates were analyzed using SDS-PAGE to detect the production of Nus-*pro-fs* (lane 1 to 7), and at 0, 4, 8, 16 h for Nus (Lane 8, 9, 11, 12). Lane 10 was loaded with Precision Plus Protein Standard (Bio-Rad). Nus-*pro-fs* was successfully expressed in *E. coli* with a molecular weight of 75 kDa and Nus of approximately 65 kDa.

A

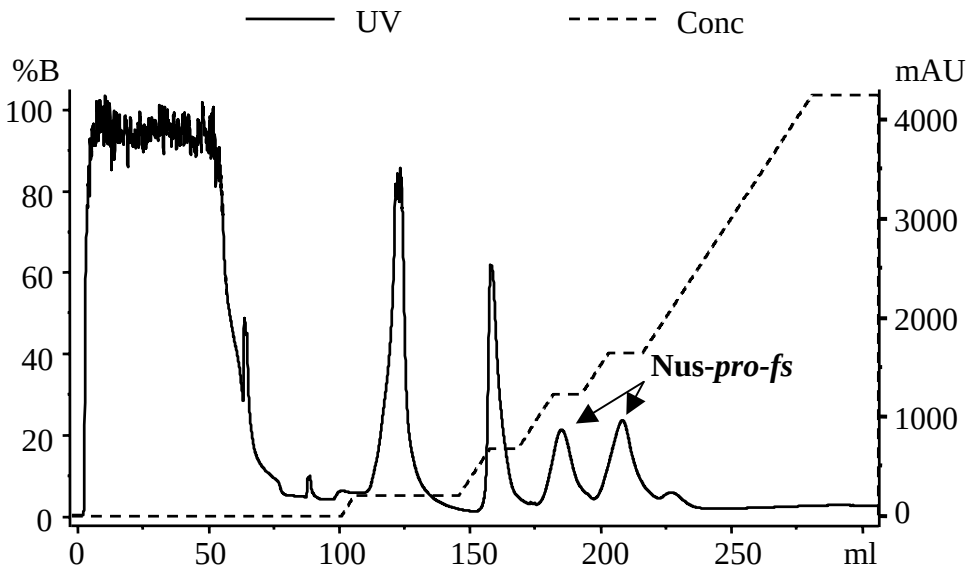
UV
Conc
%B
mAU
100
80
60
40
20
0
4000
3000
2000
1000
0
0
50
100
150
200
250
ml
Nus-*pro-fs*

B

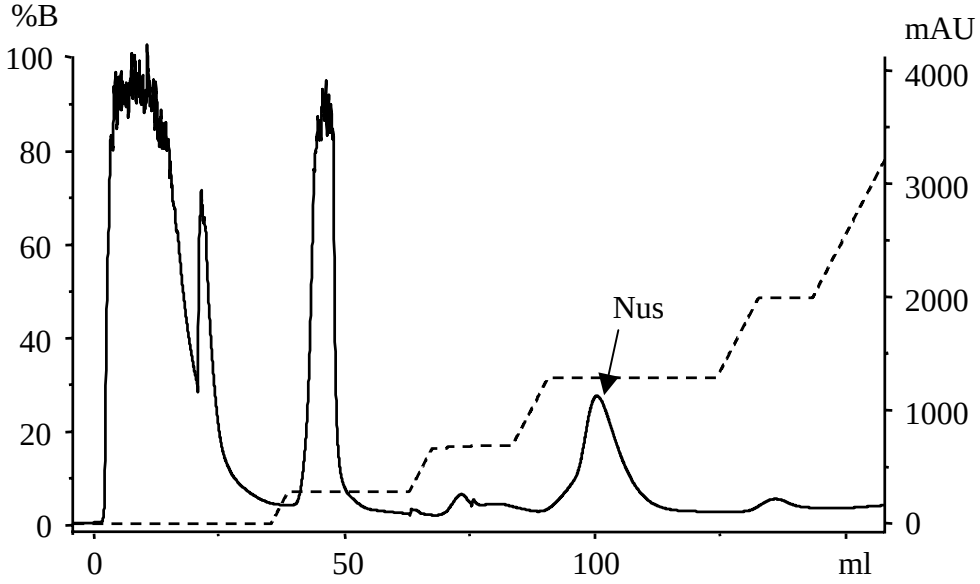
%B
mAU
100
80
60
40
20
0
4000
3000
2000
1000
0
0
50
100
ml
Nus

C

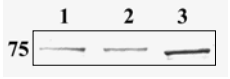
1
2
3
75

Figure 2.3. HPLC chromatographs of the purification of Nus-*pro-fs* and Nus proteins expressed in *Escherichia coli* BL21 (DE3) and Western blot analysis. (A) Column separation of whole cell lysate of bacteria expressing Nus-*pro-fs*. There are two peaks containing Nus-*pro-fs* as shown on the HPLC chromatograph when the proportion of buffer B reached 16.1% and 23.9%. The first fraction of Nus-*pro-fs* had about 70% homogeneity and the second had about 90% or more homogeneity. (B) Column separation of whole cell lysate for bacteria expressing Nus protein. Nus protein was eluted from the column when buffer B reached 31% and had more than 90% homogeneity. (C) Western blot of Nus-*pro-fs* and Nus proteins using Nus.tag antibody (Novagen). Lane C1 shows the first HPLC peak of Nus-*pro-fs* protein, lane C2 the second HPLC peak of Nus-*pro-fs*, lane C3 the HPLC peak of Nus protein. Due to the *pro-fs* domain inserted in the vector, Nus-*pro-fs* protein has a larger molecular weight than Nus protein.

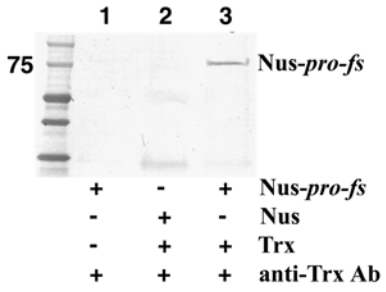

Figure 2.4. Co-immunoprecipitation of Nus-*pro-fs* and human thioredoxin (Trx)**.** Three μg of Nus-*pro-fs* and 5.5 μg of rabbit polyclonal anti-Trx were mixed without (lane 1) or with (lane 3) 2 μg of human Trx and incubated overnight at 4 °C. The mixture was then added to protein A magnetic beads to incubate for 1 h at 4 °C. Similarly expressed and purified Nus protein was used to incubate with Trx and Trx Ab by the same procedure, as a negative control (lane 2). After washing, eluting and Western blotting with mouse anti-Nus monoclonal Ab, only combined Trx + Nus-*pro-fs* gave a strong positive band (lane 3), showing that Nus-*pro-fs* bound to the beads only in the presence of Trx, and that the *pro-fs* domain was required for that binding, as Nus alone did not bind.

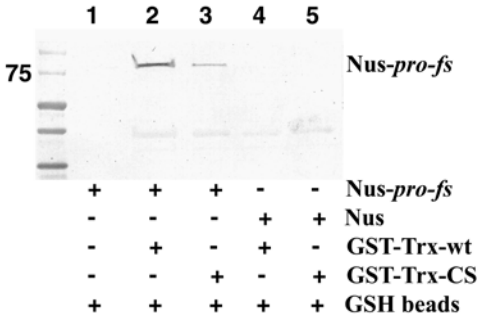

Figure 2.5. GST-pull down assay of *pro-fs*. Three μg of Nus-*pro-fs* were added to 50 μl of glutathione-Sepharose beads alone (lane 1) or beads bound with wild-type GST-Trx fusion protein (GST-Trx-wt, lane 2) or a mutant GST-Trx fusion protein (GST-Trx-CS, lane 3), in which Trx residues Cys32 and Cys35 were mutated to Ser. Three μg of Nus protein was added to GST-Trx-wt (lane 4) or GST-Trx-CS (lane 5) as negative controls. After overnight incubation at 4^{o}C, the beads were separated by centrifugation and washing (3x). The bound protein was denatured with 2X protein sample buffer, and then subjected to Western blotting with anti-Nus tag Ab as above. Nus-*pro-fs* but not Nus alone was detected in the Western blot. The stronger band in lane 2 as compared to lane 3 suggests that *pro-fs* binds Trx-wt with higher affinity than to Trx-CS.

CHAPTER 3

OLIGOMERIZATION OF A NOVEL HIV-1 ENCODED PEPTIDE VISUALIZED USING FLUORESCENCE RESONANCE ENERGY TRANSFER IN LIVING CELLS[1]

[1] Su, G. and E. W. Taylor. To be submitted to Current Biology.

ABSTRACT

A novel HIV-1 gene encoded in the overlapping –1 frameshift in the protease coding region, named *pro-fs*, has been previously demonstrated. It was shown to have significant sequence similarity to the DNA binding loop of NF-κB. Due to the nature of the –1 frameshift mechanism, the first 20 residues in N-terminal domain of *pro-fs* are identical to that in the HIV-1 protease protein. Since both the retroviral protease and NF-κB function as dimers, it is possible that *pro-fs* may also form dimers. Due to its high pI and mimicry of NF-κB, we also hypothesize that *pro-fs* localizes in the cell nucleus. Fluorescence microscopy was used to visualize the subcellular localization of *pro-fs*, and the results showed that *pro-fs* is a nuclear protein. To investigate the dimerization of *pro-fs* in living cells, we used the acceptor photobleaching method to measure fluorescence resonance energy transfer (FRET) using *pro-fs* fused to cyan fluorescent protein (CFP) and yellow fluorescent protein (YFP). Efficient energy transfer between CFP and YFP should only occur if CFP and YFP are less than 100 Å apart, which requires direct interaction of the *pro-fs* monomers fused to these fluorescent moieties. Significant FRET efficiency was detected in the nuclei of cells co-expressing CFP-*pro-fs* and YFP-*pro-fs*, indicating that *pro-fs* forms oligomers. Similar FRET results were obtained using scanning fluorometry, confirming the oligomerization of *pro-fs* in living cells.

Keywords: HIV-1; Protease; Framshift; Pro-fs; NF kappa B; FRET; CFP; YFP; Oligomerization; Scanning fluorometry.

INTRODUCTION

Previously, Taylor et al. predicted the existence of several HIV-1 encoded selenoprotein modules based on theoretical evidence [1]. One of these was an *env* variant associated with a predicted –1 frameshift site; this was named *env-fs* and later identified as a functional virally-encoded homologue of mammalian selenoprotein glutathione peroxidase [2, 3]. A second predicted HIV-1 selenoprotein, potentially expressed by a –1 frameshift from the protease coding region [1], was later named *pro-fs* [4]. The –1 frameshifting happens when the ribosome shifts upstream by one nucleotide during the course of reading the mRNA. As a consequence, the protein product is encoded in two overlapping reading frames. Due to this nature of programmed translational frameshifting, *pro-fs* would first be expressed as a *gag-pol-pro-fs* double frameshift fusion protein. After processing by the viral protease, the first 20 N-terminal residues of *pro-fs* would be identical to the protease sequence. This shared module is fused to a C-terminal domain of 49 residues encoded in the –1 reading frame to form the *pro-fs* protein. The *pro-fs* sequence contains two in-frame UGA codons (Fig. 3.1), which may encode selenocysteine (Sec) or a conventional Cys or both, depending on cellular and viral factors, and conditions such as host selenium status [4, 5]. The amino acid sequence of *pro-fs* is highly conserved in HIV-1 sequences, especially with 100% conserved for its first UGA codon [5].

Based on the protein sequence, the computed pI of *pro-fs* is 11; thus, *pro-fs* was predicted to be a very basic, positively charged protein, which suggests that it may have the ability to bind to nucleic acid [5]. Sequence analysis suggested a match to the nuclear factor kappa B (NF-κB) family of transcription factors, which contains a conserved Cys residue that aligns with the highly conserved UGA codon of *pro-fs* [5]. The frameshift site in HIV-1 protease gene occurs

just upstream of the *pro-fs* sequence (RYRSRU) [5]. The gene alignment suggests that the protease processed form of *pro-fs* could be at the least a minimal NF-κB-like DNA-binding domain. Mammalian cells co-expressing *pro-fs* and HIV long terminal repeat (LTR)-β-gal reporter gene construct showed increased β-gal activity in response to TNF-α treatment, and mutations of the NF-κB binding sites located in HIV LTR abolished the effect (Taylor et al, unpublished data).

Based on these observations, we hypothesize that *pro-fs* may localize in the nucleus. It is also perhaps significant that both retroviral proteases and NF-κB function as dimers. The arrangement of the *pro-fs* gene in HIV-1 suggests that perhaps the protease N-terminal region (the first 20 amino acid residues) functions as a common dimerization motif that can be attached to two different functional domains (protease and *pro-fs*) encoded by the same nucleic acid sequence in two different reading frames. Thus, it was previously suggested that *pro-fs* itself might exist as a dimer [1].

In the present study, we have examined the subcelluar localization of *pro-fs* and used the fluorescent resonance energy transfer (FRET) imaging paradigm to examine *pro-fs* dimerization in cells. We have also attempted to visualize the subcellular localization of fluorescent-tagged *pro-fs* in living cells. *Pro-fs* was made fluorescent by fusion to spectral variants of green fluorescent protein (GFP), specifically yellow (YFP) and cyan fluorescent (CFP) proteins, at the N-terminus of *pro-fs*. We then applied FRET microscopy to directly visualize protein-protein interactions in living cells. FRET between two fluorophores only occurs if they are less than 100 Å apart and in the right orientation, which typically requires direct interaction of tagged proteins. Hence, it is able to provide valuable information about protein/protein interactions and associated conformational changes that may occur [6, 7]. FRET has been used extensively to

study interactions between soluble proteins or a membrane protein and a soluble protein binding partner [8-13]. Various FRET-based techniques have been developed recently to monitor protein-protein interactions, including flow cytometry [14], scanning fluorometry [10, 15] and confocal microscopy [16-20]. The acceptor photobleaching procedure of FRET that we use here [11, 17, 19] is designed not only to visualize the subcelluar localization of the protein, but also to measure the donor fluorescence emission specifically without the contaminating leak-through of the acceptor emission, by comparing the quenched with the unquenched donor emission after specific photobleaching of the acceptor fluorophore [19]. FRET imaging microscopy was used herein to simultaneously visualize the subcellular localization and oligomerization of *pro-fs* in living cells. Our results confirm the oligomerization of *pro-fs* and its nuclear localization in cells.

RESULTS

Subcellular localization of *pro-fs* in cells. To examine the subcellular localization of *pro-fs*, YFP-*pro-fs* was transfected into 293T cells. DNA counterstain with 4,6-diamidino-2-phenylindole (DAPI) nuclear staining (blue fluorescence) was used to distinguish cytoplasmic and nuclear distribution. Live 293T cells expressing YFP-*pro-fs* when visualized under green fluorescent filter showed clearly that YFP-*pro-fs* co-localized with DAPI stain exclusively in the nucleus (Fig. 3.2, left panel). The merged image verifies this strong co-localization. The same results were found in YFP-*pro-fs* transfected MDCK cells (Fig. 3.2, right panel) and HeLa cells (data not shown).

Oligomerization of *pro-fs* in cells detected by confocal microscopy. We employed the FRET technique to study the oligomerization of *pro-fs*. YFP-*pro-fs* and CFP-*pro-fs* were transiently co-transfected into 293T cells. Fig. 3.3 demonstrates typical images observed from the CFP and YFP channels during the acceptor photobleaching procedure, and the resulting FRET image derived using the formula described in Materials and Methods. All colors are artificially assigned. Signals from the YFP channel are presented as yellow, signals from CFP channel as cyan, and signals for FRET are shown in pseudocolor. Numerical values from each channel represent the intensity of the signal, but do not encode color information. However, the color images in Fig. 3.3 A do illustrate the nuclear distribution of the YFP- and CFP-*pro-fs*. Owing to different expression levels of the constructs within cells and inhomogeneities in the thickness of the cells, the FRET intensities vary from cell to cell if one is only taking into account the sensitized acceptor emission. However, we applied acceptor photobleaching method to measure both the quenching of the donor signal and the sensitized acceptor emission to confirm that FRET has occurred.

Since intensity-based FRET analysis is subject to a direct fluorescent contribution from both CFP and YFP, and may suffer from a high level of "false-positive" detection if this is not properly compensated, appropriate controls are necessary for establishing a correct analysis. A CFP-YFP concatemer was used as a positive control, in which the CFP fluorophore and the YFP fluorophore were joined together with a short linker of 9 amino acid residues. Highly efficient energy transfer was expected to occur between the two fluorophores when this construct was expressed in cells. Using the protocol described in Materials and Methods, expression of the CFP-YFP concatemer produced a FRET signal of 27.0% (Fig. 3.3 B). On the other hand, since the generation of FRET requires the presence of both fluorophores, single transfection of one

fluorophore should not produce any FRET signal. Since FRET efficiency decreases as the inverse sixth power of distance, co-expression of unlinked YFP and CFP fluorophores should not generate FRET signal unless they are in direct contact. As negative controls, we used single transfection of only CFP-*pro-fs* or YFP-*pro-fs*, co-transfection of CFP-*pro-fs* and the YFP vector pair, YFP-*pro-fs* and the CFP vector pair; there was no FRET signal detected from any of these four transfections. Thus, there was no energy transfer, with a FRET of less than 1% in all negative controls (Fig. 3.3 B).

Using the same protocol for FRET signal acquisition and analysis, interaction between CFP-*pro-fs* and YFP-*pro-fs* was studied. Co-expression of these two proteins gave a FRET value of 18.2%, which showed no significant difference with the positive control and is significantly higher than all negative controls ($P<0.0001$) (Fig. 3.3 B).

Scanning fluorometry analysis of oligomerization of *pro-fs* in cells. To elucidate the question that detection of FRET in individual cell nuclei may be only due to a small subpopulation of the transfected cells, we employ the scanning fluorometry procedure [10, 15] to measure FRET based on the whole cells population, by exciting the cell suspension at 434 nm, which gives maximum excitation of CFP, and recording emission from 450 – 610 nm (see Materials and Methods). In Fig. 3.4 we present summary data for the fluorescence intensity for all combinations of CFP and YFP constructs. After subtracting cell autofluorescence and normalizing, FRET was detected in cells expressing CFP-YFP concatemer and in cells co-expressing CFP- and YFP-*pro-fs* shown in Fig. 3.4 A, indicated by the decrease in 477 nm emission and increase in 530 nm emission (e.g. sensitized YFP emission). This was not observed when cells were co-transfected with YFP vector and CFP-*pro-fs* or with CFP vector and YFP-

pro-fs. Fig. 3.4 B shows the resulted "Apparent FRET" for cells expressing CFP-YFP concatemer or coexpressing CFP- and YFP-*pro-fs* by subtracting the mean curve of the resulted curves in Fig. 3.4 A for cells co-expressing CFP vector and YFP-*pro-fs* and cells co-expressing YFP vector and CFP-*pro-fs*. This step eliminates any direct emission from CFP and YFP fluorophores upon excitation at 434 nm.

DISCUSSION

By necessity, the protein sequence of *pro-fs* N-terminus upstream of the –1 frameshift site is same as that of the HIV-1 protease N-terminus (Fig. 3.1). In addition, there is significant similarity between *pro-fs* and the DNA binding loop of NF-κB, which is also the peptide interacting with thioredoxin (Trx), with 4.5 standard deviations relative to that expected for random sequences of identical composition [5] (Chapter 2, Fig. 2.0). Since both HIV protease and NF-κB function as dimers, these structural relations between *pro-fs* and these two proteins lead to the speculation that it might also form a dimer [1, 4, 5]. We addressed this question by employing the FRET technique in live cells. The efficiency of FRET is inversely related to the sixth power of the distance between the two fluorophores. For the CFP and YFP pair we used, the critical distance is about 50 Å. Therefore, any significant FRET signal should indicate direct interactions between the tagged-proteins. The FRET efficiency for CFP-*pro-fs* and YFP-*pro-fs* was significantly higher than the negative controls, although significantly lower than the positive control, which is not surprising considering that 100% donor and acceptor pairs co-exist in the CFP-YFP concatemer within a short distance.

The current data highlight the utility of FRET in the examination of intermolecular interactions in living cells. The FRET technique used is an adaptation of a well-established tool used in biophysical studies [6]. However, although the underlying mechanism to detect FRET may be relatively straightforward, the actually data analysis is complicated if only the sensitized acceptor emission is measured. To compensate this problem, our study employed an intensity-based acceptor photobleaching method. It is known that there is a concomitant quenching of the donor fluorescence signal due to the energy transfer from the donor to the acceptor. The selective photobleaching of the acceptor fluorophore abolishes FRET, and there is an enhancement in the donor emission due to dequenching. The photobleaching method detects both the quenching of the donor signal and the sensitized acceptor emission [11, 17, 19].

Across experiments, the amount of the plasmid DNA used in the transfection was controlled to achieve relatively consistent and similar expression levels of the tagged proteins measured by scanning fluorometry, and only cells expressing similar levels of the CFP- and YFP-tagged proteins were selected for FRET detections. To check the sensitivity and selectivity of the protocol for FRET, controls were always run in parallel with our experiment samples. As expected, the positive control, a CFP-YFP concatemer, produced a FRET value significantly larger than that produced by the negative controls. Thus, we continued to apply the same method throughout this study.

For the FRET analysis to be meaningful, the fusion proteins must be correctly assembled and appropriate expressed. Fluorescent and confocal microscopy showed the same nuclear distribution of CFP- and YFP-*pro-fs* in 293T cells, MDCK cells and HeLa cells (Fig. 3.2), indicating that *pro-fs* localizes in the nucleus independent of cell lines. We carefully examined the protein sequence of HIV-1 *pro-fs* and did not find a motif that matches any known nuclear

localization signals. However, in the core of the *pro-fs* sequence spanning the first UGA codon (Fig. 3.2), there is a region containing 8 arginine (R) or lysine (K) residues over a span of 21 amino acids that may function in nuclear localization.

FRET techniques provide a way of studying protein-protein interaction in living cells as a critical test of hypotheses originating from biochemical or other experiments requiring cell disruption. The ability to assign protein-protein interactions to specific compartments of the cell opens the way to more complete understanding of the regulation of the signaling processes. However, great care must be taken to interpret the energy transfer data. Since FRET is sensitive to the distance between the two fluorophores and the dipole orientation, such effects may be so significant that different energy transfer readings could be due to either conformational changes or binding-unbinding, which cannot be distinguished from the FRET data. The true FRET efficiency is determined by the strength of protein-protein interaction and falls off with the inverse sixth power of distance. There are strong FRET signals for both CFP-YFP, and CFP-*pro-fs* and YFP-*pro-fs*, without significant difference between these two transfections (Fig. 3.3 B). In the CFP-YFP concatemer, the CFP and YFP fluorophores are simply linked together by a linker of 9 amino acids and there is no active binding activity between the two molecules. In order for FRET to happen between *pro-fs* molecules, there has to be definite active binding to result in the energy transfer. The fact that there is no significant energy transfer detected in all four negative controls (Fig. 3.3 B) strongly suggests that there is no oligomerization between CFP and YFP, or between CFP or YFP and *pro-fs* domain. Thus, the strong FRET signal detected between CFP-*pro-fs* and YFP-*pro-fs* is due to the active oligomerization of *pro-fs* domain.

In summary, these data demonstrate directly that *pro-fs* localizes in the nucleus of cells, where it forms oligomers. By structural analogy to HIV protease (the shared N-terminal domain),

and functional analogy to NF-κB, it seems most likely that the observed oligomerization is actually a dimer of *pro-fs*. In an independent study, we have also demonstrated that there is a direct interaction between Trx and *pro-fs* (see Chapter 3). Taken together, it will be important to investigate the possibilities that, in addition to modulating Trx activity by direct binding, *pro-fs* may also interact directly with the DNA recognition sites for NF-κB in the viral LTR, or with NF-κB itself, possibly by forming heterodimers, or via a ternary complex including thioredoxin.

MATERIALS AND METHODS

HEK 293T cells grown in 6-well plate were transiently transfected with YFP-*pro-fs* and were visualized under fluorescent microscope to detect the subcellular localization of *pro-fs*. 293T cells in 6-well plate co-expressing CFP-*pro-fs* and YFP-*pro-fs* were visualized using a Leica SP2 confocal microsope to detect FRET. The entire individual cell nucleus was manually selected as region of interest (ROI). Two independent transfections were performed, and 8 to 11 ROIs were selected for measurement and the FRET efficiency was averaged from multiple ROIs. Full details of techniques are available in Supplementary material.

ACKNOWLEDGEMENTS

This work was supported by PHS Grant DA13561 from National Institute of Drug Abuse (NIDA).

SUPPLEMENTARY MATERIAL

Expression constructs. To make CFP- and YFP-tagged *pro-fs* constructs, *pro-fs* coding region was amplified by PCR from Nus-*pro-fs* construct (see Chapter 2, materials and methods) using sense primer FS-ECORI, 5' CTC GTG AA TTC GTT CAA CTT CCC GC 3', containing a *EcoR*I site, and anti-sense primer FS-BamHI, 5' CCT GTA CAG GAT CCT TAT GTC CAC AGA TTT °C 3', containing a *BamH*I site. The PCR product was then digested by *EcoR*I and *BamH*I and cloned into *EcoR*I and *BamH*I sites in vectors pECFP-C1 and pEYFP-C1 (Clontech). The fusion constructs were CFP- or YFP-tagged at N-terminus of *pro-fs*. CFP-*pro-fs* and YFP-*pro-fs* constructs were then transformed into *Escherichia coli* strain DH5α using chemical transformation method followed by extraction and purification using QIAprep Miniprep Kits (Qiagen). Fidelity of the construct was verified by automated DNA sequencing (Molecular Genetics Instrumentation Facilities, University of Georgia).

Cell culture and transient transfection. The 293T cells, derived from HEK293 cells, were used. Cell culture was maintained in Dulbecco's modified Eagle's medium (DMEM) with 4 mM L-glutamine adjusted to contain 1.5 g/L sodium bicarbonate and 4.5 g/L glucose, 90% (Sigma), supplemented with 10% fetal bovine serum (FBS) at 37 °C with 5% CO_2. Cells were transiently transfected using lipofectamine 2000 (Invitrogen) following manufacture's instructions. For subcellular localization studies, cells were thinly plated on polylysine-coated 25mm glass coverslips with 8 x 10^5 cells in 35 mm dish. For FRET experiments, cells were plated in 6-well plate at 8 x 10^5 cells/well 24 h before transfection. Different amount of fluorescent constructs were used in transfection, ranging from 0.5 to 2.5 μg. The purpose was to achieve a similar

expression level, judged by intensity of fluorescence, for either CFP- or YFP-tagged constructs across different transfection pairs.

Subcellular localization study. Zeiss fluorescent microscope equipped with green fluorescent and UV filter that allows excitation and visualization of green (YFP) and blue (DAPI) fluorescence was used to visualize the YFP-*pro-fs* transfected cells. Plan NeoFluar 40x/0.75 air lens and Axiocam attached to the microscope was used to capture the images to the computer. Cells on the coverslips were stained with DAPI, a DNA stain, prior to mounting on the slides. Cells were selected for imaging if stained with DAPI and successfully expressing YFP-*pro-fs*. Three consecutive images were taken for each selected region: cells under white light, with UV filter, with green fluorescent filter. Images were then overlay on top of each other in Photoshop to observe the subcellular localization of YFP-*pro-fs*.

FRET data acquisition using confocal microscopy and analysis. Twenty-four hours after transfection, 293T cells in 6-well plates were mounted on the confocal microscope stage. All imaging experiments were performed using 60 x /1.20 water-immerse lens on a Leica SP2 confocal microscope (Leica Microsystems, Germany) equipped with an acous-to-optical beamsplitter and a 100mW argon laser (457 nm, 476 nm, 488 nm, 514 nm). The fluorescent detection channels (Ch) were set to the following ranges: Ch 1: 465-485 nm, Ch 2: 520-565 nm. Settings for gain and offset of the detectors were identical for all experiments to keep the relative contribution of the fluorophores to the detection channels constant. Images were scanned a speed of 400 Hz with a line average of 4 and a resolution of 1024 x 1024 pixels.

Acceptor photobleaching method [18] was used to assess FRET efficiency. In our acceptor photobleaching protocol, we bleached cells in YFP channel by scanning a region of interest (ROI) 60 times using the argon laser line 514 nm at 100% intensity. In brief, the selective photobleaching of the acceptor fluorophore (e.g. YFP-tagged protein) abolishes FRET, and in the region of the cell where FRET occurred, there will be an enhancement in donor emission (e.g. CFP-tagged protein) because of the dequenching. Before and after the bleach, CFP and YFP images were collected to assess the change in fluorescence. To minimize the photobleaching due to imaging, images for CFP were collected at 18% of the laser intensity, YFP at 4%. Therefore, FRET efficiency was calculated according to formula built in the Leica software:

$$FRET_{Eff} = (D_{post} - D_{pre}) / D_{post} \text{ for all } D_{post} > D_{pre}$$

D_{pre} represents the emitted donor fluorescence before and D_{post} after photobleaching of the acceptor [19]. The entire individual cell nucleus was manually selected as ROI. Two independent transfections were performed, and 8 to 11 ROIs were selected for the measurement. $FRET_{Eff}$ from all ROIs from 6-cell samples were analyzed using ANOVA and Tukey's test (SAS Institute, Cary, NC) at P=0.05.

FRET signal were recorded for 6 samples that are cells transfected with: (1) negative control cells 1 (NC1): CFP-*pro-fs* alone; (2) negative control cells 2 (NC2): YFP-*pro-fs* alone; (3) negative control cells 3 (NC3): CFP-*pro-fs* and YFP vector; (4) negative control cells 4 (NC4): YFP-*pro-fs* and CFP vector; (5) CFP-*pro-fs* and YFP-*pro-fs*; (6) positive control (PC): CFP-YFP concatemer with a short linker of 9 amino acid residues between the two fluorophores (a generous gift from Dr. Morimoto's lab, Northwestern University).

Acquistion of FRET signal by scanning fluometry and data analysis. Luminescent spectrometer LS55 (Perkin Elmer) was used to detect FRET. Scanning fluorometry method was used as described [10, 15] with modification. The excitation was set to 434 nm with a 5 nm slit, and emission spectra was set to 450-610 nm with a 2.5 nm slit. Cells in 6-well plate was trypsinized briefly with 1X trypsine-EDTA solution (Sigma), centrifuged at 1,500 rpm for 4 min, washed twice with 1X PBS, and resuspended in FRET buffer (90% 1X PBS, 10% FBS). Cells were then irradiated at 434 nm at 37 °C and were scanned at a speed of 300 nm/min to detect emission. In each FRET experiment, fluorescence emission spectra are recorded from five samples that contain the same number of cells: (1) control cells that are not transfected for autofluorescence; (2) cells that co-express CFP-*pro-fs* and YFP vector; (3) cells that co-express CFP vector and YFP-*pro-fs*; (4) cells that express CFP-YFP concatemer; (5) cells that co-express CFP- and YFP-*pro-fs*. Equivalent cell number is achieved by adjusting cell density for transfection. Data were recorded and processed using FL WinLab software from Perkin Elmer for Window 2000 Professional. The autofluorescence emission was subtracted from that obtained with cells expressing fluorescent proteins. The resulted emission, which only due to direct excitation of the fluorophores, were then normalized based on the emission at 477 nm to observe the pattern of the spectrum across all of the transfected cells. Apparent FRET was calculated for (4) and (5) by subtracting the mean curve of normalized curves for (2) and (3) from normalized curves of (4) and (5).

REFERENCES

1. Taylor, E.W., et al., *A Basis for New Approaches to the Chemotherapy of AIDS: Novel Genes in HIV-1 Potentially Encode Selenoproteins Expressed by Ribosomal Frameshifting and Termination Suppression.* J. Med. Chem., 1994. **37**: p. 2637-2654.
2. Taylor, E.W., et al., *HIV-1 encodes a sequence overlapping env gp41 with highly significant similarity to selenium-dependent glutathione peroxidases.* J. Acquir. Immune. Defic. Syndr. Hum. Retrovirol., 1997. **15**(5): p. 393-394.
3. Zhao, L., et al., *Molecular modeling and in vitro activity of an HIV-1-encoded glutathione peroxidase.* Proc. Natl. Acad. Sci. U.S.A., 2000. **97**(12): p. 6356-6361.
4. Taylor, E.W., R.G. Nadimpalli, and C.S. Ramanathan, *Genomic structures of viral agents in relation to the biosynthesis of selenoproteins.* Biol. Trace. Elem. Res., 1997. **56**: p. 63-91.
5. Taylor, E.W., et al., *Nutrition, HIV, and drug abuse: the molecular basis of a unique role for selenium.* J Acquir Immune Defic Syndr, 2000. **25 Suppl 1**: p. S53-61.
6. Clegg, R.M., *Fluorescence resonance energy transfer.* Current Opinion in Biotechnology, 1995. **6**(1): p. 103-110.
7. Pollok, B.A. and R. Heim, *Using GFP in FRET-based applications.* Trends in Cell Biology, 1999. **9**(2): p. 57-60.
8. Sorkin, A., et al., *Interaction of EGF receptor and Grb2 in living cells visualized by fluorescence resonance energy transfer (FRET) microscopy.* Current Biology, 2000. **10**(21): p. 1395-1398.

9. Jiang, X. and A. Sorkin, *Coordinated Traffic of Grb2 and Ras during Epidermal Growth Factor Receptor Endocytosis Visualized in Living Cells.* Mol. Biol. Cell, 2002. **13**(5): p. 1522-1535.

10. Overton, M.C. and K.J. Blumer, *G-protein-coupled receptors function as oligomers in vivo.* Current Biology, 2000. **10**(6): p. 341-344.

11. Sharma, N., et al., *A Close Association of TorsinA and {{alpha}}-Synuclein in Lewy Bodies : A Fluorescence Resonance Energy Transfer Study.* Am J Pathol, 2001. **159**(1): p. 339-344.

12. Valenzuela-Fernandez, A., et al., *Optimal Inhibition of X4 HIV Isolates by the CXC Chemokine Stromal Cell-derived Factor 1alpha Requires Interaction with Cell Surface Heparan Sulfate Proteoglycans.* J. Biol. Chem., 2001. **276**(28): p. 26550-26558.

13. Weiss, T.S., et al., *Galpha i3 binding to calnuc on Golgi membranes in living cells monitored by fluorescence resonance energy transfer of green fluorescent protein fusion proteins.* PNAS, 2001. **98**(26): p. 14961-14966.

14. He, L., et al., *Flow cytometric measurement of fluorescence (Förster) resonance energy transfer from cyan fluorescent protein to yellow fluorescent protein using single-laser excitation at 458 nm.* Cytometry Part A, 2003. **53A**(1): p. 39-54.

15. Overton, M.C. and K.J. Blumer, *Use of fluorescence resonance energy transfer to analyze oligomerization of G-protein-coupled receptors expressed in yeast.* Methods, 2002. **27**(4): p. 324-332.

16. Bastiaens, P.I.H. and R. Pepperkok, *Observing proteins in their natural habitat: the living cell.* Trends in Biochemical Sciences, 2000. **25**(12): p. 631-637.

17. Day, R.N., A. Periasamy, and F. Schaufele, *Fluorescence Resonance Energy Transfer Microscopy of Localized Protein Interactions in the Living Cell Nucleus.* Methods, 2001. **25**(1): p. 4-18.

18. Kenworthy, A.K., *Imaging Protein-Protein Interactions Using Fluorescence Resonance Energy Transfer Microscopy.* Methods, 2001. **24**(3): p. 289-296.

19. Wouters, F.S., P.J. Verveer, and P.I.H. Bastiaens, *Imaging biochemistry inside cells.* Trends in Cell Biology, 2001. **11**(5): p. 203-211.

20. Zimmermann, T., et al., *Spectral imaging and linear un-mixing enables improved FRET efficiency with a novel GFP2-YFP FRET pair*. FEBS Letters, 2002. **531**(2): p. 245-249.

HIV-1 *PRO-FS* PQITLWQRPL VTIKIGGQLK* GSSIRYRSR**U** YSIRRNEFAR

KMETKNDRGN WRFYQSKTV**U** SDTHRNLWT

HIV-1 PROTEASE PQITLWQRPL VTIKIGGQLK* EALLDTGADD TVLEEMSLPG

RWKPKMIGGI GGFIKVRQYD QILIEICGHK AIGTVLVGPT

PVNIIGRNLL TQIGCTLNF

Figure 3.1. Amino acid sequence of HIV-1 *pro-fs*, comparing to that of HIV-1 protease (1HHP), modified from Table 1 of Taylor et al. [1]. The predicted frameshift site at lysine codon (K) is indicated by asterisk. Sequence at the frameshift site was translated according to a hypothetical single lysine tRNA P-site slippage mechanism [1]. The sequence after the asterisk is encoded in the –1 reading frame; the sequence up to the asterisk, the underlined region, is identical to the known protein sequence of HIV-1 protease in the zero reading frame. The two letters **U** in HIV-1 *pro-fs* sequence represent the selenocysteine residues encoded by the two in-frame UGA codons.

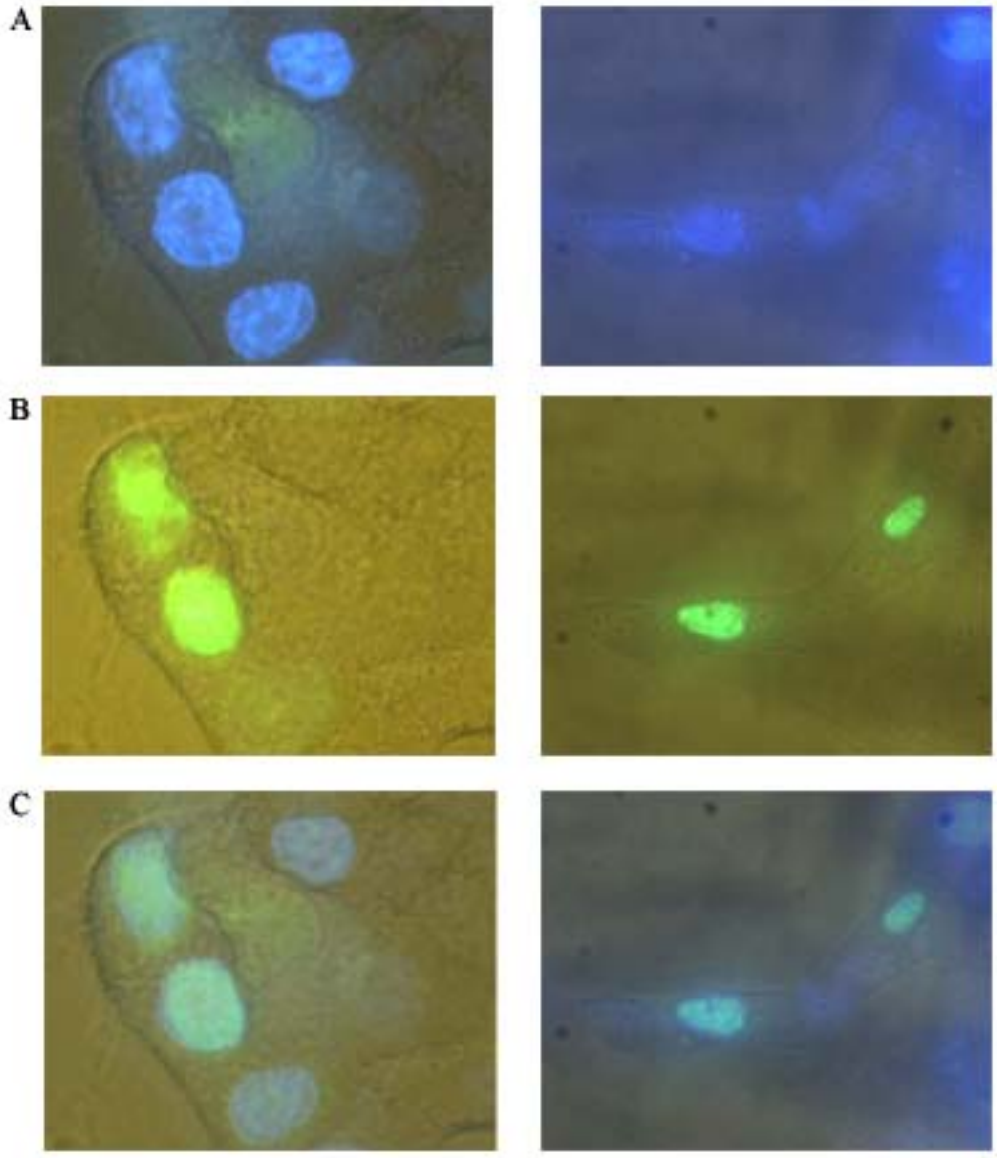
A
B
C

Figure 3.2. Subcellular localization of YFP-*pro-fs* in 293T (left panel) and MDCK (right panel) cells visualized by fluorescent microscope. Cells were transiently transfected with YFP-*pro-fs* and were visualized 24 h post-transfection. Cells were stained with 4,6-diamidino-2-phenylindole (DAPI) nuclear staining (blue fluorescence) and visualized under UV filter (A) or green fluorescent filter (B). White light was used as background combined with both filters to visualize the outline of cells. A merged image of the two panels is shown in (C), which verifies this strong co-localization. Shown are cells from one of two independent experiments.

A

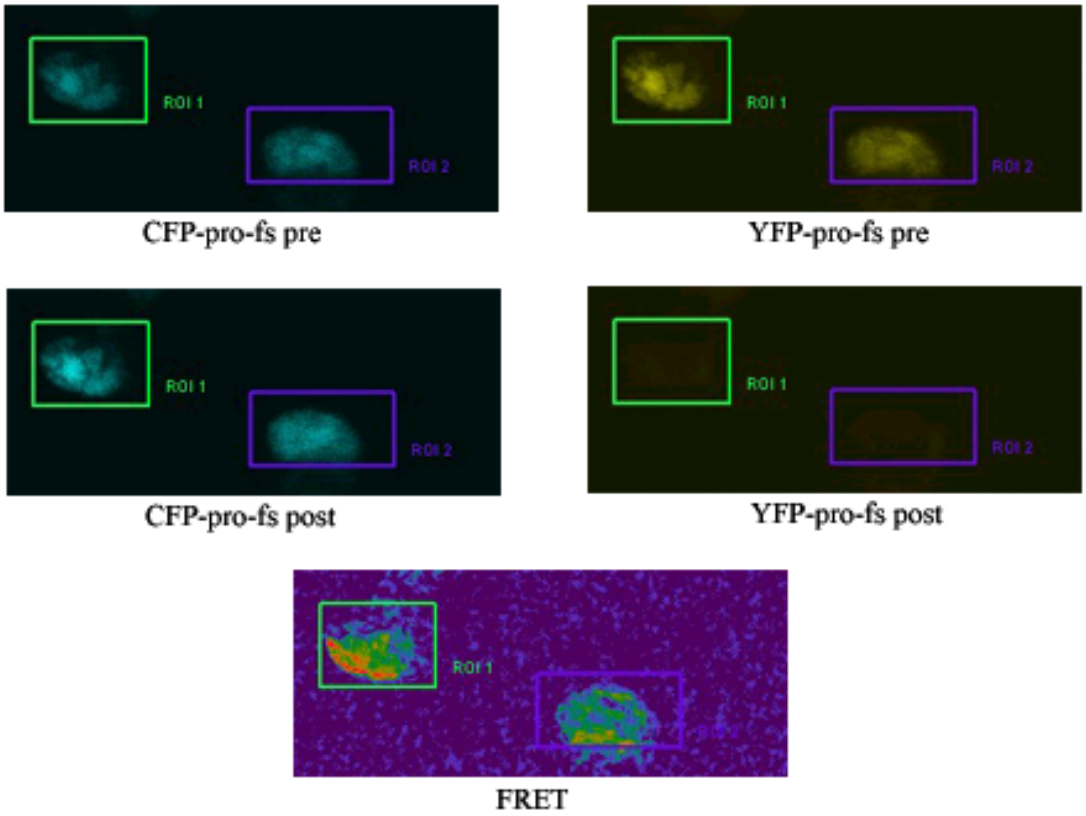
ROI 1
ROI 2
CFP-pro-fs pre
YFP-pro-fs pre
CFP-pro-fs post
YFP-pro-fs post
FRET

B

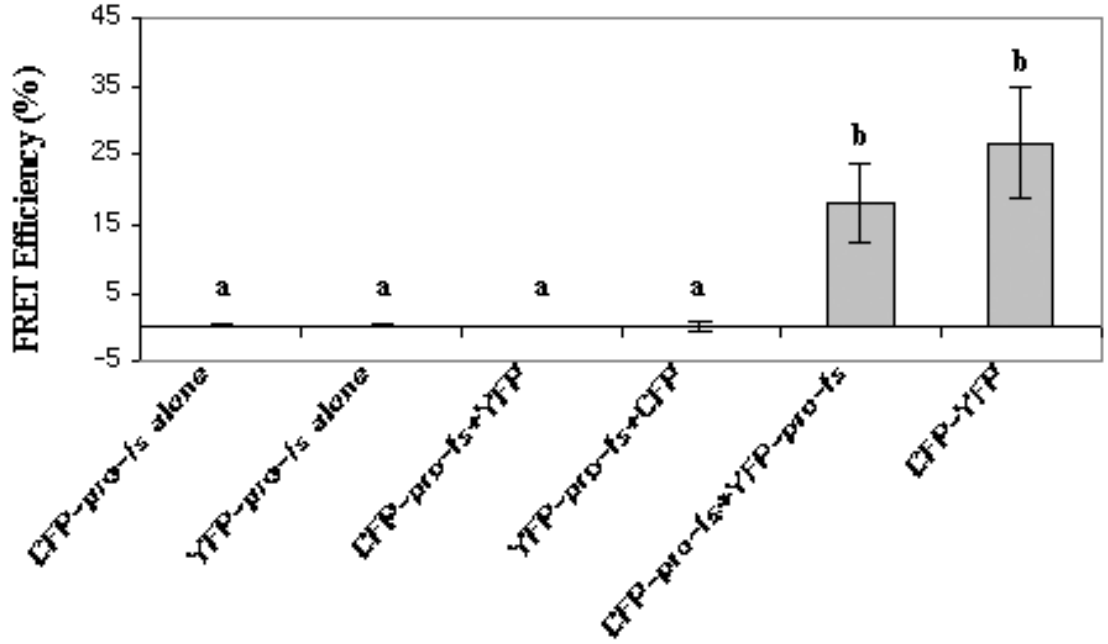
FRET Efficiency (%)
45
35
25
15
5
-5
a
a
a
a
b
b
CFP-pro-fs alone
YFP-pro-fs alone
CFP-pro-fs+YFP
YFP-pro-fs+CFP
CFP-pro-fs+YFP-pro-fs
CFP-YFP

Figure 3.3. Oligomerization of *pro-fs* in cells detected by FRET using confocal microscopy. Cells were transfected with indicated constructs. FRET signal acquisition was carried out 24 h post transfection via acceptor photobleaching method using confocal microscopy (see Materials and Methods). Cells were only analyzed when both tagged proteins were expressed at similar level when co-transfected. FRET efficiencies obtained for all transfections were analyzed using ANOVA with Tukey's test (P=0.05) as described in Materials and Methods. (A) Representative fluorescent signals observed from two channels through photobleaching process are shown. *Pre* stands from before photobleaching and *post* after photobleaching. FRET image was drived as described in Materials and Methods. All colors are arbitrarily assigned to indicate signal strength. (B) Summery of FRET between different protein pairs as indicated. CFP-YFP is a construct, in which CFP and YFP fluorophores are directly linked (see *Materials and Methods*). Data are plotted as mean +/- SEM. Letters above each bar indicates the significance among groups separated by Tukey's test.

A

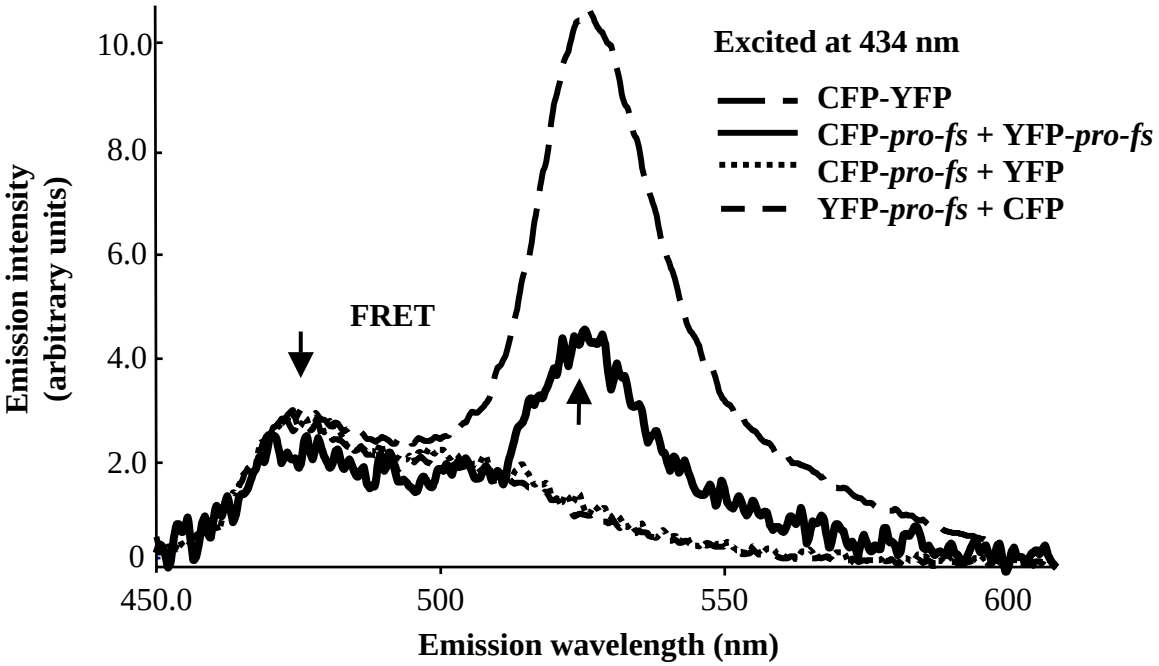
Excited at 434 nm
CFP-YFP
CFP-*pro-fs* + YFP-*pro-fs*
CFP-*pro-fs* + YFP
YFP-*pro-fs* + CFP
FRET
Emission intensity (arbitrary units)
10.0
8.0
6.0
4.0
2.0
0
450.0
500
550
600
Emission wavelength (nm)

B

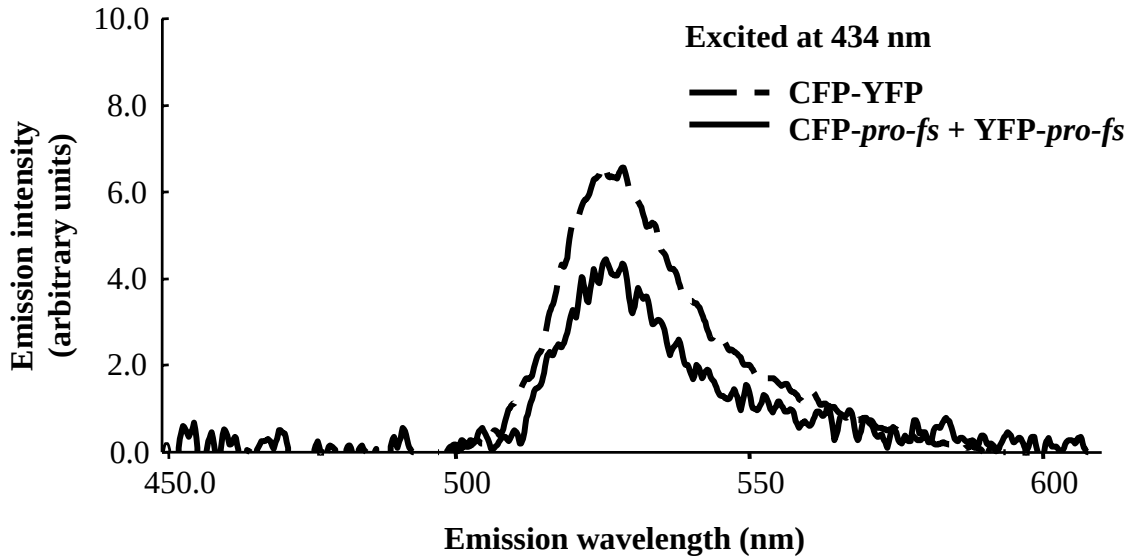
Excited at 434 nm
CFP-YFP
CFP-*pro-fs* + YFP-*pro-fs*
Emission intensity (arbitrary units)
10.0
8.0
6.0
4.0
2.0
0.0
450.0
500
550
600
Emission wavelength (nm)

Figure 3.4. Oligomerization of *pro-fs* detected in cells by FRET using scanning fluorometry. 293T cells untransfected, or expressing CFP-YFP, co-expressing CFP vector and YFP-*pro-fs*, or YFP vector and CFP-*pro-fs*, or CFP- and YFP-*pro-fs* were irradiated at 434 nm and fluorescence emission intensity was recorded from 450 to 610 nm. The results shown are the average of two independent experiments. (A) Emission intensity from untransfected 293T cells was subtracted from all other emission scan results as cell autofluorescence. The resulting values are then normalized based on its emission at 477 nm, which is the maximum emission wavelength for CFP, using FL WinLab software (Perkin Elmer). In the cells expressing CFP-YFP, which is a concatemer with CFP and YFP fluorophores linked together by 9 amino acid residues, or co-expressing CFP- and YFP-*pro-fs* the decrease in 477 nm emission and increase in 530 nm emission (e.g. sensitized YFP emission) implies that FRET is occurring. This was not observed when cells were co-transfected with YFP vector and CFP-*pro-fs* or with CFP vector and YFP-*pro-fs*. (B) Apparent FRET was obtained for cells expressing CFP-YFP and cells co-expressing CFP- and YFP-*pro-fs* by subtracting the mean curve of the resulted curves in (A) for cells co-expressing CFP vector and YFP-*pro-fs* and cells co-expressing YFP vector and CFP-*pro-fs*. This step eliminates any direct emission from CFP and YFP fluorophore upon excitation at 434 nm.

CHAPTER 4

FLUORESCENCE RESONANCE ENERGY TRANSFER STUDIES ON THE INTERACTION BETWEEN A NOVEL HIV-1 ENCODED NF KAPPA B-LIKE PEPTIDE AND THIOREDOXIN IN LIVING CELLS[1]

[1] Su, G. and E. W. Taylor. To be submitted to Molecular Biology of the Cell.

ABSTRACT

The gene encoded in the overlapping –1 reading frame of HIV-1 protease, named *pro-fs*, has been shown to have significant similarity to the DNA binding loop of NF-κB, which is known to bind thioredoxin (Trx) as part of the process of NF-κB activation. It was previously demonstrated that the putative HIV-1 *pro-fs* gene product localizes in cell nuclei and binds Trx with high affinity in vitro. The hypothesis that *pro-fs* associate directly with Trx in living mammalian cells was investigated in this study by fluorescent resonance energy transfer (FRET) analysis in 293T cells expressing cyan fluorescent protein (CFP) and yellow fluorescent protein (YFP) tagged *pro-fs* and Trx pairs. Confocal microscopy was utilized to quantify the FRET efficiency in living cells using the acceptor photobleaching method. Efficient energy transfer between CFP and YFP should only occur if CFP and YFP are less than 100 Å apart, which requires direct interaction of the *pro-fs* molecules fused to these fluorescent moieties. We observed partial nuclear translocation of Trx protein in cells treated with phorbol 12-myristate 13-acetate (PMA). Significant FRET efficiency was detected in the nuclei of PMA-stimulated cells co-expressing *pro-fs* and wild type human Trx (Trx-wt) or the double mutant of Trx (Trx-CS), in which the two conserved Cys residues in the active center are mutated to Ser. The results indicate that *pro-fs* binds both Trx-wt and Trx-CS, suggesting that Trx-*pro-fs* binding is a structurally specific interaction that involves multiple amino acid residues in addition to the Cys of *pro-fs* and Trx in the interactive region.

Keywords: Frameshift; HIV-1; Protease; Pro-fs; NF kappa B; Thioredoxin; Selenocysteine; Cysteine; Fluorescent resonance energy transfer; FRET; Photobleaching; CFP; YFP; Confocal microscopy; PMA.

INTRODUCTION

Pro-fs is a human immunodeficiency type 1 (HIV-1) encoded putative selenoprotein that was predicted by Taylor et al. based on computational analysis of the viral genome; it is potentially expressed by a –1 frameshift from the protease-coding region [1, 2]. *Pro-fs* contains two in-frame UGA codons, generally a stop codon, which is now well known for its role in coding for selenocysteine (Sec) in both eukaryotic and prokaryotic genomes [3-5]. The amino acid sequence of *pro-fs* is highly conserved in HIV-1 sequences, especially in the region spanning the UGA codons [6, 7]. Sequence analysis suggested a match to the NF-κB/Rel family of transcription factors, in which the conserved amino acid Cys62 residue aligns with a conserved UGA codon of *pro-fs* [7]. The frameshift site in the HIV-1 protease gene occurs just upstream of the *pro-fs* sequence (RYRSRU), which matches the sequence of the NF-κB/Rel family DNA binding domain (RFRYXC) [7].

NF-κB is an inducible, multisubunit transcription factor of higher eukaryotes that belongs to the NF-κB/Rel family. It is recognized as a key regulator of HIV replication. NF-κB/Rel family proteins are encoded by five genes: p50/p105, p65/RelA, c-Rel, RelB, and p52/p100, all of which share a conserved Rel homology domain (RHD) that is important for DNA binding, dimerization, nuclear localization, and interaction with IκB molecules (reviewed in [8]). NF-κB is composed of homo- or heterodimers of Rel family proteins, among which the heterodimer (p50/p65) is the major form. NF-κB is sequestered in the cytosol by interaction with the inhibitory molecule IκB family proteins [8]. Activation of cells with appropriate stimuli results in phosphorylation and degradation of IκB by IκB Kinase (IKK), which results in nuclear translocation of NF-κB. In the nucleus, NF-κB dimers bind to a specific DNA consensus

sequence, e.g. the two conserved κB sites at the long terminal repeat (LTR) promoter region of HIV, to start gene transcription [9-14].

The transcriptional activation of HIV LTR via NF-κB can be stimulated by a variety of proinflammatory or pathogenic stimuli including inflammatory cytokines, phorbol 12-myristate 13-acetate (PMA), T-cell mitogens, lipopolysaccharide (LPS), hydrogen peroxide (H_2O_2) and by tumor necrosis factor-α (TNF-α) [15-18], which function at least in part by forming reactive oxygen species (ROS). In addition to HIV replication, NF-κB also regulates hundreds of cellular genes involved in immune activation and cellular responses to stress, including cytokine genes associated with T cell activation and inflammation responses (for example, GM-CSF, IL-6, IL-8, IL-2, etc.), adhesion molecules (for example, VCAM-1 and E-selectin), and genes that regulate cell proliferation and apoptosis [13, 19-21], as well as gene expression of cytomegalovirus and simian virus 40 [22, 23].

NF-κB is susceptible to regulation by alterations in the intracellular reduction-oxidation (redox) state [13, 21]. Just as oxidants can activate NF-κB, antioxidants, such as N-acetylcysteine (NAC), lipoic acid, gold ion, and selenium (Se), can effectively suppress the activation of NF-κB [16, 24-29]. Se is an essential trace element important for various aspects of human health (reviewed in [30]). Its most important function, antioxidative function, is associated with specific selenoproteins including glutathione peroxidase (GPx) and thioredoxin reductase (TR) in the form of selenocysteine (Sec), an analog of Cys. Growing evidence links Se deficiency to the occurrence, virulence, or disease progression of several viral infections, such as Coxsackie virus, HIV-1, and hepatitis virus (B or C) [31-37]. Se supplementation was shown to suppress HIV replication induced by TNF-α or IL-1 by increasing the concentration of cellular selenoproteins GPx and TR [19, 27, 38, 39]. A statistically significant correlation between HIV

disease outcome and patient Se status has been widely documented. Moreover, Se is also an independent predictor of mortality in HIV infection [31, 33, 35].

Activation of NF-κB was shown to be regulated by the cellular selenoprotein TR and its substrate thioredoxin (Trx) through oxidoreduction (redox). Mammalian TR has two redox active centers. The N-terminal center, conserved in all species that encodes Trx, is formed by two Cys residues. The one in the C-terminus is found only in TR expressed in mammals and *C. elegans*, and is formed by a conserved Sec residue and a conserved Cys residue. This Sec is required for catalytic activity of mammalian TR, whose activity is therefore tightly regulated by dietary Se status [40, 41]. Trx is a small ubiquitous protein, known to be an important endogenous redox-regulating molecule with thiol reducing activity [42-44]. It has two Cys residues in its catalytic center with the consensus amino acid sequence Trp-Cys-Gly-Pro-Cys-Lys. Trx participates in redox reactions by reversible oxidation of the dithiol of the amino acid Cys32 and Cys35 residues to an intramolecular disulfide bond. It catalyzes dithiol-disulfide exchange reactions involving many thiol-dependent cellular processes, including intracellular signaling, gene regulation, resistance to oxidant stress, and control of apoptosis [44-46]. Hirota et al. demonstrated that Trx plays a dual and opposing role in the regulation of NF-κB. Overexpression of wild-type Trx suppressed NF-κB activation in the cytoplasm, while overexpression of nuclear-targeted Trx enhanced NF-κB-dependent transcription in the nucleus [42]. A growing body of evidence shows that Trx serves as a reductive catalyst in the reduction reaction of the Cys62 residues in NF-κB RHD, and needs to be maintained in a reduced (thiol) state in order for NF-κB to bind to DNA [21, 42, 47]. It was demonstrated that the reduction of the Cys62 residue of NF-κB requires direct association between the active center of Trx and the DNA binding loop of NF-κB [42, 48].

Trx is also known to regulate the DNA binding ability of cellular transcription factor activator protein 1 (AP-1), another cellular transcription factor that activates HIV transcription. It was demonstrated that Trx directly associates with redox factor 1 (Ref-1), which is known to stimulate AP-1 DNA binding activity and also possesses an apurinic/apyrimidinic (AP) endonuclease DNA repair activity [49-51]. In addition, Trx is required by retroviruses for formation of their DNA provirus because of its role of being hydrogen donor for ribonucleotide reductase, which is essential for DNA synthesis [52]. Clinically, an increase in plasma Trx levels in HIV disease, particularly in the later stages, has been reported [53].

Previously, we have demonstrated that *pro-fs* resides in cell nuclei and forms oligomers in living mammalian cells. In vitro experiments showed that *pro-fs* could bind Trx with high affinity. In the present studies, we have applied the FRET imaging paradigm to examine whether Trx and *pro-fs* interact in living mammalian cells. Our results demonstrate that in living cells, *pro-fs* interacts with both wild type human Trx and the double CS mutants of human Trx, in which the two Cys residues in the active center are mutated to Ser.

MATERIAL AND METHODS

Expression constructs of HIV-1 *pro-fs* and Trx. CFP- and YFP-tagged *pro-fs* constructs were made previously (see Chapter 3, materials and methods). To make CFP- and YFP-tagged Trx constructs, Trx-wt and Trx-CS coding region was amplified by PCR from Flag-tagged Trx constructs, which were provided by Dr. Wang Min (University of Rochester, NY) [43], using sense primer Trx-EcoRI, 5’ GGT GGA ATT CGC CTT GTG GTA 3’, containing a *EcoR*I site, and anti-sense primer Trx-XbaI, 5’ CGG GCC CTC TAG ACT TAG AC 3’, containing a *Xba*I

site. The PCR product was then digested by *EcoR*I and *Xba*I and cloned into *EcoR*I and *Xba*I sites in vectors pECFP-C1 and pEYFP-C1 (Clontech). The fusion constructs were CFP- or YFP-tagged at N-terminus of Trx-wt and Trx-CS. All expression constructs were then transformed into *Escherichia coli* strain DH5α using chemical transformation method followed by extraction and purification using QIAprep Miniprep Kits (Qiagen). Fidelity of the construct was verified by automated DNA sequencing (Molecular Genetics Instrumentation Facilities, University of Georgia).

Cell culture and transient transfection. The 293T cells, derived from HEK293 cells, were used. Cell culture was maintained in Dulbecco's modified Eagle's medium (DMEM) with 4 mM L-glutamine adjusted to contain 1.5 g/L sodium bicarbonate and 4.5 g/L glucose, 90% (Sigma), supplemented with 10% fetal bovine serum (FBS) at 37 °C with 5% CO_2. Cells were transiently transfected using lipofectamine 2000 (Invitrogen) following manufacture's instructions. For subcellular localization studies, cells were thinly plated on polylysine-coated 25mm glass coverslips with 8 x 10^5 cells in 35 mm dish. For FRET experiments, cells were plated in 6-well plate at 8 x 10^5 cells/well 24 h before transfection. Different amount of fluorescent constructs were used in transfection, ranging from 0.5 to 3.0 μg for 6-well plate. The purpose was to achieve a similar expression level across different CFP-tagged constructs, and a similar level for all YFP-tagged constructs, judged by intensity of fluorescence detected by Luminescent Spectrometer LS55 (Perkin Elmer) as decribed in Chapter 3. Cells were treated with or without phorbol 12-myristate 13-acetate (PMA, 50ng/ml) (Sigma) 16 hours post-transfection, and incubated for additional 24 h before subjecting to the subcellular localization study and FRET analysis.

Subcellular localization study of Trx. Nuclear localization of *pro-fs* was determined previously (see Chapter 3). In order to determine if *pro-fs* and Trx co-localize in the same subcellular compartment, we studied the subcellular localization of Trx. This was performed as previously described (see Chapter 3, materials and methods). Briefly, a Zeiss fluorescent microscope equipped with green fluorescent and UV filters were used, allowing the visualization of green (YFP) and blue fluorescence (DNA counterstain with 4,6-diamidino-2-phenylindole (DAPI) nuclear staining) of the YFP-Trx-wt in the transfected cells. DAPI nuclear staining permits the distinction between cytoplasmic and nuclear distributions. Plan NeoFluar 40x/0.75 air lens and Axiocam attached to the microscope was used to capture the images digitally. Cells on the polylysine-coated glass coverslips were stained with DAPI prior to mounting on the slides. Cells were selected for imaging if stained with DAPI and successfully expressing YFP-Trx-wt. Two consecutive images were taken for each selected region of cells: with UV filter and with green fluorescent filter. Images were then overlaid on top of each other in Photoshop to observe the subcellular localization of fluorescent protein. The localization of YFP-Trx-CS was determined using the same method described above.

FRET data acquisition using confocal microscopy and analysis. FRET experiments were carried out as described previously (see Chapter 3, Supplementary Material). Briefly, acceptor photobleaching method [54, 55] was used to assess FRET efficiency in transfected 293T cells using confocal microscopy. The fluorescent detection channels were set to 465-485 nm (for CFP) and 520-565 nm (for YFP) on a Leica SP2 confocal microscope (Leica Microsystems, Germany). FRET efficiency was calculated according to formula: $FRET_{Eff} = (D_{post} - D_{pre}) / D_{post}$ for all $D_{post} > D_{pre}$, in which D_{pre} represents the emitted donor fluorescence before and D_{post}

after photobleaching of the acceptor [55]. To limit the effect of heterogeneity of expression levels, only cells with similar expression level of CFP-tagged and YFP-tagged constructs across different transfections were selected. The individual cell nuclei were selected as area of interests (ROIs). Two independent transfections were performed, and 10 to 15 ROIs were selected for the measurement. $FRET_{Eff}$ of all of the ROIs from all transfections were analyzed using ANOVA and Tukey's test (SAS Institute, Cary, NC) at P=0.05.

Since intensity-based FRET analysis is subject to direct fluorescent contribution from both CFP and YFP, and may suffer from a high level of "false-positive" detection, appropriate controls were used to properly compensate for this problem. A CFP-YFP concatemer was used as a positive control, in which the CFP fluorophore and the YFP fluorophore were joined together with a short linker of 9 amino acid residues (a generous gift from Dr. R. Morimoto's lab, Northwestern University, Chicago, IL). Strong energy transfer was expected to occur between the two fluorophores when this construct was expressed in cells. FRET signal were recorded for 7 different transfections for studying interaction between Trx-wt and *pro-fs*. Cells transfected with: (1) negative control cells 1 (NC1): CFP-Trx-wt alone; (2) negative control cells 2 (NC2): YFP-*pro-fs* alone; (3) negative control cells 3 (NC3): CFP-Trx-wt and YFP vector; (4) negative control cells 4 (NC4): YFP-*pro-fs* and CFP vector; (5) CFP-Trx-wt and YFP-*pro-fs*, not treated with PMA; (6) CFP-Trx-wt and YFP-*pro-fs*, treated with PMA; (7) positive control (PC): CFP-YFP concatemer. FRET was also carried out to determine interaction between YFP-Trx-wt and CFP-*pro-fs*, CFP-Trx-CS and YFP-*pro-fs*, and YFP-Trx-CS and CFP-*pro-fs* as described above.

RESULTS

Expression and subcellular localization of Trx-wt, Trx-CS, and *pro-fs* constructs in cells. Each one of the eight constructs (Fig. 4.1) was successfully expressed in 293T, MDCK and HeLa cells and could be visualized in live cells using fluorescent or confocal microscope, and detected by Luminescent Spectrometer LS55. Previously, we discovered that *pro-fs* localizes in cell nuclei in all tested cell lines, including 293T, MDCK and HeLa cells (see Chapter 3, Fig. 3.1). It was reported that Trx predominantly localizes in the cytoplasm, and treatments with UV irradiation, PMA (50 ng/ml) or TNFα (100ng/ml) induce the translocation of Trx into the nucleus [42]. We then examined whether PMA treatment alters the subcellular localization of fluorescent-tagged Trx fusion protein, YFP-Trx-wt or YFP-Trx-CS. In transfected cells not treated with PMA, YFP-Trx-wt was visualized in both cytoplasm and the nucleus in 293T cells (Fig. 4.2, A, left panel), which was confirmed with DAPI stain (Fig. 4.2, B, left panel), but with more protein in cytoplasm then in nucleus. The merged image verifies this subcellular localization of YFP-Trx-wt (Fig. 4.2, C, left panel). Treatment with PMA led to an enhanced fluorescent intensity in the nucleus with a decrease in the cytoplasm of 293T cells, indicating that PMA triggered some nuclear translocation of YFP-Trx-wt (Fig. 4.2 A-C, right panel). Similar results were observed in YFP-Trx-CS transfected cells (data not shown).

Trx interacts with *pro-fs* in PMA-stimulated 293T cells. We employed the FRET technique to study the protein-protein interaction between Trx and *pro-fs*. YFP-*pro-fs* and CFP-Trx-wt or CFP-Trx-CS were transiently co-transfected into 293T cells. Fig. 4.3 demonstrates representative images observed from the CFP and YFP channels during acceptor photobleaching procedure,

and the resulting FRET images derived using the formula described in Materials and Methods. All colors are artificially assigned. Signals from the YFP channel are presented as yellow, signals from CFP channel as cyan, and signals for FRET are shown in pseudocolor. Numerical values from each channel represent the intensity of the signal, but do not encode color information. The color images in Fig. 4.3 do illustrate the distribution of CFP-Trx-wt and -CS in both cytoplasm and nucleus and the exclusive nuclear distribution of the YFP-*pro-fs*. We applied the acceptor photobleaching method to measure both the quenching of the donor signal and the sensitized acceptor emission to confirm that FRET has occurred, and to eliminate the effect caused by different expression levels of the constructs within cells and inhomogeneities in the thickness of the cells.

Using the protocol described in Materials and Methods, expression of the CFP-YFP concatemer produced a FRET signal of 27% (Fig. 4.4). Since the generation of FRET requires the presence of both fluorophores, single transfection of one fluorophore should not produce any FRET signal. Base on the theory behind FRET method, co-expression of unlinked YFP and CFP fluorophores should not generate FRET signal unless they are in direct contact. In cells singly transfected with only CFP- or YFP-tagged Trx-wt, Trx-CS or *pro-fs*, co-transfected with CFP-*pro-fs* and the YFP vector pair, YFP-*pro-fs* and the CFP vector pair, CFP-Trx-wt or -CS and YFP vector pair, YFP-Trx-wt or –CS and CFP vector pair, there was only marginal FRET signal detected, with a FRET efficiency of less than 1% (Fig. 4.4). Thus, there was no energy transfer in these transfections. FRET efficiency in the positive control was significantly higher than that in all the negative controls ($P<0.0001$).

Using the same protocol for FRET signal acquisition and analysis, interaction between fluorescent tagged-Trx and *pro-fs* was studied, as described in Materials and Methods. In PMA-

stimulated cells, co-expression of CFP-*pro-fs* and YFP-Trx-wt, YFP-*pro-fs* and CFP-Trx-wt, and YFP-*pro-fs* and CFP-Trx-CS gave a FRET efficiency of 8.2%, 4.6%, and 6.6%, respectively (Fig. 4.4 A-D), which are all significantly higher than all negative controls ($P<0.0001$). FRET efficiency detected between *pro-fs* + Trx-wt and *pro-fs* + Trx-CS do no significantly differ from each other (Fig. 4.4 D). In cells unstimulated with PMA, co-expression of CFP-*pro-fs* and YFP-Trx-wt, and YFP-*pro-fs* and CFP-Trx-CS gave only marginal FRET signals, 0.4% and 0.5%, respectively, and thus showed no significance difference from the negative controls (Fig. 4.4 A and C). All FRET efficiencies between Trx and *pro-fs* in PMA-stimulated cells were significantly higher than that seen in unstimulated cells, and significantly lower than that seen in positive control cells (Fig. 4.4 D).

DISCUSSION

There are two in-frame UGA codons in *pro-fs* sequence for possible incorporation of Sec. Since UGA is normally read as a stop codon, the decoding of UGA as Sec requires translational reprogramming during the biosynthesis of selenoproteins. In eukaryotes, this process requires a complex of the Sec insertion sequence (SECIS element), SECIS-binding protein 2 (SBP2), eEFSec, and Sec-tRNA^{Sec} that are dedicated to Sec incorporation. Because of the inherent competition against termination, Sec incorporation is often precluded by termination (reviewed in [56]). In FRET assay, similar expression levels of the two tagged proteins are required in order to correctly detect the energy transfer between the two fluorophores. The inefficiency and complexity of selenoprotein production in mammalian cells may result in a very low level of *pro-fs* expression that might not permit its stoichiometric interaction with Trx. Moreover, it was

shown previously in our in vitro studies that the Cys mutant of *pro-fs*, in which the two UGA codons were mutated to Cys residues, binds Trx with high affinity (Chapter 2). Thus, the Cys mutant of *pro-fs* was used in current studies.

In this study, we observed the nuclear translocation of the cellular antioxidative protein Trx in response to PMA stimulation, and demonstrate that the putative HIV-1 encoded peptide, *pro-fs*, interacts with Trx in vivo, which is consistent with the results of our previous in vitro studies (see Chapter 2, Fig. 2.4 and 2.5). Moreover, both wild type (Trx-wt) and the double Cys mutant (Trx-CS) of Trx binds to *pro-fs* in PMA-stimulated cells, but not in cells untreated with PMA (Fig. 4.4). In agreement with the previous in vitro demonstration, our results indicate that Trx-*pro-fs* binding is a structurally specific interaction that involves multiple amino acid residues in the interactive surface, not merely due to the formation of an intermolecular disulfide bond between the Cys residues in the active site of Trx and the Sec of *pro-fs*. These results are consistent with the modeling results of Taylor, et al. (unpublished data), which demonstrate that Trx binds *pro-fs* with a more favorable energy compared to Trx binding to its known ligand, the DNA binding loop of NF-κB, and that at least 8 amino acid residues are involved in the protein-protein interaction.

Accumulating evidence implicates that the intracellular localization of proteins are crucial components of signal transduction. For example, NF-κB heterodimer is normally sequestered in the cytoplasm associating with inhibitory molecule IκB, but upon activation, the free NF-κB dimers translocate into the nucleus, which is important for NF-κB-induced gene expression (reviewed in [8]). PMA treatment is known to induce the activation and nuclear translocation of NF-κB by generating ROS in the cytoplasm. In HeLa cells, PMA is also shown to efficiently translocate Trx into the nucleus [49]. In the case of redox regulation of NF-κB

function by Trx, the reduced Trx inhibits NF-κB activation in the cytoplasm, but upon nuclear translocation of NF-κB and Trx, Trx potentiates the DNA binding activity of NF-κB [42]. Moreover, the nuclear translocation of Trx induced by PMA is essential for AP-1 activation mediated by Trx and Ref-1, which results from Trx association with Ref-1 in the nucleus [49]. It was also reported that the nuclear translocalization of mitogen-activated protein kinase appears to be an important regulatory step for mitogen-induced gene expression and cell cycle re-entry [57]. Thus, it may be important to investigate the regulation of the signal transduction mechanisms with respect to cellular compartments. Fig. 4.2 shows that Trx fusion proteins, which are predominantly expressed in the cytoplasm (Fig. 4.2, left panel), partially translocate in the nucleus of 293T cells after PMA treatment (Fig. 4.2, right panel). We previously demonstrated that *pro-fs* localizes exclusively in cell nucleus in 293T, MDCK and HeLa cells (Chapter 3, Fig. 3.2). As shown in Fig. 4.4, overexpression of Trx and *pro-fs* alone was not sufficient to have significant interaction that can be detected using FRET, and these results suggest that nuclear localization of Trx by PMA is indispensable for binding to *pro-fs*.

Trx participates in redox regulation in the cell by reversible oxidation of the free dithiol to an intramolecular disulfide bond between the two active center Cys residues. Since Trx exerts dual and opposing effects in regulating NF-κB activation in different subcellular compartments [42], Trx needs to be in the cell nucleus in a reduced state in order to enhance HIV-1 replication regulated by NF-κB. The only enzyme known to catalyze this reaction is the cellular selenoprotein TR, whose activity is dependent upon Se status because the Sec residue is required for its catalytic activity in mammals [40, 41, 52]. Since *pro-fs* can be a selenoprotein containing one or two Sec residues, upon nuclear translocation of Trx induced by PMA, *pro-fs* may act as a nuclear TR to keep recycling Trx from the oxidazied state to the reduced state in cell nucleus,

which in turn enhance NF-κB activation to promote HIV-1 replication. The structural specificity between Trx and *pro-fs* observed in vivo in this study and in previous in vitro studies provides experimental basis for this speculation.

The structurally specific association of *pro-fs* and Trx also suggest that *pro-fs* might participate in other functions of Trx. It was shown that Trx plays a key role in inhibiting apoptosis of HIV-infected cells, which requires that Trx in a reduced form binds to the N-terminal portion of apoptosis signaling kinase 1 (ASK1) to block its activation by TNF-α [43, 58]. The oxidized form (intramolecular disulfide bond between C32 and C35) and the redox-inactive form (Trx-CS) of Trx do not bind to ASK1. Mutagenesis studies showed that the presence of at least one of the two conserved Cys residues in the redox center is required for Trx to inhibit ASK1-dependent apoptosis [43]. Thus, if *pro-fs* can catalyze reduction reaction of Trx, HIV-1 would be able to employ *pro-fs* to participate in the regulation of apoptosis process in infected cells. There is evidence indicates that the pleiotropic HIV-1 nef protein participates in the process of inhibiting ASK1-dependent apoptosis, by preventing stimulus-coupled release of Trx from ASK1 in HIV infected cells [59]. Trx also regulates the activation of AP-1 via direct association with Ref-1. Since AP-1 is also a redox responsive transcription factor that activates HIV replication, *pro-fs* may have regulating effect over AP-1, thus HIV replication. Furthermore, because of the role of Trx in the formation of proviral DNA by retroviruses for being a reducing agent for ribonucleotide reductase [52], it is possible that *pro-fs* might contribute to viral DNA synthesis.

HIV-encoded proteins, most importantly tat and nef proteins, are known to directly participate and play major roles in the process of viral reproduction by altering the cellular redox state (as in the case of tat) or by directly activating cellular transcription factors NF-κB and AP-1

(as in the case of nef) [60-62]. Given the importance of redox regulation of gene expression, it is reasonable for viruses to try to encode homologues of the regulatory proteins involved. We previously shown that *pro-fs* has high homology to the DNA binding loop of NF-κB (Chapter 2) and is a nuclear protein (Chapter 3). In the present study and the previous in vitro studies, we demonstrate that Trx interacts with *pro-fs* in a structural specific manner. Because interaction between Trx and NF-κB is also structural specific and Trx was shown to be a reducing agent of NF-κB required to activate the DNA binding activity of NF-κB [42, 48], we suggest that Trx may catalyze the reduction of *pro-fs*. Taylor et al. demonstrate that *pro-fs* is a potent activator of HIV-1 LTR and functions via NF-κB in a HIV-1 LTRlacZ reporter system (Taylor, et al., unpublished data). Taken together, our results suggest that *pro-fs* may function as a mimic of NF-κB in activation of HIV-1 transcription by binding to the HIV LTR. The existence of this protein might provide an alternative way for virus to survive the battle against host antioxidative defense system and continue to replicate. Moreover, since NF-κB regulates the expression of hundreds of genes involved in host immune responses and cellular defense against stress, it is possible for *pro-fs* to regulate other κB sites located in host DNA to activate cellular genes, enabling HIV to directly interfere with host defense mechanisms.

We should not ignore the value of *pro-fs* as a potential selenoprotein that possibly allows HIV to fight against cellular antioxidant defense. The role of ROS and oxidative stress in general in HIV pathogenesis has received considerable attention in recent years due to their roles in inducing activation of HIV transcription. NF-κB plays a key role in regulating HIV-1 replication and was the first transcription factor found to respond to oxidative stress mediated by prooxidants and pathogenic stimuli [15-18]. Conversely, this activation can be inhibited by various antioxidants [24-26]. It has been reported that low dose of Se supplementation can

suppress NF-κB activation in response to TNF-α and H_2O_2 in vitro, via increased production of the cellular selenoprotein GPx [27]. It seems feasible for viruses to have a self-defensive mechanism against environmental stress via encoding viral selenoproteins. Such phenomenon is not unprecedented. A functional GPx enzyme encoded by *Molluscum contagiosum*, a poxvirus that causes persistent skin neoplasms in children and acquired immunodeficiency syndrome (AIDS) patients, was shown to protect human keratinocytes against cytotoxic effects of ultraviolet irradiation and hydrogen peroxide [63, 64]. HIV-1 also encodes a highly truncated GPx enzyme [1] that showed measurable GPx activity [65].

It must be pointed out that, at this stage, *pro-fs* is still a hypothetical protein. There are several reasons why *pro-fs* has escaped detection before now. *Pro-fs* can only be expressed as a double frameshift protein since *pro-fs* is encoded in the overlapping –1 reading frame in HIV-1 protease-coding region, which as part of the pol gene, overlaps the gag-coding region in the –1 frameshift from. Due to the inefficiency of ribosomal frameshifting, which only occurs during by 1-10% of translational events [1], *pro-fs* only has 1% or less chance to be expressed as compared to HIV structural proteins. This would result in the very low abundance of *pro-fs* in HIV-infected cells. In addition, HIV only intends to make necessary enzyme proteins when necessary, it makes hard to detect the presence of *pro-fs*. The other reason might be because *Pro-fs* has a low molecular weight of approximately either 7.2 or 8.3 kDa, depending on whether one or both in-frame UGA codons are decoded as Sec. However, it is possible that the expression of *pro-fs* has been overlooked in a study of the effect of HIV-infection on selenoprotein expression in ^{75}Se-labeled human Jurkat T cells. Their results showed some low molecular mass Se-labeled compounds in HIV-infected cells without further investigation (Fig. 2.1 B in [66]). The position

of a wide band partially overlapping a known the 6 kDa cellular selenoprotein is in the correct size range to correspond to predicted isoforms of *pro-fs*.

In this paper, we have shown that human Trx translocates into the nucleus from the cytoplasm when stimulated by PMA. We have also demonstrated that this putative HIV-1 encoded peptide, *pro-fs*, a mimic of NF-κB, interacts with human Trx in the cell nucleus in vivo when cells are stimulated with PMA, and that the interaction is structurally specific. Given the complexity of the multiple factors involved, consideration of the outcome of this interaction in host cellular response in regard to HIV infection and disease progression should be further explored.

ACKNOWLEDGEMENTS

This work was supported by PHS Grant DA13561 from National Institute of Drug Abuse (NIDA).

REFERENCES

1. Taylor, E.W., et al., *A Basis for New Approaches to the Chemotherapy of AIDS: Novel Genes in HIV-1 Potentially Encode Selenoproteins Expressed by Ribosomal Frameshifting and Termination Suppression.* J. Med. Chem., 1994. **37**: p. 2637-2654.
2. Taylor, E.W., R.G. Nadimpalli, and C.S. Ramanathan, *Genomic structures of viral agents in relation to the biosynthesis of selenoproteins.* Biol. Trace. Elem. Res., 1997. **56**: p. 63-91.

3. Berry, M.J., et al., *Functional characterization of the eukaryotic SECIS elements which direct selenocysteine insertion at UGA codons.* EMBO J., 1993. **12**: p. 3315-3322.

4. Bock, A., et al., *Selenocysteine: the 21st amino acid.* Mol. Microbiol., 1991. **5**: p. 515-520.

5. Shen, Q., F.F. Chu, and P.E. Newburger, *Sequences in the 3'-untranslated region of the human cellular glutathione peroxidase gene are necessary and sufficient for selenocysteine incorporation at the UGA codon.* J. Biol. Chem., 1993. **268**: p. 11463-11469.

6. Taylor, E.W., et al., *HIV-1 encodes a sequence overlapping env gp41 with highly significant similarity to selenium-dependent glutathione peroxidases.* J. Acquir. Immune. Defic. Syndr. Hum. Retrovirol., 1997. **15**(5): p. 393-394.

7. Taylor, E.W., et al., *Nutrition, HIV, and drug abuse: the molecular basis of a unique role for selenium.* J Acquir Immune Defic Syndr, 2000. **25 Suppl 1**: p. S53-61.

8. Baldwin, A.S., *THE NF-κB AND IκB PROTEINS: New Discoveries and Insights.* Annual Review of Immunology, 1996. **14**(1): p. 649-681.

9. Antoni, B.A., S.B. Stein, and A.B. Rabson, *Regulation of human immunodeficiency virus infection: implications for pathogenesis.* Adv Virus Res, 1994. **43**: p. 53-145.

10. Baeuerle, P. and D. Baltimore, *A 65-kappaD subunit of active NF-kappaB is required for inhibition of NF-kappaB by I kappaB.* Genes Dev., 1989. **3**(11): p. 1689-1698.

11. Bednarik, D.P. and T.M. Folks, *Mechanisms of HIV-1 latency.* AIDS, 1992. **6**(1): p. 3-16.

12. Doerre, S., et al., *The c-rel Protooncogene Product Represses NF-{kappa}B p65-Mediated Transcriptional Activation of the Long Terminal Repeat of Type 1 Human Immunodeficiency Virus.* PNAS, 1993. **90**(3): p. 1023-1027.

13. Kawakami, K., C. Scheidereit, and R.G. Roeder, *Identification and purification of a human immunoglobulin-enhancer-binding protein (NF-kappa B) that activates transcription from a human immunodeficiency virus type 1 promoter in vitro.* PNAS, 1988. **85**(13): p. 4700-4704.

14. Rabson, A.B. and H.-C. Lin, *NF-κB and HIV: Linking Viral and Immune Activation*, in *HIV-1: Molecular Biology and Pathogenesis - Viral Mechanisms*, K.-T. Jeang, Editor. 2000, Academic Press. p. 161-207.

15. Griffin, G.E., et al., *Activation of HIV gene expression during monocyte differentiation by induction of NF-kappa B.* Nature, 1989. **339**(6219): p. 70-73.

16. Schreck, R., P. Rieber, and P.A. Baeuerle, *Reactive oxygen intermediates as apparently widely used messengers in the activation of the NF-kappa B transcription factor and HIV-1*. The EMBO Journal, 1991. **10**(8): p. 2247-2258.

17. Schreck, R., K. Albermann, and P. Bauerle, *Nuclear factor κB: An oxidative stress-response transcription factor of eukaryotic cells.* Free Rad. Res. Comm., 1992. **17**: p. 221-237.

18. Schulze-Osthoff, K., et al., *Depletion of the mitochondrial electron transport abrogates the cytotoxic and gene-inductive effects of TNF*. EMBO J., 1993. **12**(8): p. 3095-3104.

19. Brigelius-Flohe, R., et al., *Interleukin-1-induced nuclear factor kappa B activation is inhibited by overexpression of phospholipid hydroperoxide glutathione peroxidase in a human endothelial cell line.* Biochemical Journal, 1997. **328**: p. 199-203.

20. Kim, I.Y. and T.C. Stadtman, *Inhibition of NF-kappaB DNa binding and nitric oxide induction in human T cells and lung adenocarcinoma cellsby selenite treatment.* Proc Natl Acad Sci, 1997. **94**: p. 12904-12907.

21. Mitomo, K., et al., *Two different cellular redox systems regulate the DNA-binding activity of the p50 subunit of NF-kappa B in vitro.* Gene, 1994. **145**: p. 197-203.

22. Phares, W., B.R.J. Franza, and W. Herr, *The kappa B enhancer motifs in human immunodeficiency virus type 1 and simian virus 40 recognize different binding activities in human Jurkat and H9 T cells: evidence for NF-kappa B-independent activation of the kappa B motif.* J Virol., 1992. **66**(12): p. 7490-7498.

23. Sambucetti, L.C., et al., *NF-kappa B activation of the cytomegalovirus enhancer is mediated by a viral transactivator and by T cell stimulation.* EMBO J., 1989. **8**(13): p. 4251-4258.

24. Beg, A., et al., *Tumor necrosis factor and interleukin-1 lead to phosphorylation and loss of I kappa B alpha: a mechanism for NF-kappa B activation.* Mol. Cell. Biol., 1993. **13**(6): p. 3301-3310.

25. Henkel, T., et al., *Rapid proteolysis of I kappa B-alpha is necessary for activation of transcription factor NF-kappa B.* Nature, 1993. **365**(6442): p. 182-185.

26. Kretz-Remy, C., et al., *Inhibition of I kappa B-alpha phosphorylation and degradation and subsequent NF-kappa B activation by glutathione peroxidase overexpression.* J. Cell Biol., 1996. **133**(5): p. 1083-1093.

27. Makropoulos, V., T. Brüning, and K. Schulze-Osthoff, *Selenium-mediated inhibition of transcription factor NF kappa B and HIV-1 LTR promoter activity.* Archives of Toxicology, 1996. **70**(5): p. 277 - 283.

28. Suzuki, Y.J., B.B. Aggarwal, and L. Packer, *Alpha-lipoic acid is a potent inhibitor of NF-kappa B activation in human T cells.* Biochem Biophys Res Commun, 1992. **189**(3): p. 1709-1715.

29. Yang, J.-P., et al., *Inhibition of the DNA-binding activity of NF-kappa B by gold compounds in vitro.* FEBS Lett, 1995. **361**(1): p. 89-96.

30. Sunde, R.A., *Selenium*, in *Handbook of Nutritionally Essential Minerals*, B.L. O'Dell and R.A. Sunde, Editors. 1997, Marcel Dekker: New York. p. 493-556.

31. Allavena, C., et al., *Relationship of trace-element, immunological markers, and HIV infection progression.* Biol. Trace Elem. Res., 1995. **47**(133-138).

32. Beck, M.A., et al., *Rapid genomic evolution of a non-virulent coxsackievirus B3 in selenium-deficient mice results in selection of identical virulent isolates.* Nature Medicine, 1995. **1**(5): p. 433-436.

33. Baum, M.K., et al., *High risk of HIV-related mortality is associated with selenium deficiency.* J Acquir Immune Defic Syndr Hum Retrovirol, 1997. **15**: p. 370-376.

34. Constans, J., et al., *Serum selenium predicts outcome in HIV infection.* J. Acquir. Immune. Defic. Syndr. Hum. Retrovirol., 1995. **10**(3): p. 392.

35. Dworkin, B.M., *Selenium deficiency in HIV infection and the acquired immunodeficiency syndrome (AIDS).* Chem. Biol. Interact., 1994. **91**: p. 181-186.

36. Yu, S.Y., Y.J. Zhu, and W.G. Li, *Protective role of selenium against hepatitis B virus and primary liver cancer in Qidong.* Biological Trace Element Research, 1997. **56**(1): p. 117-124.

37. Yu, M.W., et al., *Plasma selenium levels and risk of hepatocellular carcinoma among men with chronic hepatitis virus infection.* American Journal Of Epidemiology, 1999. **150**(4): p. 367-374.

38. Hori, L., et al., *Selenium supplementation suppresses tumor necrosis factor α-induced human immunodeficiency virus type 1 replication in vitro.* AIDS Research And Human Retroviruses, 1997. **13**: p. 1325-1332.

39. Sappey, C., et al., *Stimulation of glutathione peroxidase activity decreases HIV type 1 activation after oxidative stress.* AIDS. Res. Hum. Retroviruses., 1994. **10**(11): p. 1451-1461.

40. Gallegos, A., et al., *Mechanisms of the regulation of thioredoxin reductase activity in cancer cells by the chemopreventive agent selenium.* Cancer Res, 1997. **57**(21): p. 4965-4970.

41. Hadley, K.B. and R.A. Sunde, *Selenium regulation of thioredoxin reductase activity and mRNA levels in rat liver.* The Journal of Nutritional Biochemistry, 2001. **12**(12): p. 693-702.

42. Hirota, K., et al., *Distinct Roles of Thioredoxin in the Cytoplasm and in the Nucleus. A TWO-STEP MECHANISM OF REDOX REGULATION OF TRANSCRIPTION FACTOR NF-kappa B.* J. Biol. Chem., 1999. **274**(39): p. 27891-27897.

43. Liu, Y. and W. Min, *Thioredoxin Promotes ASK1 Ubiquitination and Degradation to Inhibit ASK1-Mediated Apoptosis in a Redox Activity-Independent Manner.* Circ Res, 2002. **90**(12): p. 1259-1266.

44. Tanaka, T., et al., *Redox regulation by thioredoxin superfamily; protection against oxidative stress and aging.* Free Radic Res, 2000. **33**(6): p. 851-855.

45. Arner, E.S.J. and A. Holmgren, *Physiological functions of thioredoxin and thioredoxin reductase.* Eur J Biochem, 2000. **267**(20): p. 6102-6109.

46. Powis, G., D. Mustacich, and A. Coon, *The role of the redox protein thioredoxin in cell growth and cancer.* Free Radic Biol Med, 2000. **29**(3-4): p. 312-322.

47. Matthews, J.R., et al., *Thioredoxin regulates the DNA binding activity of NF-κB by reduction of a disulphide bond involving cysteine 62.* Nucleic Acids Research, 1992. **20**(15): p. 3821-3830.

48. Qin, J., et al., *Solution structure of human thioredoxin in a mixed disulfide intermediate complex with its target peptide from the transcription factor NF-κB.* Structure, 1995. **3**: p. 289-297.

49. Hirota, K., et al., *AP-1 transcriptional activity is regulated by a direct association between thioredoxin and Ref-1.* PNAS, 1997. **94**(8): p. 3633-3638.

50. Xanthoudakis, S. and T. Curran, *Identification and characterization of Ref-1, a nuclear protein that facilitates AP-1 DNA-binding activity.* EMBO J., 1992. **11**(2): p. 653-665.

51. Xanthoudakis, S., et al., *Redox activation of Fos-Jun DNA binding activity is mediated by a DNA repair enzyme.* EMBO J., 1992. **11**(9): p. 3323-3335.

52. Bjornstedt, M., et al., *Selenium and the thioredoxin and glutaredoxin systems.* Biomed Environ Sci, 1997. **10**((2-3)): p. 271-279.

53. Nakamura, H., et al., *Elevation of plasma thioredoxin levels in HIV-infected individuals.* Int. Immunol., 1996. **8**(4): p. 603-611.

54. Kenworthy, A.K., *Imaging Protein-Protein Interactions Using Fluorescence Resonance Energy Transfer Microscopy.* Methods, 2001. **24**(3): p. 289-296.

55. Wouters, F.S., P.J. Verveer, and P.I.H. Bastiaens, *Imaging biochemistry inside cells.* Trends in Cell Biology, 2001. **11**(5): p. 203-211.

56. Driscoll, D.M. and P.R. Copeland, *MECHANISM AND REGULATION OF SELENOPROTEIN SYNTHESIS.* Annual Review of Nutrition, 2003. **23**(1): p. 17-40.

57. Brunet, A., et al., *Nuclear translocation of p42/p44 mitogen-activated protein kinase is required for growth factor-induced gene expression and cell cycle entry.* EMBO J., 1999. **18**(3): p. 664-674.

58. Saitoh, M., et al., *Mammalian thioredoxin is a direct inhibitor of apoptosis signal-regulating kinase (ASK) 1* . EMBO J., 1998. **17**(9): p. 2596-2606.

59. Geleziunas, R., et al., *HIV-1 Nef inhibits ASK1-dependent death signalling providing a potential mechanism for protecting the infected host cell.* Nature, 2001. **412**(6830): p. 834-838.

60. Gentz, R., C.H. Chen, and C.A. Rosen, *Bioassay for trans-activation using purified human immunodeficiency virus tat-encoded protein: trans-activation requires mRNA synthesis.* PNAS, 1989. **86**(3): p. 821-824.

61. Westendorp, M.O., et al., *HIV-1 Tat potentiates TNF-induced NF-kappa B activation and cytotoxicity by altering the cellular redox state.* EMBO J., 1995. **14**(3): p. 546-554.

62. Varin, A., et al., *Exogenous Nef Protein Activates NF-kappa B, AP-1, and c-Jun N-Terminal Kinase and Stimulates HIV Transcription in Promonocytic Cells. ROLE IN AIDS PATHOGENESIS.* J. Biol. Chem., 2003. **278**(4): p. 2219-2227.

63. Senkevich, T.G., et al., *Genome sequence of a human tumorigenic poxvirus: prediction of specific host response-evasion genes.* Science, 1996. **273**(5276): p. 813-816.

64. Shisler, J.L., et al., *Ultraviolet-induced cell death blocked by a selenoprotein from a human dermatotropic poxvirus.* Science, 1998. **279**(5347): p. 102-105.

65. Zhao, L., et al., *Molecular modeling and in vitro activity of an HIV-1-encoded glutathione peroxidase.* Proc. Natl. Acad. Sci. U.S.A., 2000. **97**(12): p. 6356-6361.

66. Gladyshev, V.N., et al., *Levels of major selenoproteins in T cells decrease during HIV infection and low molecular mass selenium compounds increase.* PNAS, 1999. **96**(3): p. 835-839.

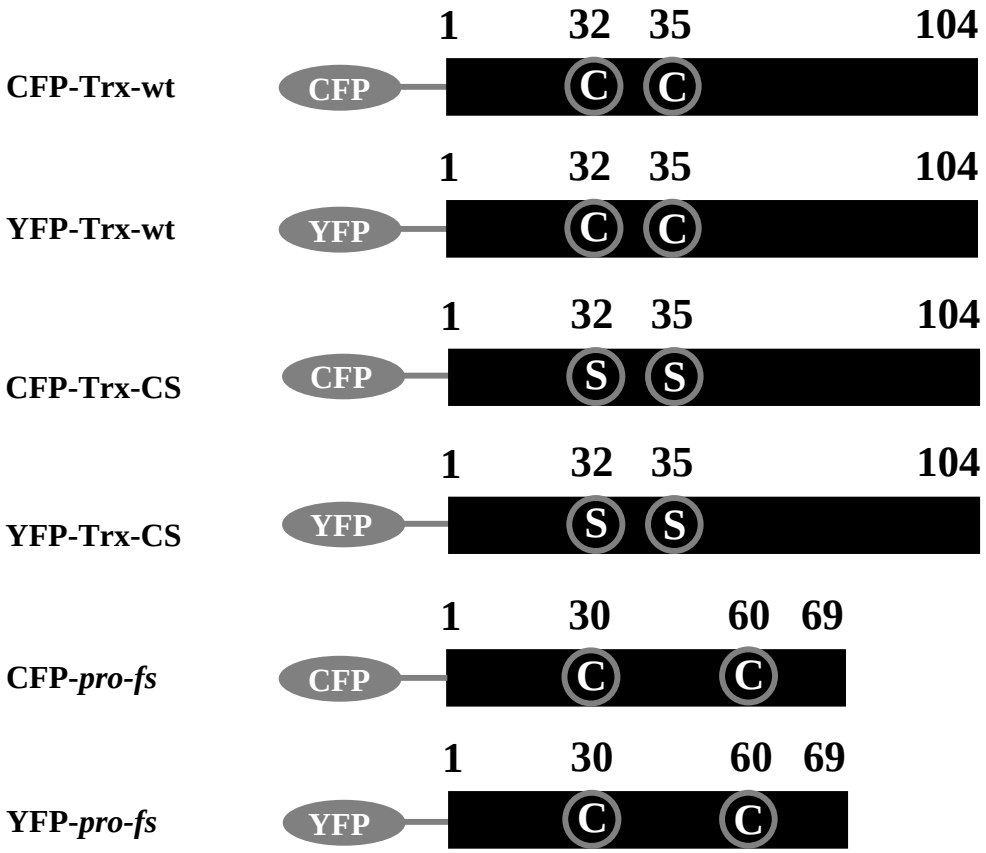

Figure 4.1. Schematic structures of N-terminal CFP- or YFP- tagged Trx-wt, Trx-CS and *pro-fs* constructs. Artificial linkers constructed from the polylinker region of pECFP-C1 and pEYFP-C1 (Clontech) are drawn in gray lines. All fusion constructs were CFP- or YFP-tagged at their N-termini. Trx-CS is a double mutant generated from Trx-wt, with two Ser residues in place of Cys residues in the active center {Liu, 2002 #12}. In order to express *pro-fs* in sufficient amount for FRET studies, we continued to use the mutant of *pro-fs*, with two Cys residues in the place of Sec residues, which are encoded by UGA codons in the wild-type *pro-fs* (see Chapter 4, Materials and Methods for further details).

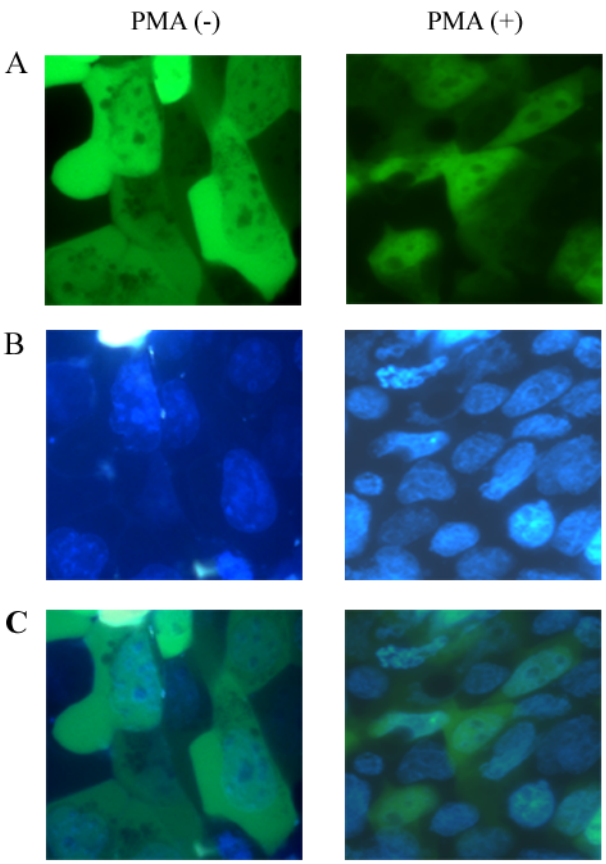

Figure 4.2. Effect of PMA treatment on subcellular localization of YFP-Trx-wt in 293T cells. Cells were transiently transfected with YFP-Trx-wt and were treated with (left panel) or without (right panel) PMA (50 ng/ml) 16 h post-transfection. After another 24 h incubation, cells were stained with 4,6-diamidino-2-phenylindole (DAPI) nuclear staining (blue fluorescence) and visualized with UV filter (A) or with green fluorescent filter (B). A merged image of the two panels is shown in (C), which verifies subcellular localization of YFP-Trx-wt. In cells untreated with PMA, YFP-Trx-wt predominantly localizes in the cytoplasm then in the nuclei (A, left panel), whereas in PMA-stimulated cells, more YFP-Trx-wt localizes in the cell nuclei than in the cytoplasm (A, right panel).

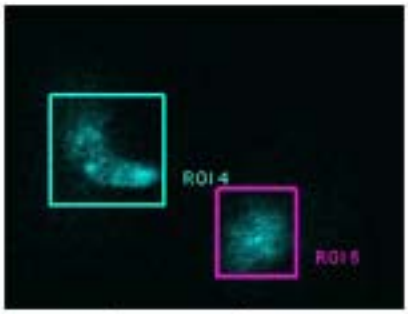

CFP-pro-fs pre

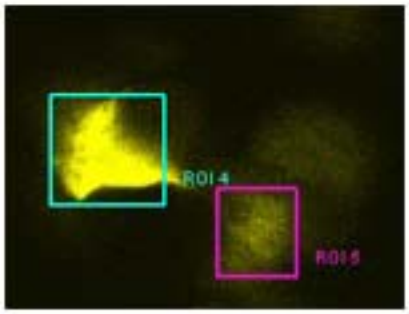

YFP-Trx-wt pre

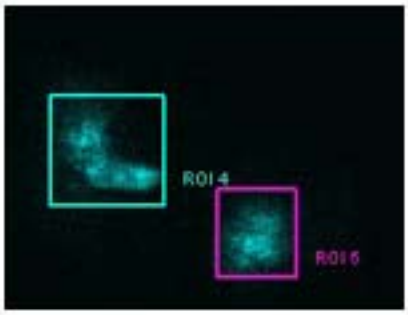

CFP-pro-fs post

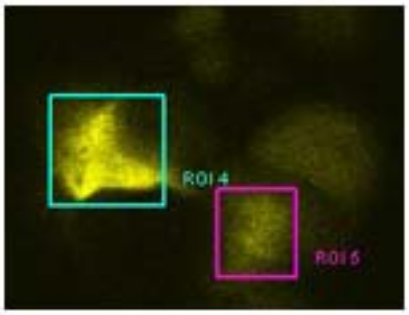

YFP-Trx-wt post

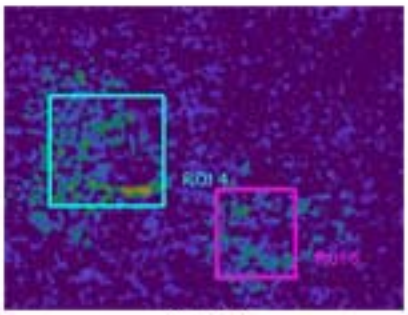

FRET

FRET Eff of ROI 4: 10.33%

FRET Eff of ROI 5: 6.87%

Figure 4.3. Representative FRET images by confocal microscopy through photobleaching process. 293T cells were transfected with CFP-*pro-fs* and YFP-Trx-wt. Transfected cells were stimulated with PMA (50ng/ml) 16 h post-transfection. FRET signal acquisition was carried out after another 24 h incubation via acceptor photobleaching method using confocal microscope (see Materials and Methods). Cells were only analyzed when both tagged proteins were expressed at similar level. Images represent fluorescent signals observed from two channels through photobleaching process. Individual nucleus was selected as area of interest and FRET image was obtained as described in Materials and Methods. *Pre* stands from before photobleaching and *post* after photobleaching. All colors are arbitrarily assigned to indicate signal strength. FRET efficiency is represented as pseudocolor.

A

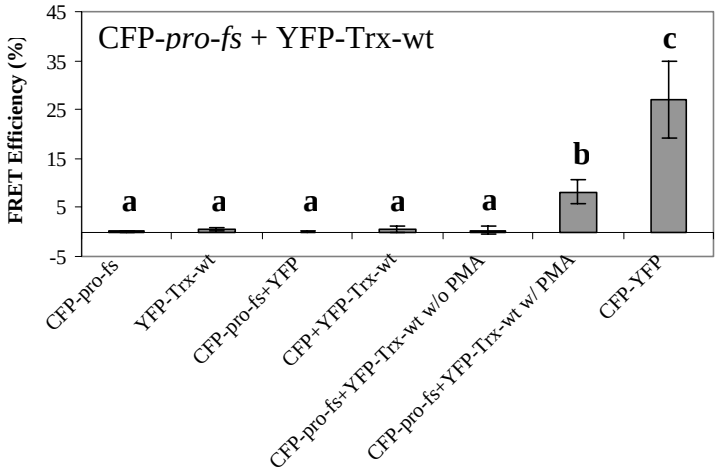
CFP-*pro-fs* + YFP-Trx-wt
FRET Efficiency (%)
45
35
25
15
5
-5
a
a
a
a
a
b
c
CFP-pro-fs
YFP-Trx-wt
CFP-pro-fs+YFP
CFP+YFP-Trx-wt
CFP-pro-fs+YFP-Trx-wt w/o PMA
CFP-pro-fs+YFP-Trx-wt w/ PMA
CFP-YFP

B

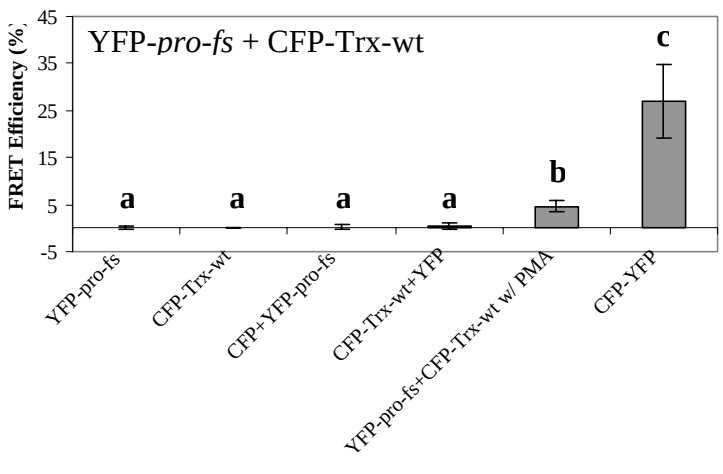
YFP-*pro-fs* + CFP-Trx-wt
FRET Efficiency (%)
45
35
25
15
5
-5
a
a
a
a
b
c
YFP-pro-fs
CFP-Trx-wt
CFP+YFP-pro-fs
CFP-Trx-wt+YFP
YFP-pro-fs+CFP-Trx-wt w/ PMA
CFP-YFP

C

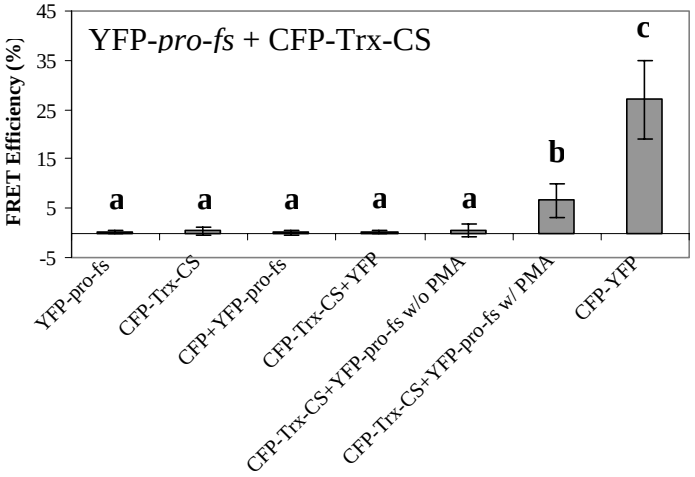
YFP-*pro-fs* + CFP-Trx-CS
FRET Efficiency (%)
45
35
25
15
5
-5
a
a
a
a
a
b
c
YFP-pro-fs
CFP-Trx-CS
CFP+YFP-pro-fs
CFP-Trx-CS+YFP
CFP-Trx-CS+YFP-pro-fs w/o PMA
CFP-Trx-CS+YFP-pro-fs w/ PMA
CFP-YFP

D

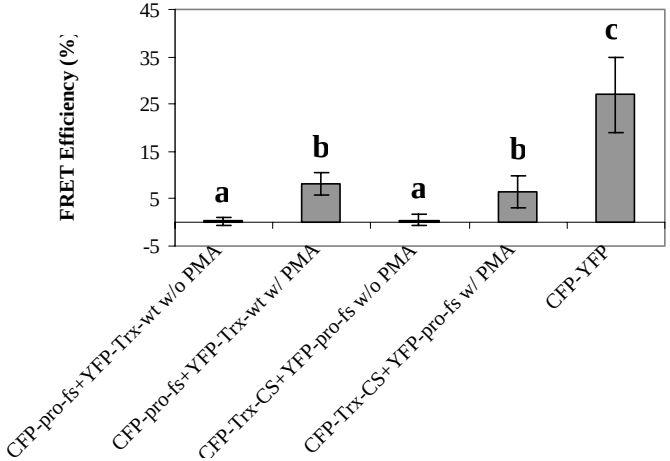
FRET Efficiency (%)
45
35
25
15
5
-5
a
b
a
b
c
CFP-pro-fs+YFP-Trx-wt w/o PMA
CFP-pro-fs+YFP-Trx-wt w/ PMA
CFP-Trx-CS+YFP-pro-fs w/o PMA
CFP-Trx-CS+YFP-pro-fs w/ PMA
CFP-YFP

Figure 4.4. Interaction between thioredoxin (Trx) and *pro-fs* detected in PMA-stimulated cells by FRET using confocal microscopy. 293T cells were transfected with different expression constructs as shown in the graphs. CFP-YFP is a construct that CFP and YFP fluorophores are directly linked (see Materials and Methods). Cells were treated or not treated with PMA (50ng/ml) 16 h post-transfection, and incubated for additional 24 h. FRET efficiency cross different transfections were then detected using photobleaching method by confocal microscopy (see Materials and Methods for details). $FRET_{Eff}$ of all samples were analyzed using ANOVA and Tukey's test (SAS Institute, Cary, NC) at P=0.05. (A) FRET efficiency in PMA-stimulated cells co-expressing CFP-*pro-fs* and YFP-Trx-wt is significantly higher than that in unstimulated cells co-expressing both proteins and all negative controls, but is significantly lower than that in CFP-YFP transfected cells. (B) Significant FRET efficiency was also detected in PMA-stimulated cells co-expressing YFP-*pro-fs* and CFP-Trx-wt. (C) FRET efficiency detected in PMA-stimulated cells co-expressing YFP-*pro-fs* and CFP-Trx-CS is significantly higher than in unstimulated cells co-expressing both proteins and all of the negative controls, is significantly lower than in CFP-YFP transfected cells. (D) There is no significant difference between FRET efficiencies detected in PMA-stimulated cells co-expressing CFP-*pro-fs* + YFP-Trx-wt and YFP-*pro-fs* + CFP-Trx-CS, which are both significantly higher than that in unstimulated cells and lower than that in CFP-YFP transfected cells.

CHAPTER 5

KINETIC MODELING ON REDOX REGULATION OF NF KAPPA B AND HIV-1 GENE TRANSCRIPTION[1]

[1] Su, G., J. L. Hargrove, and E. W. Taylor. To be submitted to Journal of Biological Systems.

ABSTRACT

Selenium (Se) is a crucial nutrient for HIV-infected individuals and a potent inhibitor of HIV replication in vitro. Se-deficient HIV patients showed a mortality risk from HIV-related causes nearly 20 times that of those with adequate levels. Oxidative stress induced by reactive oxygen species (ROS) plays a role in HIV-1 replication and disease progression, especially by activating NF-κB, a key cellular transcription factor in regulating HIV replication. TNF-α is one of the stimuli that can induce ROS production. Se supplementation was shown to suppress this activation by increasing production and activity of cellular antioxidative selenoproteins including glutathione peroxidase and thioredoxin reductase. Thus, our hypothesis is that antioxidant defense (Se supplementation) can inhibit oxidative stress-induced HIV transcription by suppressing NF-κB. In this paper, we generated a computer simulation model using the STELLA program to monitor the redox regulation of NF-κB activation and HIV-1 replication. Both experimental data from various publications and some arbitrary values were used to implement this model in order to simulate the effects of Se supplementation and TNF-α in the system. The results showed that our model strongly support our hypothesis, and indicate the benefits of Se supplementation as a nutritional therapeutic adjuvant to drug or chemotherapy to slow down disease progression in HIV-infected patients.

Keywords: HIV; STELLA; Simulation; Model; Compartment; Selenium; Selenoprotein; TNF alpha; NF kappa B; ROS; Thioredoxin; Thioredoxin reductase; Glutathione peroxidase; Oxidative stress.

INTRODUCTION

Selenium (Se) is a nutritionally essential mineral and seems to be crucial for HIV-infected individuals because of its role in cellular antioxidant defense. A correlation between HIV-1 disease outcome and patient's Se status has been widely documented. Se deficiency exposes the host to a more significant risk than deficiency of any other nutrient. Plasma Se is not only correlated with various indicators of disease progression, but also an independent predictor of mortality in HIV-1 infection, being a significantly greater risk factor for mortality than low helper-T-cell count in some studies [1-4]. A progressive decline in plasma Se in parallel with the on-going loss of CD4 T cells in HIV-1 infection was documented [5]. Se-deficient HIV-1 patients showed a mortality risk from HIV-related causes with nearly 20 times that of those with adequate levels [2]. It was shown that Se supplementation suppressed HIV-1 replication induced by H_2O_2 and tumor necrosis factor-α (TNF-α) in acute infected cells via increasing concentration of selenoproteins glutathione peroxidase (GPx) and thioredoxin reductase (TR) [6-9]. Therefore, adequate Se is essential to maintain a reductive cytoplasmic milieu in HIV-infected cells to suppress the rate of HIV-1 replication.

The transcriptional activation of HIV-1 was clearly shown to depend on cellular transcription factor NF-κB when exposed to oxidative stress mediated by either H_2O_2 or TNF-α [10-13]. NF-κB is sequestered in the cytosol by interaction with the inhibitory molecule IκB family proteins [14]. Activation of cells with appropriate stimuli results in phosphorylation and degradation of IκB by IκB Kinase (IKK), which results in nuclear translocation of NF-κB. In nucleus, NF-κB dimers bind to a specific DNA consensus sequence, e.g. the two conserved κB sites at the long terminal repeat (LTR) promoter region of HIV-1, to start gene transcription [15-

20]. A large variety of stimuli are now known to induce the activation of NF-κB, including phorbol ester (such as PMA), phytohaemmaglutinin (PHA), TNF-α, LPS, HIV-1 protease, calcium ionophores and H_2O_2. These stimuli function at least in part by involving reactive oxygen species (ROS) [11, 21-25]. Antioxidants such as N-acetylcysteine (NAC), lipoic acid, gold ion, and Se were shown to efficiently reduce NF-κB activation in the signaling pathway in the cells [8, 11, 26, 27]. Therefore, in general, antioxidants are considered to be effective NF-κB inhibitors.

Overexpression of cytosolic or phospholipid hydroperoxide GPx has shown to inhibit NF-κB activation and subsequent HIV-1 replication induced by H_2O_2, TNF-α or IL-1 [6, 8, 28, 29]. Being selenoprotein, the activity of GPx depends on the amount of Se available for their biosynthesis. In vitro experiments have demonstrated that optimal Se-supplementation in the growth medium significantly increases the GPx activity in cultured cells, and such cells exhibit an increased resistance against oxidative stress and a decrease in activation of NF-κB induced by IL-1 [6, 8]. In vivo studies showed that the abundance of cytosolic GPx mRNA in Se-adequate rat liver was 30-fold higher than glyceraldehyde-3-phosphate dehydrogenase (GAPDH) mRNA, whereas it is similar to that in Se-deficient rat liver [30]. Se supplementation appears to switch cytosolic GPx mRNA from nonsense-mediated degradation to translation, thus resulting an increase of approximately 20-fold in translational efficiency of cytosolic GPx mRNA, which preceded the increase in liver GPx activity [31, 32]. In liver supernatant of Se-deficient rats, the cytosolic GPx mRNA was significantly reduced to 10% and activity to 25% of the levels in Se-adequate rats [30].

NF-κB is susceptible for regulation by the mammalian selenoprotein TR and its substrate thioredoxin (Trx) through oxidoreduction. Mammalian TR has two redox catalytic centers. The

N-terminal center is formed by two conserved cysteine (Cys) residues, and the C-terminal one is formed by a Cys and a selenocysteine (Sec) residue [33]. This Sec is required for catalytic activity of mammalian TR, whose activity is therefore tightly regulated by dietary Se status in a dose-dependent manner [34, 35]. It was shown that there was about 8-37 folds increase in TR activity produced by supplementing 1 μM of Se in the medium of cultured cells compared to cells in medium without adding Se, which is accompanied by an relatively small increase in TR mRNA levels by only 2-5 fold and TR protein levels only up to 3-fold [34]. Studies also demonstrated that the amount of Se incorporated into TR increased from 0.01 to 0.98 Se unit per TR monomer as the Se concentration in the medium increased from 27 nM to 1 μM, with an increase in stability of TR mRNA [34]. In COS-1 cells transfected with rat TR1, it was shown that TR1 activity increased as the Se concentration in the medium increased, without a concomitant elevation in TR1 protein levels [36]. In agreement with cell culture studies, in vivo studies also demonstrated that deficient level of dietary Se intake by rats caused down-regulation of TR activity, mRNA and protein level in the liver, kidney and lung [34, 37, 38], whereas tissues from rats fed with super-nutritional levels of Se showed a transient increase in TR activity without an increase in TR protein level [37]. Both cell culture and in vivo studies suggest that most of the increase in TR activity detected following the addition of Se is mostly due to an increase in the incorporation of Se into the enzyme without much increase in protein synthesis of TR.

Alternations in TR activity might regulate the activities of its substrate, Trx, since it is the only known enzyme class to reduce oxidized Trx. Trx is a small ubiquitous protein, known to be an important endogenous redox-regulating molecule with thiol reducing activity [39-41]. Trx participates in redox reactions by reversible oxidation of the dithiol of the active center Cys32

and Cys35 residues to an intramolecular disulfide bond. It catalyzes dithiol-disulfide exchange reactions involving many thiol-dependent cellular processes, including intracellular signaling, gene regulation, resistance to oxidant stress, and control of apoptosis [41-43]. Hirota et al. demonstrated that Trx plays a dual and opposing role in the regulation of NF-κB. Overexpression of wild-type Trx suppressed NF-κB activation in the cytoplasm while nuclear-localized Trx enhanced NF-κB-dependent transcription [39]. TNF-α, PMA and UV irradiation are shown to induce the translocation of Trx from the cytoplasm to the nucleus [39, 44].

In this paper, we generated a computer simulation model using the STELLA program to test the hypothesis that adequate dietary Se can inhibit oxidative stress-induced HIV-1 transcription by suppressing NF-κB activation. We monitored the effects of Se supplementation and TNF-α treatment in the redox regulation of NF-κB and HIV-1 transcription. The results showed that our model strongly support our hypothesis, and indicate the benefits of Se supplementation as a nutritional therapeutic adjuvant to drug or chemotherapy to slow down disease progression in HIV-1-infected patients.

MODEL DESIGN

STELLA 5.1.1 was utilized to implement this model. The model diagram is shown in Fig. 5.1. The core of this model is the activation of NF-κB, which involves the phosphorylation and degradation of IκB and resulted disassociation of the IκB/NF-κB complex. Then, activated NF-κB dimers translocate into the nucleus, where it binds to HIV-1 LTR, triggers the gene transcription. Therefore, it is critical to inhibit or reduce the level of IκB phosphorylation in order to prevent NF-κB activation, control HIV-1 replication in the cell, and reduce viral

budding from the cell. The IκB/NF-κB complex is represented by compartment called “IκB and NFκB complex”. The initial level of this complex was arbitrarily set as 1. The inflow is a representation of the formation of the complex in the cytosol, which is “IkB and NFkB complex formation”. In a normal healthy cell, the level of this complex is assumed to remain at a steady state. There are two outflows from this compartment: one of them, “complex degradation”, represents the degradation of the IκB/NF-κB complex, whose half-life was arbitrarily set as 1 day; the other, “IkB phosphorylation”, represents the disassociation of the IκB from NF-κB dimer due to the phosphorylation of IκB, which is negatively affected by the level of GPx and Trx activity but is upregulated by TNF-α treatment. Because of the interactive relationship between GPx, Trx, TNF-α and IκB/NF-κB complex, modulators were connected to “IκB phosphorylation” from these factors. As described previously, after phosphorylation of IκB, free NF-κB dimers translocate into nucleus. So, “Activated NFκB in cytosol” and "Activated NFκB in nucleus" are two compartments followed after the IκB/NF-κB complex to represent the amount of activated NF-κB in the cytosol and nucleus, respectively. The compartment "Activated NFκB in nucleus" outflows via two path: one is “NFκB degradation”, which represents the degradation of the NF-κB dimers that do not bind to the LTR of HIV, the half-life of which is arbitrarily set as 0.6 days; the other is “NFκB binding to HIV-1 LTR”, which represents the part of the dimer population that actually binds to LTR to initiate HIV-1 transcription. These continuous three compartments of the model are represented by the equations listed below (1-3):

(1) IkB_and_NFkB_complex(t) = IkB_and_NFkB_complex(t - dt) +
(IkB_and_NFkB_complex_formation - IkB_phosphorylation - complex_degradation) * dt

INIT: IkB_and_NFkB_complex = 1

INFLOWS:

IkB_and_NFkB_complex_formation = 0.693*2

OUTFLOWS:

IkB_phosphorylation =

IkB_and_NFkB_complex*TNF_alpha_effect_on_NFkB*Trx_effect_on_NFkB*GPx_eff

ect_on_NFkB

complex_degradation = IkB_and_NFkB_complex*0.693

(2) Activated_NFkB_in_cytosol(t) = Activated_NFkB_in_cytosol(t - dt) + (IkB_phosphorylation - NFkB_translocation) * dt

INIT: Activated_NFkB_in_cytosol = 0

INFLOWS:

IkB_phosphorylation =

IkB_and_NFkB_complex*TNF_alpha_effect_on_NFkB*Trx_effect_on_NFkB*GPx_eff

ect_on_NFkB

OUTFLOWS:

NFkB_translocation = Activated_NFkB_in_cytosol

(3) Activated_NFkB_in_nucleus(t) = Activated_NFkB_in_nucleus(t - dt) + (NFkB_translocation - NFkB_degradation) * dt

INIT: Activated_NFkB_in_nucleus = 0

INFLOWS:

NFkB_translocation = Activated_NFkB_in_cytosol

OUTFLOWS:

NFkB_degradation = Activated_NFkB_in_nucleus*0.693/0.6

GPx is represented in a single compartment called “GPx level in cytosol” with its synthesis as inflow and its degradation as outflow. The initial level of GPx in cytosol is arbitrarily set as 1. In a normal healthy cell, the GPx level should remain at a steady state. The half-life of GPx in cytosol is 5 days. Since the synthesis of GPx protein increases with increasing level of Se in the cell, the modulator of Se is connected with the inflow of GPx synthesis. This compartment is represented by the equations listed below (4):

(4) GPx_level_in_cytosol(t) = GPx_level_in_cytosol(t - dt) + (GPx_synthesis - GPx_degradation) * dt

INIT: GPx_level_in_cytosol = 1

INFLOWS:

GPx_synthesis = Ks*Selenium

OUTFLOWS:

GPx_degradation = GPx_level_in_cytosol*Ke

In above equations, Ks is the synthesis factor and Ke is the elimination factor. Their equations are:

(5) Ks = 0.693/0.1

(6) Ke = 0.693/5

In addition to affect the synthesis of the GPx protein, Se level also affects the GPx activity. This effect is represented by an effect graph based on the data published by Sappey, et al. [8]. The equation for this modulator is:

(7) Se_effect_on_GPx_activity = GRAPH(Selenium)

(0.00, 1.00), (25.0, 2.73), (50.0, 2.67), (75.0, 2.50), (100, 2.13)

Therefore, the GPx activity is affect by Se through two paths: the synthesis of the protein and activity/unit of protein. Thus, the modulator “GPx activity” is represented by equation (8):

(8) GPx_activity = Se_effect_on_GPx_activity*GPx_level_in_cytosol.

Based on the experiment data, the assumption of nonlinear effect of GPx on NF-κB activation was made and was represented in the model as an effect graph called “GPx effect on NFkB”. The equation is:

(9) GPx_effect_on_NFkB = GRAPH(GPx_activity)

(0.00, 1.00), (200, 0.665), (400, 0.495), (600, 0.375), (800, 0.29), (1000, 0.225), (1200, 0.165), (1400, 0.12), (1600, 0.09), (1800, 0.065), (2000, 0.055)

Se level also affects the Trx effect on NF-κB activation in an indirect way via selenoprotein TR. TR is represented in a compartment with its synthesis as inflow and its degradation as outflow. The initial level and half-life of TR in cytosol are both arbitrarily set as 1. The Se modulator is connected to TR synthesis inflow through an effect modulator called “Se effect on TR synthesis” since the synthesis of this protein and incorporation of Se increases with increase of Se level in the cytosol. The Se modulator is also connected to TR activity through an effect modulator “Se effect on TR activity”. The reason to use two separate paths to represent TR is because the synthesis of TR protein increases to a lesser extent than the enzyme activity with the increase of Se in the cell. These two effect graphs were derived from data published by Gallegos, et al. [34]. Thus, the TR compartment in the model is represented by the equations listed below (10-13):

(10) TR_in_cytosol(t) = TR_in_cytosol(t - dt) + (TR_synthesis - TR_degradation) * dt

INIT: TR_in_cytosol = 1

INFLOWS:

TR_synthesis = Se_effect_on_TR_synthesis*0.693

OUTFLOWS:

TR_degradation = TR_in_cytosol*0.693

(11) Se_effect_on_TR_synthesis = GRAPH(Selenium)

(0.00, 1.00), (10.0, 2.30), (20.0, 3.03), (30.0, 3.50), (40.0, 3.73), (50.0, 3.95), (60.0, 4.05), (70.0, 4.15), (80.0, 4.20), (90.0, 4.25), (100, 4.28)

(12) Se_effect_on_TR_activity = GRAPH(Selenium)

(0.00, 0.3), (7.14, 16.3), (14.3, 18.1), (21.4, 19.6), (28.6, 21.0), (35.7, 22.2), (42.9, 23.4), (50.0, 24.3), (57.1, 25.2), (64.3, 25.9), (71.4, 26.6), (78.6, 27.1), (85.7, 27.6), (92.9, 28.1), (100.0, 28.5)

(13) TR_activity = Se_effect_on_TR_activity*TR

Trx is modeled in three continuous compartments, by the name of “Oxidized Trx in cytosol”, “Reduced Trx in cytosol” and “Reduced Trx in nucleus”, respectively. The inflow into the compartment “Oxidized Trx in cytosol” is “Trx synthesis”. The flow connecting this compartment and “Reduced Trx in cytosol” is “Trx reduction”, which represents the reduction of Trx from oxidized state to reduced state by TR. The modulator “TR activity” is connected to “Trx reduction”. The flow from “Reduced Trx in cytosol” to “Reduced Trx in nucleus” is called “Trx nuclear translocation”, which is activated by TNF-α treatment, and thus the TNF-α modulator is connected to “Trx nuclear translocation” through an effect modulator called “TNF alpha effect on Trx translocation”, whose effects were represented as an effect graph based on the data published by Hirota et al. [39]. The outflow of the compartment is “Degradation of reduced Trx in nucleus”. The half-life is arbitrarily set as 0.1. The Trx compartments, therefore, are represented by the equations below (14-17):

(14) Oxidized_Trx_in_cytosol(t) = Oxidized_Trx_in_cytosol(t - dt) + (Trx_synthesis - Trx_reduction) * dt

INIT: Oxidized_Trx_in_cytosol = 1

INFLOWS:

Trx_synthesis = 0.693*5

OUTFLOWS:

Trx_reduction = Oxidized_Trx_in_cytosol*TR_activity/(100+Oxidized_Trx_in_cytosol)

(In this equation, K_m for enzyme activity is arbitrarily set as 100).

(15) Reduced_Trx_in_cytosol(t) = Reduced_Trx_in_cytosol(t - dt) + (Trx_reduction - Trx_nuclear_translocation) * dt

INIT: Reduced_Trx_in_cytosol = 0

INFLOWS:

Trx_reduction = Oxidized_Trx_in_cytosol*TR_activity/(100+Oxidized_Trx_in_cytosol)

OUTFLOWS:

Trx_nuclear_translocation =

Reduced_Trx_in_cytosol*TNF_alpha_effect_on_Trx_translocation

(16) Reduced_Trx_in_nucleus(t) = Reduced_Trx_in_nucleus(t - dt) + (Trx_nuclear_translocation - Degradation_of_reduced_Trx_in_nucleus) * dt

INIT: Reduced_Trx_in_nucleus = 0

INFLOWS:

Trx_nuclear_translocation =

Reduced_Trx_in_cytosol*TNF_alpha_effect_on_Trx_translocation

OUTFLOWS:

Degradation_of_reduced_Trx_in_nucleus = Reduced_Trx_in_nucleus*0.693/0.1

(17) TNF_alpha_effect_on_Trx_translocation = GRAPH(TNF_alpha_level)

(0.00, 0.01), (10.0, 0.04), (20.0, 0.075), (30.0, 0.115), (40.0, 0.165), (50.0, 0.22), (60.0, 0.295), (70.0, 0.38), (80.0, 0.48), (90.0, 0.62), (100, 0.8)

Since Trx plays a duel and opposing role in regulating NF-κB activation and DNA binding ability, two effect graphs, “Trx effect on NF-κB activation in cytosol” and “Reduced Trx effect on NF-κB binding to LTR in nucleus”, are designed to represent the experimental data [39]. The assumption of nonlinear effect of Trx on NF-κB activation was made. The equations are (18-19):

(18) Trx_effect_on_NFkB_activation_in_cytosol = GRAPH(Reduced_Trx_in_cytosol)

(0.00, 0.995), (10.0, 0.72), (20.0, 0.575), (30.0, 0.465), (40.0, 0.39), (50.0, 0.335), (60.0, 0.3), (70.0, 0.27), (80.0, 0.25), (90.0, 0.23), (100, 0.22)

(19) Reduced_Trx_effect_on_NFkB_binding_to_LTR_in_nucleus = GRAPH(Reduced_Trx_in_nucleus)

(0.00, 0.825), (10.0, 1.88), (20.0, 2.45), (30.0, 2.85), (40.0, 3.08), (50.0, 3.30), (60.0, 3.48), (70.0, 3.65), (80.0, 3.83), (90.0, 3.95), (100, 4.00)

The modulator “TNF alpha level” models the changes of TNF-α level in the cell. TNF-α treatment exposes the cell under oxidative stress, and results in the activation of NF-κB in the absence or inadequacy of selenoproteins. This modulator is connected to the outflow from “Reduced Trx in cytosol”, which was described above, and is connected to “ IκB phosphorylation” through an effect graph modulator called “TNF alpha effect on NFκB”, which is represented by the equation (20):

(20) TNF_alpha_effect_on_NFkB = GRAPH(TNF_alpha_level)

(0.00, 0.1), (200, 3.90), (400, 3.70), (600, 3.40), (800, 3.00), (1000, 2.70), (1200, 2.56)

The nuclear activated NF-κB activates the HIV-1 transcription by binding to the κB sites located on the LTR region. The reduced state Trx in nucleus was shown to enhance NF-κB binding to DNA up to 4 folds [39]. Therefore, the modulator of “NFkB binding to HIV1 LTR” can be directly influenced by the compartment "Activated NFkB in nucleus", and at the same time, by the compartment “Reduced Trx in nucleus” through an effect modulator called “Reduced Trx effect on NFkB binding to LTR in nucleus”. Thus, the modulator “NFkB binding to HIV1 LTR” is represented using equation (21):

(21) NFkB_binding_to_HIV1_LTR =

Activated_NFkB_in_nucleus*Reduced_Trx_effect_on_NFkB_binding_to_LTR_in_nucleus

Since there are binding sites for other cellular transcription factors in HIV-1 LTR region besides NF-κB, the effect of the nucleus activated NF-κB was assumed to account for only 2/3 of overall activation of HIV-1 transcription.

Thus, the compartment “HIV1 mRNA” is modeled based on the effect that allows the quantity of "Activated NFkB in nucleus" to directly alter the rate of its inflow, which is “Transcription”, through the modulator “NFkB binding to HIV1 LTR”. The initial value of this compartment is arbitrarily set as 0. The outflow of “HIV1 mRNA” is labeled as “mRNA degradation” with half-life of mRNA arbitrarily set as 0.5 day. In the model, the “HIV1 mRNA” compartment is represented using equation (22):

(22) HIV1_mRNA(t) = HIV1_mRNA(t - dt) + (Transcription - mRNA_degradation) * dt

INIT: HIV1_mRNA = 0

INFLOWS:

Transcription = 2/3*NFkB_binding_to_HIV1_LTR*0.693/0.1

OUTFLOWS:

mRNA_degradation = HIV1_mRNA*0.693/0.5

The last compartment of the model is a representation of the HIV-1 viral load in the cell. This compartment monitors the accumulation of new virus particles in the cell and the release of virus into the blood stream via viral budding. The inflow to the compartment “HIV1” from “HIV1 mRNA” represents the directly contribution of HIV-1 transcription to the viral load in the cells. The initial value is arbitrarily set as 0. The outflow “Viral budding” is arbitrarily assumed to occur in one half-life, 1 day. When the cells are under oxidative stress when treated with TNF-α at the absence or low concentration of Se, the viral replication is then triggered by NF-κB binding to HIV-1 LTR. Then this compartment contains the amount of replicated virus. The “HIV1” compartment is represented in equations listed below (23):

(23) HIV1(t) = HIV(t - dt) + (Translation - Viral_budding) * dt

INIT: HIV1 = 0

INFLOWS:

Translation = HIV1_mRNA*0.693

OUTFLOWS:

Viral_budding = HIV1*.693/0.8

In this model, Se and TNF-α levels are the only variables whose values can be set within the range of 0—100 and 0—1200, respectively (Fig. 5.2). These two factors have opposing effects on NF-κB regulation. Therefore, this model can be test by comparing results generated by changing values of these two factors.

RESULTS

In the model, when both of the Se and TNF-α level are set as 0, HIV-1 shows a basal level replication, which results in a fairly low level of viral population in the cell (Fig. 5.3). The HIV-1 viral load increases by more than 6-fold when the TNF-α level in the cell increases up to 200, but decreases to a lesser level when TNF-α level reaches 1200. Therefore, TNF-α has the largest enhancing effect on HIV-1 replication at 200 (Fig. 5.3). When the Se level increases from 0 to 25 and TNF-α is fixed at 200, the viral load decreases to a steady state over the 14-day period, which is an approximately 1.5-fold increase of the basal level. When the Se level is set at 100, the viral load reaches the same steady state as when Se level was 25 but more rapidly (Fig. 5.3). Therefore, Se has the largest effect on inhibiting HIV-1 replication at level 25.

The behavior of the major compartments in the model is tested for a 14-day period by setting the levels of Se and TNF-α to different values. When Se and TNF-α are both at their basal values, which is 0, the quantity of GPx in cytosol is decreasing over time, TR remains at a steady state, and there is a slightly increase for reduced Trx in cytosol and nucleus due to its reduction by TR (Fig. 5.4 A). There is also a very low level of NF-κB activation in the nucleus, which results in a low basal level of HIV-1 replication in the cell (Fig. 5.4 B).

When Se level is 0 and TNF-α level is 200, both GPx and TR compartments behave in the same pattern as shown in Fig. 5.4 A. Due to the TNF-α treatment, which induces the nuclear translocation of the reduced Trx, by the end of the 14-day period, the amount of reduced Trx in the cytosol decreases about 6-fold while increases about 9-fold in the nucleus comparing to its basal values shown in Fig. 5.4 A (Fig. 5.5 A). The amount of IκB/NF-κB complex in the cytosol decreases for about 1.3-fold, whereas the amount of activated NF-κB in the nucleus increases for

about 18.5-fold and the amount of HIV-1 viral load in the cell 22-fold, comparing to their values in Fig. 5.4 B (Fig. 5.5 B).

When Se level is at 25 and TNF-α level is kept at 0, the amount of selenoprotein GPx in cytosol increases dramatically for about 9,000-fold at the end of the 14-day period. The amount of selenoprotein TR increases by 3.3-fold comparing to their values shown in Fig. 5.4 A. As a result, the amount of the reduced Trx in the cytosol increased by 57.7-fold, and the reduced Trx in the nucleus increases by 35-fold comparing to that shown in Fig. 5.4 A (Fig. 5.6 A). The amount of IκB/NF-κB complex in the cytosol increases slightly by 1-fold, whereas the amount of activated NF-κB in the nucleus and the amount of HIV-1 in the cell decrease by 15-fold and 33-fold, respectively, comparing to their values shown in Fig. 5.4 B (Fig. 5.6 B).

When Se is set at 25 and TNF-α is set at 200, GPx and TR behave the same as in Fig. 5.6 A (Fig. 5.7 A). The amount of reduced Trx in both cytosol and nucleus increases for about 36-fold and 38-fold (Fig. 5.7 A), respectively, comparing to their values when Se is at 0 and TNF-α is at 200, as shown in Fig. 5.5 A. However, the amount of the reduced Trx decreases by 9.6-fold in the cytosol and increases by approximately 10-fold in the nucleus while comparing to its value when Se is at 25 and TNF-α is at 0 (Fig. 5.6 A), due to TNF-α effect on Trx nuclear translocation. The amount of IκB/NF-κB complex in the cytosol shows a slight increase by 1.1-fold, whereas the amount of activated NF-κB in the nucleus and the amount of HIV-1 in the cell decreased for about 10.7- and 16-fold (Fig. 5.7 B), respectively, comparing to the values when Se is at 0 and TNF-α is at 200 (Fig. 5.5 B).

CONCLUSION AND DISCUSSION

Inducible gene expression is the major regulatory mechanism allowing cells to respond to changes in their environment. Gene expression induced by growth factors, cytokines, hormones, and other pathogenic stimuli mediated by ROS plays critical roles in HIV infection. As a key regulator of HIV-1 replication, the role of NF-κB in redox regulation is being intensively investigated. Numerous studies demonstrated that various antioxidants inhibit NF-κB activation and the expression of NF-κB target genes is upregulated in HIV-1 infected individuals. This model is designed to represent the dynamic behavior of NF-κB in the cytosol and nucleus under oxidative stress induced by TNF-α with or without Se supplementation. In addition, the model also monitors the relationship between Se supplementation (antioxidant level), TNF-α treatment (oxidative stress level) and the change of the level of HIV-1 replication in the cell over time.

High level of TNF-α is found in serum of AIDS patients and suggests its possible involvement in disease progression [45]. It is also known to induce the release of ROS into the cell [9] and exhibits a strong activating effect on HIV-1 replication via NF-κB. Dietary Se uptake is known to enhance the resistance of the cell to ROS and other mediators of oxidative stress [46]. It was demonstrated that low dose of Se can efficiently suppress NF-κB activation in response to TNF treatment [8, 29]. In the model, while cells are under oxidative stress and Se-deficient conditions, e.g. Se level is at 0 and TNF-α is 200, both NF-κB activation and HIV-1 viral load are very high (Fig. 5.5). Treatment with Se, e.g. Se level increases to 25 while TNF-α remains at 200, reduces both NF-κB activation and HIV-1 viral load dramatically (Fig. 5.7). This protective effect of Se is mainly attributed by its enhancing effect on synthesis and activity of selenoproteins GPx and TR. It was shown that very low concentration of Se are sufficient to

increase activity of GPx and TR. When Se increases from 0 to 25 in the model, there is dramatic increase of both selenoproteins, as shown in Fig. 5.6 and Fig. 5.7. Thus, based on the results (Fig. 5.3 through Fig. 5.7), we conclude the model well represents that the effect of TNF-α in inducing HIV-1 replication via promoting NF-κB activation, and that Se supplementation can partially reduce the oxidative stress induced by TNF-α in the cell to a lower level, thus reduces NF-κB activation and HIV-1 replication (Fig. 5.6 B and Fig. 5.7 B). These findings are in agreement with the results demonstrated experimentally [7-9, 29]. In addition to its effect on directly reducing HIV-1 transcription via inhibiting NF-κB binding of HIV-1 LTR, Se also inhibit the expression of NF-κB regulated expression of TNF noted in HIV-1 infection, thus decreases the oxidant level [47]. Due to complexity of the situation, this effect is not included in the model.

Trx plays opposite roles in the cytosol and in the nucleus in redox regulation of NF-κB. In the cytosol it inhibits the NF-κB activation whereas it promotes NF-κB binding to DNA in the nucleus [39]. TNF-α is known to induce nuclear translocation of Trx [39]. Thus, TNF-α not only activates NF-κB in cytosol, also enhances NF-κB binding to HIV-1 LTR via Trx, as shown in Fig. 5.4 through Fig. 5.7.

Activation of HIV-1 transcription in vivo is a very complicated process. AP-1 is another antioxidant-responsive transcription factor that can bind to LTR region to activate the HIV-1 transcription [51, 52]. In contrast to NF-κB, activation of AP-1 was not inhibited but slightly enhanced by Se supplementation in cell cultures [29]. A strong activation of AP-1 in cells treated with Trx was also observed [53]. Thus, in the model, NF-κB activated HIV-1 replication only accounts for 2/3 of all possible activation of HIV-1 transcription based on speculation and published experimental data [54, 55], and Se supplementation can only partially reduce the HIV-

1 transcription via inhibiting NF-κB activation. Therefore, increasing Se from 0 to 25 reduces the amount of HIV-1 in the cell to a lower level than that in the cell treated with only TNF-α, but still higher its basal level (Fig. 5.3, Fig. 5.4 B and Fig. 5.7 B).

Numerous oxidant stimuli are known to activate HIV-1 transcription in vivo. In addition to TNF-α, H_2O_2 and IL-1 were also reported to increase NF-κB activated HIV-1 transcription [6]. Besides Se, trace element zinc was also shown to significantly reduce NF-κB and AP-1 binding to HIV-1 LTR [56] [57]. The nature of HIV-caused disease is a continuous process involves immune dysfunction and depletion of $CD4^+$ helper T cells, mostly bystander uninfected cells, through apoptosis in vivo [58, 59]. It was suggested that TNF stimulation and expression of HIV-1 Nef protein could inhibit apoptosis in HIV-1-infected $CD4^+$ T lymphocytes [59, 60]. Due to the high level of the complexity of HIV-1 infection, the roles of other cellular transcription factors and oxidant stimuli, the apoptosis of $CD4^+$ T cells, and other HIV-1 proteins in the disease progression are not included in the model.

It is worth to mention that several selenoprotein modules encoded by HIV-1 were proposed based on theoretical evidence [48]. One of them is *env-fs*, later identified as vGPx, which has high sequence similarities to the mammalian GPx and has functional GPx activity when expressed as a selenoprotein in mammalian cells [49, 50]. The other selenoprotein possibly encoded by HIV-1 in overlapping protease-coding region is *pro-fs*, which is now identified as a mimic of NF-κB. When expressed in mammalian cells, *pro-fs* localizes in the nuclei as a dimer and exerts bioactivity in activating HIV LTR via NF-κB (Chapter 3; Taylor, et al., unpublished data). Both in vitro and in vivo studies showed that *pro-fs* is a substrate of Trx that the interaction of these two proteins is structural specific (Chapter 2 and 4). The actual role of these viral selenoproteins in HIV-1 infection and disease progression is not clear yet. It is well known

that Se is a potent regulator of both NF-κB activity and HIV-1 transcription via cellular selenoproteins. It is therefore reasonable that HIV-1 could have evolved to directly participate in redox signaling cascades by encoding its own selenoprotein. Simply put, viral selenoproteins could very well hijack host Se from cellular selenoprotein, thus, interferes with the immune antioxidant defense of the infected host [50]. As in the case of *pro-fs*, it might also participate in activating HIV transcription as well. Thus, the existence of HIV-encoded selenoproteins can help to understand the disease pathogenic mechanism and to explain why the effects of HIV-1 infection are exacerbated in Se-deficient patients [50].

Most of the data used in the model were obtained from publications although some arbitrary values were used because of short of experimental information, such as the half-life of TR, Trx, IκB/NF-κB complex, activated NF-κB in nucleus, HIV-1 mRNA and HIV-1 in human cell. Arbitrary numbers were set to serve the purpose of the model design. To fulfill the use of this model, the model needs to be tested using more published data on this subject.

Regardless, the model is successful because it exhibited the primary objectives of the model design and answered the question, " Can Se supplementation maintain the HIV-1 in the cell at a low level when the cell is under oxidative stress?" The model helps to understand the importance of trace element supplementation (in this case, Se) that Se administration may provide beneficial effects in the treatment of HIV-infected individuals. Dietary Se uptake may be used as an alternative way or in combination with current expensive and lots-of-side-effect drug therapy to inhibit HIV replication, and thereby to prolong the latency period of the virus. It is conceivable that adjuvant therapy with Se may prove to be efficient not only inhibiting HIV replication but also in enhancing the resistance of T cell toward oxidative stress and apoptosis.

REFERENCES

1. Allavena, C., et al., *Relationship of trace-element, immunological markers, and HIV infection progression.* Biol. Trace Elem. Res., 1995. **47**(133-138).
2. Baum, M.K., et al., *High risk of HIV-related mortality is associated with selenium deficiency.* J Acquir Immune Defic Syndr Hum Retrovirol, 1997. **15**: p. 370-376.
3. Constans, J., et al., *Serum selenium predicts outcome in HIV infection.* J. Acquir. Immune. Defic. Syndr. Hum. Retrovirol., 1995. **10**(3): p. 392.
4. Dworkin, B.M., *Selenium deficiency in HIV infection and the acquired immunodeficiency syndrome (AIDS).* Chem. Biol. Interact., 1994. **91**: p. 181-186.
5. Look, M.P., et al., *Serum selenium versus lymphocyte subsets and markers of disease progression and inflammatory response in human immunodeficiency virus-1 infection.* Biological Trace Element Research, 1997. **56**(1): p. 31-41.
6. Brigelius-Flohe, R., et al., *Interleukin-1-induced nuclear factor kappa B activation is inhibited by overexpression of phospholipid hydroperoxide glutathione peroxidase in a human endothelial cell line.* Biochemical Journal, 1997. **328**: p. 199-203.
7. Hori, L., et al., *Selenium supplementation suppresses tumor necrosis factor α-induced human immunodeficiency virus type 1 replication in vitro.* AIDS Research And Human Retroviruses, 1997. **13**: p. 1325-1332.
8. Sappey, C., et al., *Stimulation of glutathione peroxidase activity decreases HIV type 1 activation after oxidative stress.* AIDS. Res. Hum. Retroviruses., 1994. **10**(11): p. 1451-1461.

9. Tolando, R., et al., *Reactive oxygen species and proinflammatory cytokine signaling in endothelial cells: effect of selenium supplementation.* Free Radical Biology and Medicine, 2000. **28**(6): p. 979-986.

10. Griffin, G.E., et al., *Activation of HIV gene expression during monocyte differentiation by induction of NF-kappa B.* Nature, 1989. **339**(6219): p. 70-73.

11. Schreck, R., P. Rieber, and P.A. Baeuerle, *Reactive oxygen intermediates as apparently widely used messengers in the activation of the NF-kappa B transcription factor and HIV-1.* The EMBO Journal, 1991. **10**(8): p. 2247-2258.

12. Schreck, R., K. Albermann, and P. Bauerle, *Nuclear factor κB: An oxidative stress-response transcription factor of eukaryotic cells.* Free Rad. Res. Comm., 1992. **17**: p. 221-237.

13. Schulze-Osthoff, K., et al., *Depletion of the mitochondrial electron transport abrogates the cytotoxic and gene-inductive effects of TNF.* EMBO J., 1993. **12**(8): p. 3095-3104.

14. Baldwin, A.S., *THE NF-κB AND IκB PROTEINS: New Discoveries and Insights.* Annual Review of Immunology, 1996. **14**(1): p. 649-681.

15. Antoni, B.A., S.B. Stein, and A.B. Rabson, *Regulation of human immunodeficiency virus infection: implications for pathogenesis.* Adv Virus Res, 1994. **43**: p. 53-145.

16. Baeuerle, P. and D. Baltimore, *A 65-kappaD subunit of active NF-kappaB is required for inhibition of NF-kappaB by I kappaB.* Genes Dev., 1989. **3**(11): p. 1689-1698.

17. Bednarik, D.P. and T.M. Folks, *Mechanisms of HIV-1 latency.* AIDS, 1992. **6**(1): p. 3-16.

18. Doerre, S., et al., *The c-rel Protooncogene Product Represses NF-{kappa}B p65-Mediated Transcriptional Activation of the Long Terminal Repeat of Type 1 Human Immunodeficiency Virus.* PNAS, 1993. **90**(3): p. 1023-1027.

19. Kawakami, K., C. Scheidereit, and R.G. Roeder, *Identification and purification of a human immunoglobulin-enhancer-binding protein (NF-kappa B) that activates transcription from a human immunodeficiency virus type 1 promoter in vitro.* PNAS, 1988. **85**(13): p. 4700-4704.

20. Rabson, A.B. and H.-C. Lin, *NF-κB and HIV: Linking Viral and Immune Activation*, in *HIV-1: Molecular Biology and Pathogenesis - Viral Mechanisms*, K.-T. Jeang, Editor. 2000, Academic Press. p. 161-207.

21. Brown, K., et al., *Mutual regulation of the transcriptional activator NF-kappa B and its inhibitor, I kappa B-alpha.* Proceedings Of The National Academy Of Sciences Of The United States Of America, 1993. **90**(6): p. 2532-2536.

22. Ginn-Pease, M.E. and R.L. Whisler, *Optimal NF[kappa]B Mediated Transcriptional Responses in Jurkat T Cells Exposed to Oxidative Stress Are Dependent on Intracellular Glutathione and Costimulatory Signals.* Biochemical and Biophysical Research Communications, 1996. **226**(3): p. 695-702.

23. Menon, S.D., G.R. Guy, and Y.H. Tan, *Involvement of a putative protein-tyrosine phosphatase and I kappa B-alpha serine phosphorylation in nuclear factor kappa B activation by tumor necrosis factor.* The Journal Of Biological Chemistry, 1995. **270**(32): p. 18881-18887.

24. Sen, R. and D. Baltimore, *Inducibility of kappa immunoglobulin enhancer-binding protein Nf-kappa B by a posttranslational mechanism.* Cell, 1986. **47**(6): p. 921-928.

25. Zhang, D., et al., *HIV type 1 protease activation of NF-kappa B within T lymphoid cells.* AIDS Research And Human Retroviruses, 1995. **11**(2): p. 223-230.

26. Suzuki, Y.J., B.B. Aggarwal, and L. Packer, *Alpha-lipoic acid is a potent inhibitor of NF-kappa B activation in human T cells.* Biochem Biophys Res Commun, 1992. **189**(3): p. 1709-1715.

27. Yang, J.-P., et al., *Inhibition of the DNA-binding activity of NF-kappa B by gold compounds in vitro.* FEBS Lett, 1995. **361**(1): p. 89-96.

28. Kretz-Remy, C., et al., *Inhibition of I kappa B-alpha phosphorylation and degradation and subsequent NF-kappa B activation by glutathione peroxidase overexpression.* J. Cell Biol., 1996. **133**(5): p. 1083-1093.

29. Makropoulos, V., T. Brüning, and K. Schulze-Osthoff, *Selenium-mediated inhibition of transcription factor NF kappa B and HIV-1 LTR promoter activity.* Archives of Toxicology, 1996. **70**(5): p. 277 - 283.

30. Weiss, S.S. and R.A. Sunde, *Selenium regulation of transcript abundance and translational efficiency of glutathione peroxidase-1 and -4 in rat liver.* Biochem J., 2001. **357**(Pt 3): p. 851-858.

31. Weiss, S.L., et al., *The selenium requirement for glutathione peroxidase mRNA level is half of the selenium requirement for glutathione peroxidase activity in female rats.* J. Nutrition, 1996. **126**(9): p. 2260-2267.

32. Weiss, S.L., et al., *Dietary selenium regulation of glutathione peroxidase mRNA and other selenium-dependent parameters in male rats.* The Journal of Nutritional Biochemistry, 1997. **8**(2): p. 85-91.

33. Gladyshev, V.N., K.-T. Jeang, and T.C. Stadtman, *Selenocysteine, identified as the penultimate C-terminal residue in human T-cell thioredoxin reductase, corresponds to TGA in the human placental gene.* PNAS, 1996. **93**(12): p. 6146-6151.

34. Gallegos, A., et al., *Mechanisms of the regulation of thioredoxin reductase activity in cancer cells by the chemopreventive agent selenium.* Cancer Res, 1997. **57**(21): p. 4965-4970.

35. Hadley, K.B. and R.A. Sunde, *Selenium regulation of thioredoxin reductase activity and mRNA levels in rat liver.* The Journal of Nutritional Biochemistry, 2001. **12**(12): p. 693-702.

36. Fujiwara, N., et al., *Functional expression of rat thioredoxin reductase: selenocysteine insertion sequence element is essential for the active enzyme.* Biochem J., 1999. **340**(Pt 2): p. 439-444.

37. Berggren, M., et al., *Cellular thioredoxin reductase activity is regulated by selenium.* Anticancer Res., 1997. **17**(5A): p. 3377-3380.

38. Hill, K.E., et al., *Thioredoxin Reductase Activity Is Decreased by Selenium Deficiency.* Biochemical and Biophysical Research Communications, 1997. **234**(2): p. 293-295.

39. Hirota, K., et al., *Distinct Roles of Thioredoxin in the Cytoplasm and in the Nucleus. A TWO-STEP MECHANISM OF REDOX REGULATION OF TRANSCRIPTION FACTOR NF-kappa B.* J. Biol. Chem., 1999. **274**(39): p. 27891-27897.

40. Liu, Y. and W. Min, *Thioredoxin Promotes ASK1 Ubiquitination and Degradation to Inhibit ASK1-Mediated Apoptosis in a Redox Activity-Independent Manner.* Circ Res, 2002. **90**(12): p. 1259-1266.

41. Tanaka, T., et al., *Redox regulation by thioredoxin superfamily; protection against oxidative stress and aging.* Free Radic Res, 2000. **33**(6): p. 851-855.

42. Arner, E.S.J. and A. Holmgren, *Physiological functions of thioredoxin and thioredoxin reductase.* Eur J Biochem, 2000. **267**(20): p. 6102-6109.

43. Powis, G., D. Mustacich, and A. Coon, *The role of the redox protein thioredoxin in cell growth and cancer.* Free Radic Biol Med, 2000. **29**(3-4): p. 312-322.

44. Hirota, K., et al., *AP-1 transcriptional activity is regulated by a direct association between thioredoxin and Ref-1.* PNAS, 1997. **94**(8): p. 3633-3638.

45. Kobayashi, S., et al., *Serum level of TNF alpha in HIV-infected individuals.* AIDS, 1990. **4**(2): p. 169-170.

46. Taylor, E.W., et al., *Nutrition, HIV, and drug abuse: the molecular basis of a unique role for selenium.* J Acquir Immune Defic Syndr, 2000. **25 Suppl 1**: p. S53-61.

47. Droge, W., H.-P. Eck, and S. Mihm, *HIV-induced cysteine deficiency and T-cell dysfunction -- a rationale for treatment with N-acetylcysteine.* Immunology Today, 1992. **13**(6): p. 211-214.

48. Taylor, E.W., et al., *A Basis for New Approaches to the Chemotherapy of AIDS: Novel Genes in HIV-1 Potentially Encode Selenoproteins Expressed by Ribosomal Frameshifting and Termination Suppression.* J. Med. Chem., 1994. **37**: p. 2637-2654.

49. Zhang, W., et al., *Selenium-dependent glutathione peroxidase modules encoded by RNA viruses.* Biol. Trace. Elem. Res., 1999. **70**(2): p. 97-116.

50. Zhao, L., et al., *Molecular modeling and in vitro activity of an HIV-1-encoded glutathione peroxidase.* Proc. Natl. Acad. Sci. U.S.A., 2000. **97**(12): p. 6356-6361.

51. Meyer, M., R. Schreck, and P. Baeuerle, *H2O2 and antioxidants have opposite effects on activation of NF-kappa B and AP-1 in intact cells: AP-1 as secondary antioxidant-responsive factor.* EMBO J., 1993. **12**(5): p. 2005-2015.

52. Schulze-Osthoff, K., H. Schenk, and W. Droge, *Effects of thioredoxin on activation of transcription factor NF-kappa B.* Methods Enzymol, 1995. **252**: p. 253-64.

53. Schenk, H., et al., *Distinct Effects of Thioredoxin and Antioxidants on the Activation of Transcription Factors NF-{kappa}B and AP-1.* PNAS, 1994. **91**(5): p. 1672-1676.

54. Luciw, P.A. and B.L. Shacklett, *Molecular biology of the human and simian immunodeficiency viruses.*, in *HIV Molecular Organization, Pathogenicity and Treatment.*, W.J.W. Morrow and N.L. Haigwood, Editors. 1993, Elsevier Science Publishers. p. 123-219.

55. Ross, E.K., et al., *Contribution of NF-kappa B and Sp1 binding motifs to the replicative capacity of human immunodeficiency virus type 1: distinct patterns of viral growth are determined by T-cell types.* J Virol., 1991. **65**(8): p. 4350-4358.

56. Connell, P., et al., *Zinc attenuates tumor necrosis factor-mediated activation of transcription factors in endothelial cells.* J Am Coll Nutr, 1997. **16**(5): p. 411-417.

57. Hennig, B., et al., *Antioxidant-Like Properties of Zinc in Activated Endothelial Cells.* J Am Coll Nutr, 1999. **18**(2): p. 152-158.

58. Goldberg, B. and R.B. Stricker, *Apoptosis and HIV infection: T-cells fiddle while the immune system burns.* Immunology Letters, 1999. **70**(1): p. 5-8.

59. Kirchhoff, F., et al., *Absence of Intact nef Sequences in a Long-Term Survivor with Nonprogressive HIV-1 Infection.* N Engl J Med, 1995. **332**(4): p. 228-232.

60. Mahlknecht, U., et al., *Resistance to Apoptosis in HIV-Infected CD4+ T Lymphocytes Is Mediated by Macrophages: Role for Nef and Immune Activation in Viral Persistence.* J Immunol, 2000. **165**(11): p. 6437-6446.

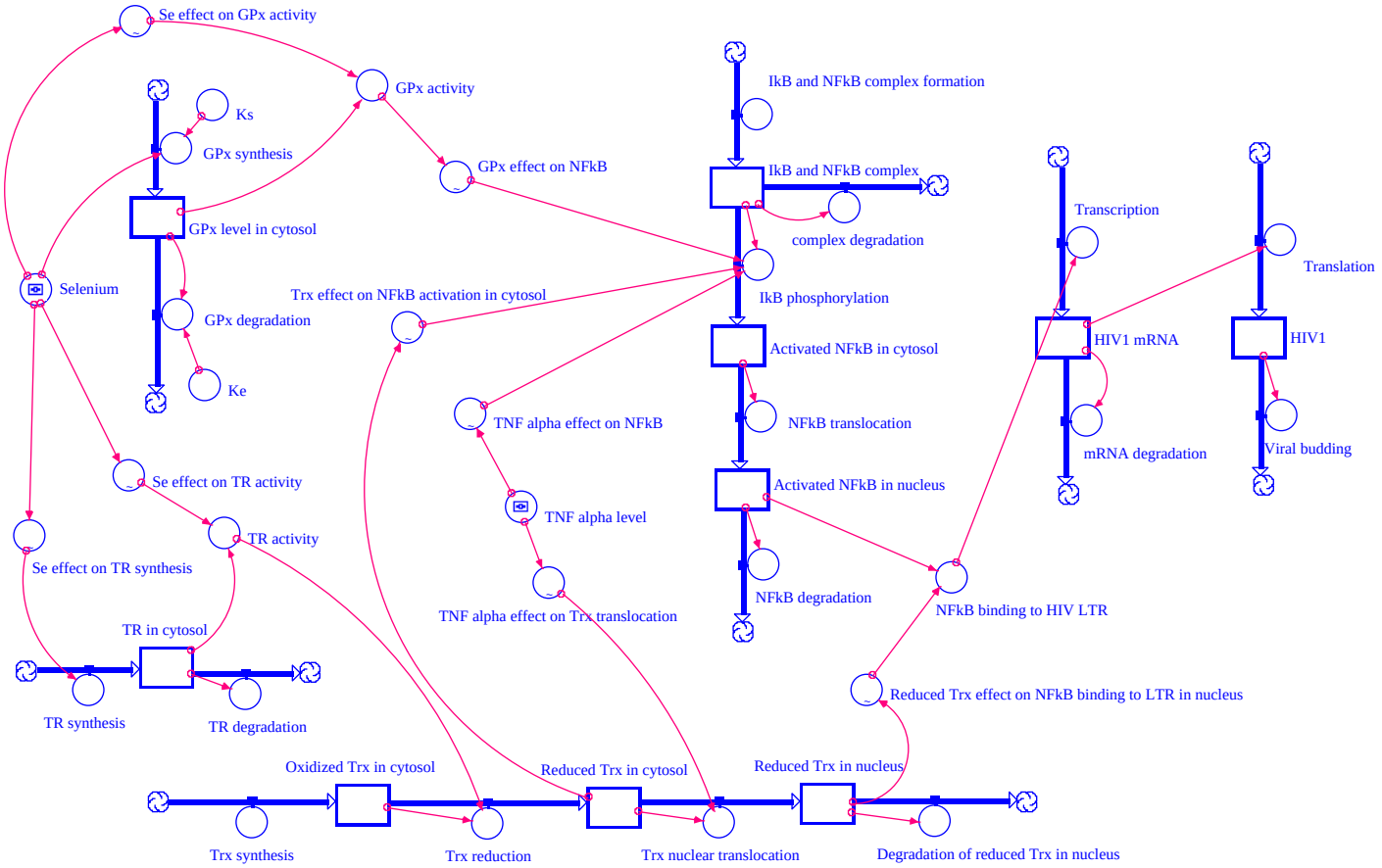

Figure 5.1. The scheme of STELLA model (see Model Design in Chapter 5 for detail description).

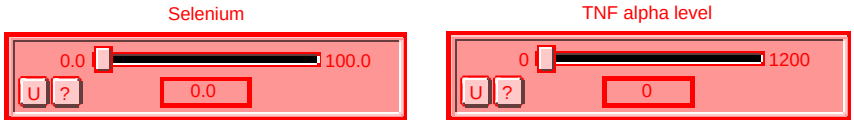

Figure 5.2. Selenium and TNF-α are the two variables in the STELLA model. Selenium level was set with a range of 0-100, and TNF-α level was set with a range of 0-1200.

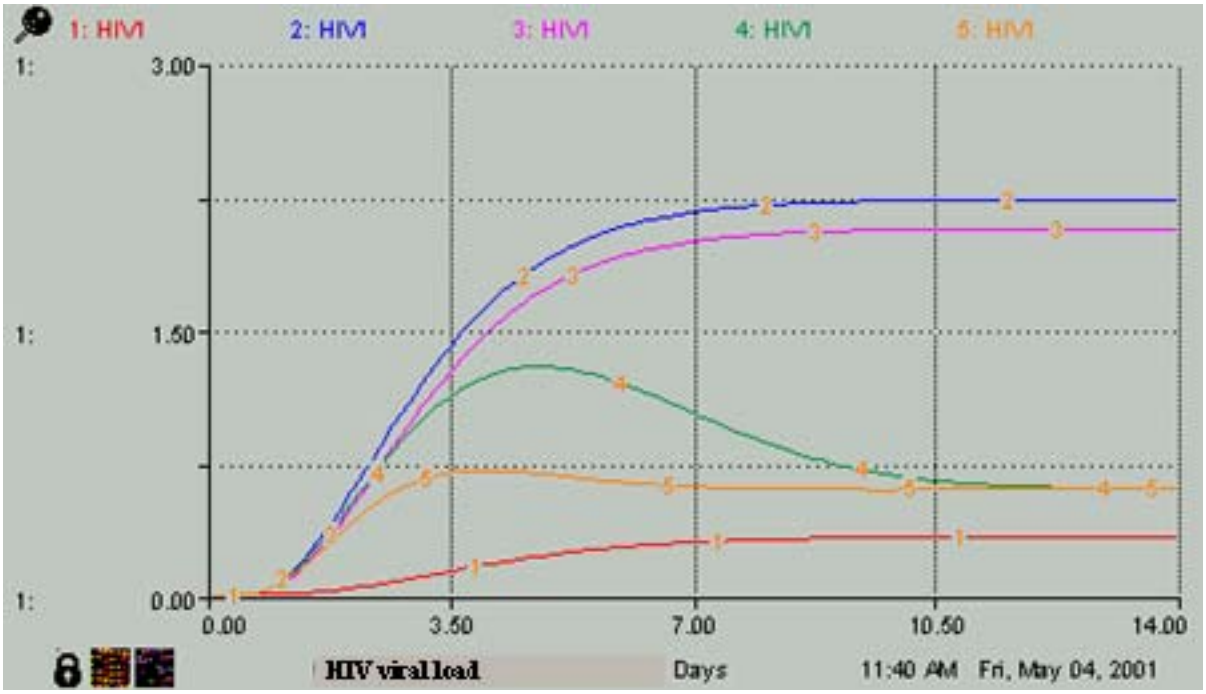

Figure 5.3. The change of HIV-1 viral load in the cell when expose to various levels of oxidative stress (TNF-α) and antioxidant status (Se) in a 14-day period. The curves are color coded, matching with the numbers. (1) HIV-1 viral load when both Se and TNF-α are 0. (2) HIV-1 viral load when Se is 0 and TNF-α is 200, which is the maximum effect level for TNF-α. (3) HIV-1 viral load when Se is 0 and TNF-α is 1200. (4) HIV-1 viral load when Se is 25 and TNF-α is 200. (5) HIV-1 viral load when Se is 100 and TNF-α is 200.

A

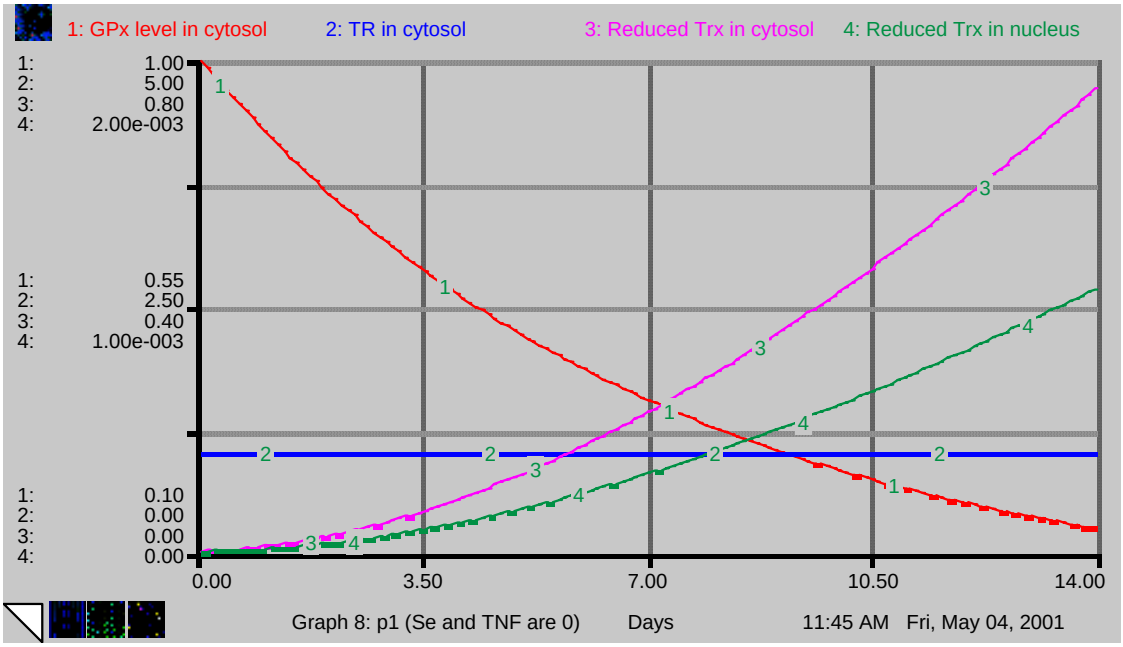
1: GPx level in cytosol
2: TR in cytosol
3: Reduced Trx in cytosol
4: Reduced Trx in nucleus
1: 1.00
2: 5.00
3: 0.80
4: 2.00e-003
1: 0.55
2: 2.50
3: 0.40
4: 1.00e-003
1: 0.10
2: 0.00
3: 0.00
4: 0.00
0.00
3.50
7.00
10.50
14.00
Graph 8: p1 (Se and TNF are 0)
Days
11:45 AM Fri, May 04, 2001

B

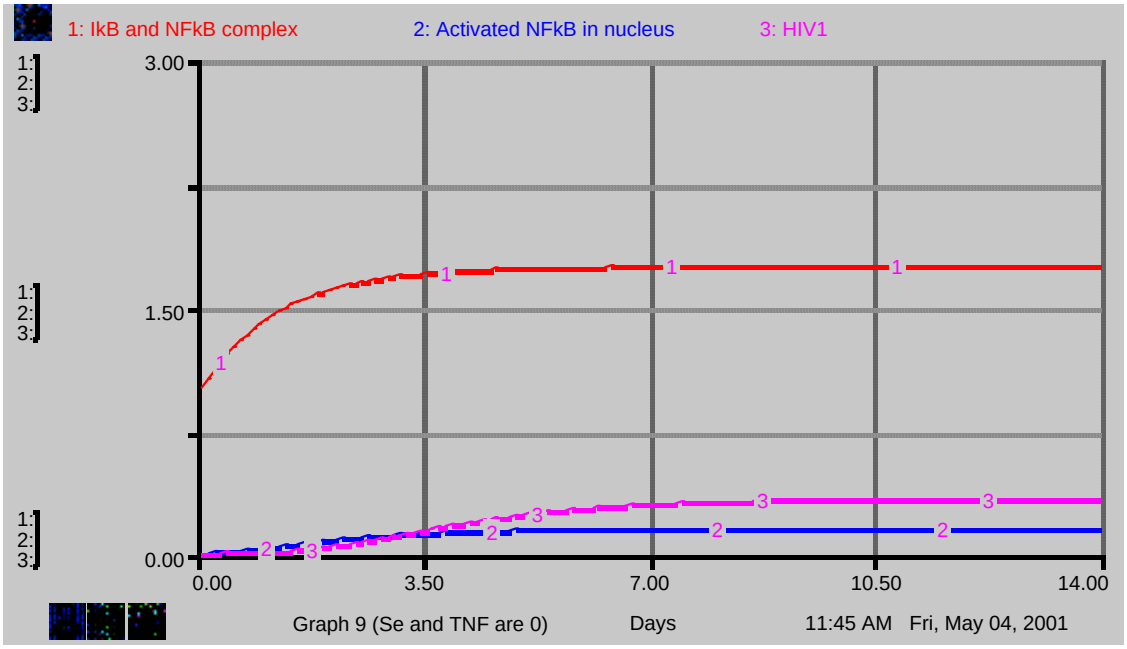
1: IkB and NFkB complex
2: Activated NFkB in nucleus
3: HIV1
3.00
1.50
0.00
0.00
3.50
7.00
10.50
14.00
Graph 9 (Se and TNF are 0)
Days
11:45 AM Fri, May 04, 2001

Figure 5.4. Dynamic behavior of the system in the model during a 14-day period when Se and TNF-α are both set at 0, their initial level. The curves are color coded, matching with the number. **A.** (1) Amount of GPx in cytosol. (2) Amount of TR in cytosol. (3) Amount of reduced state Trx in cytosol. (4) Amount of reduced Trx in nucleus. **B.** (1) Amount of IκB/NF-κB complex in cytosol. (2) Amount of activated NF-κB in nucleus. (3) Amount of HIV-1 in the cell.

A

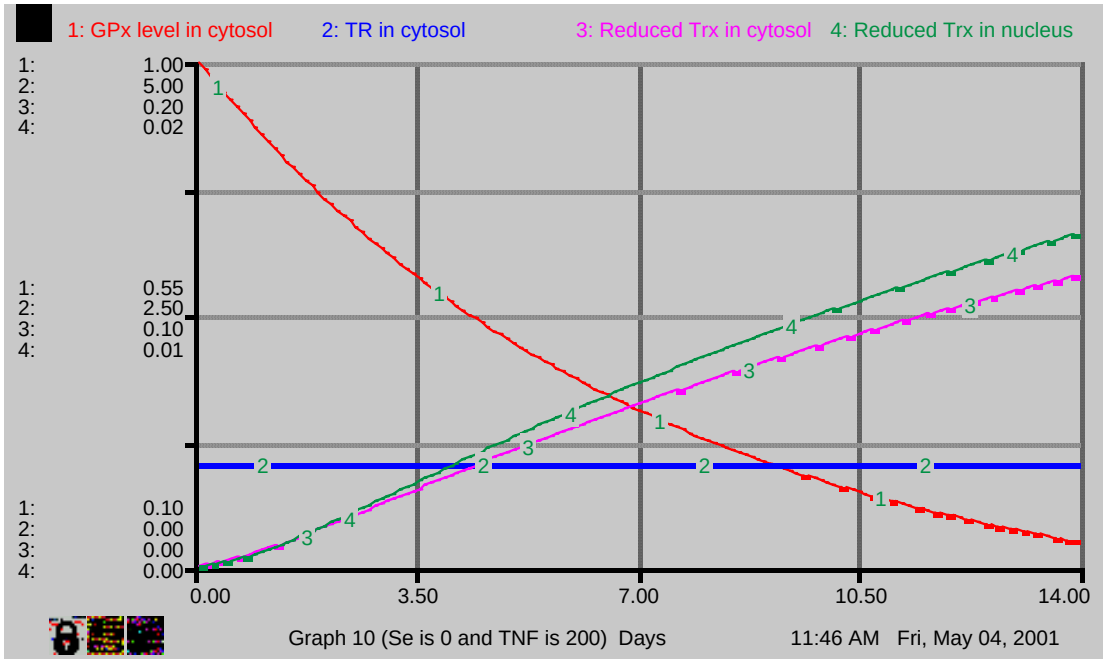
1: GPx level in cytosol
2: TR in cytosol
3: Reduced Trx in cytosol
4: Reduced Trx in nucleus
1: 1.00
2: 5.00
3: 0.20
4: 0.02
1: 0.55
2: 2.50
3: 0.10
4: 0.01
1: 0.10
2: 0.00
3: 0.00
4: 0.00
0.00
3.50
7.00
10.50
14.00
Graph 10 (Se is 0 and TNF is 200) Days
11:46 AM Fri, May 04, 2001

B

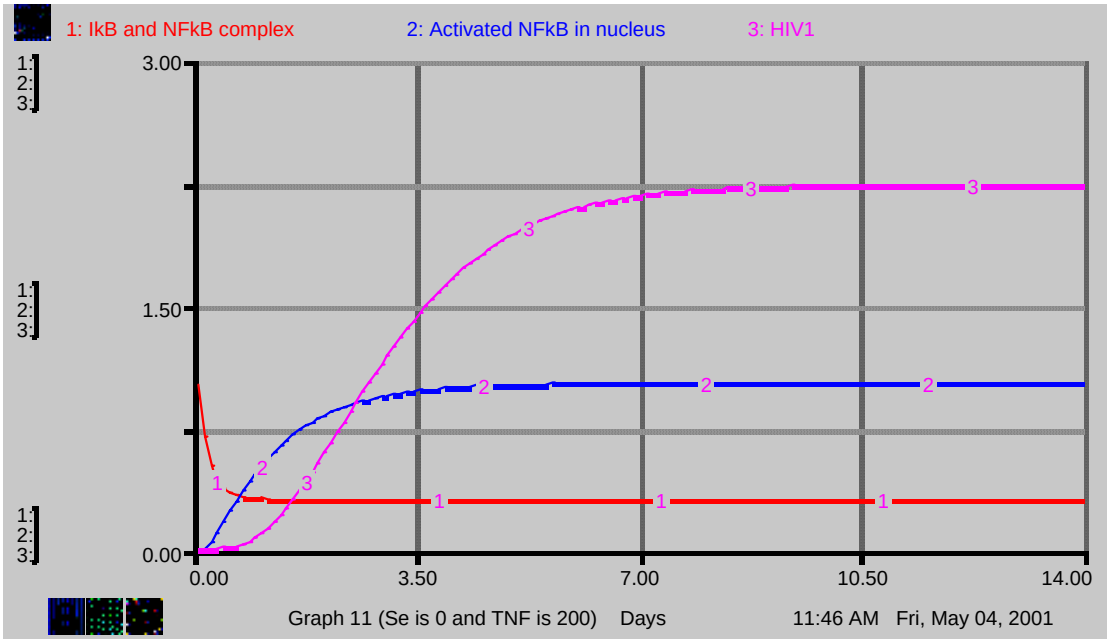
1: IkB and NFkB complex
2: Activated NFkB in nucleus
3: HIV1
3.00
1.50
0.00
0.00
3.50
7.00
10.50
14.00
Graph 11 (Se is 0 and TNF is 200) Days
11:46 AM Fri, May 04, 2001

Figure 5.5. Dynamic behavior of the system in the model during a 14-day period when Se is set at 0 and TNF-α is set at 200. The curves are color coded, matching with the number. **A.** (1) Amount of GPx in cytosol; (2) Amount of TR in cytosol; (3) Amount of reduced state Trx in cytosol; (4) Amount of reduced Trx in nucleus. **B.** (1) Amount of IκB/NF-κB complex in cytosol; (2) Amount of activated NF-κB in nucleus; (3) Amount of HIV-1 in the cell.

A

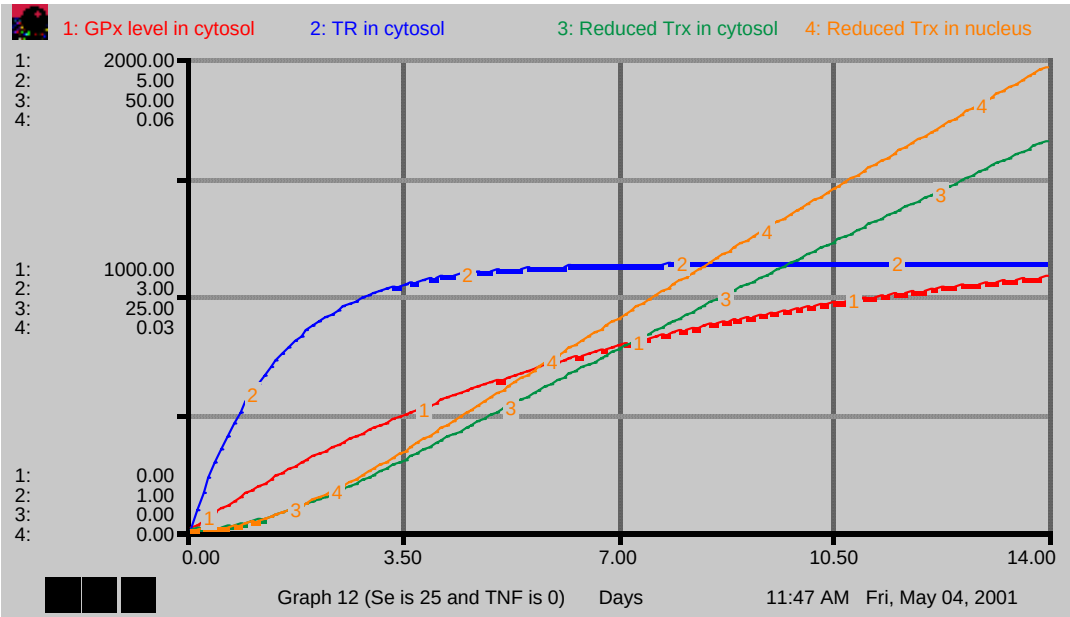
1: GPx level in cytosol
2: TR in cytosol
3: Reduced Trx in cytosol
4: Reduced Trx in nucleus
2000.00
5.00
50.00
0.06
1000.00
3.00
25.00
0.03
0.00
1.00
0.00
0.00
0.00
3.50
7.00
10.50
14.00
Graph 12 (Se is 25 and TNF is 0)
Days
11:47 AM Fri, May 04, 2001

B

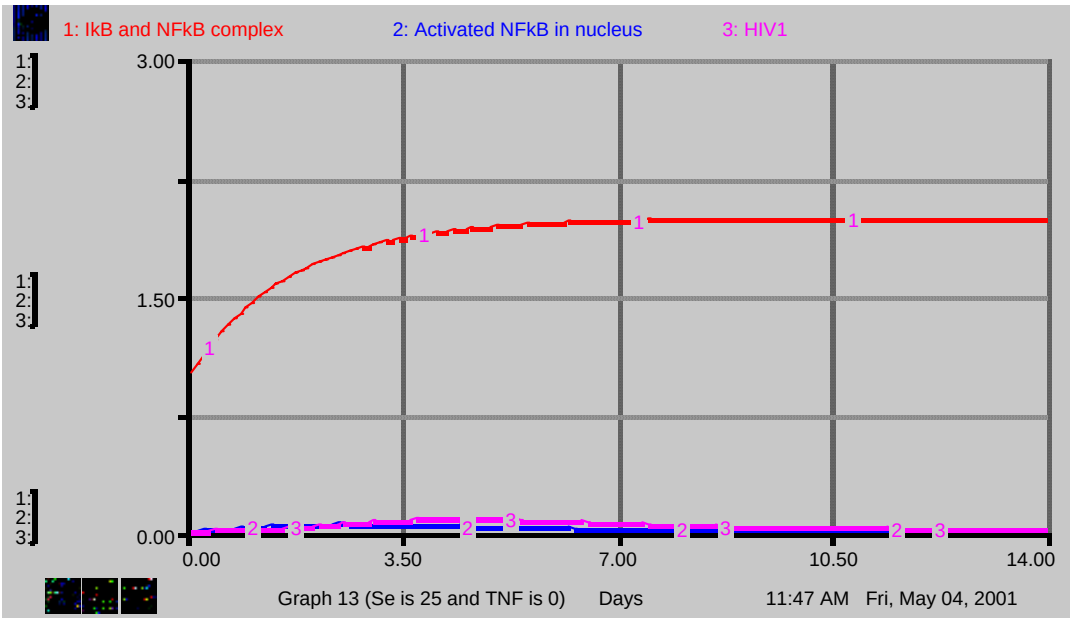
1: IkB and NFkB complex
2: Activated NFkB in nucleus
3: HIV1
3.00
1.50
0.00
0.00
3.50
7.00
10.50
14.00
Graph 13 (Se is 25 and TNF is 0)
Days
11:47 AM Fri, May 04, 2001

Figure 5.6. Dynamic behavior of the system in the model during a 14-day period when Se is 25 and TNF-α is 0. The curves are color coded, matching with the number. **A.** (1) Amount of GPx in cytosol; (2) Amount of TR in cytosol; (3) Amount of reduced state Trx in cytosol; (4) Amount of reduced Trx in nucleus. **B.** (1) Amount of IκB/NF-κB complex in cytosol; (2) Amount of activated NF-κB in nucleus; (3) Amount of HIV-1 in the cell.

A

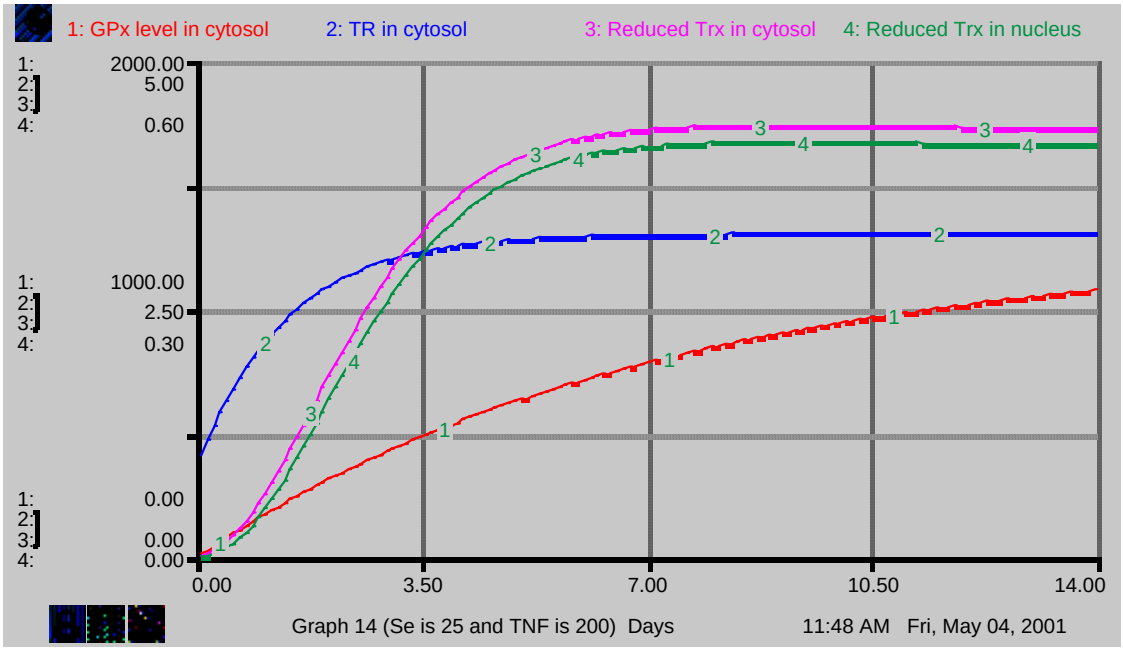
1: GPx level in cytosol
2: TR in cytosol
3: Reduced Trx in cytosol
4: Reduced Trx in nucleus
2000.00
5.00
0.60
1000.00
2.50
0.30
0.00
0.00
0.00
0.00
3.50
7.00
10.50
14.00
Graph 14 (Se is 25 and TNF is 200) Days
11:48 AM Fri, May 04, 2001

B

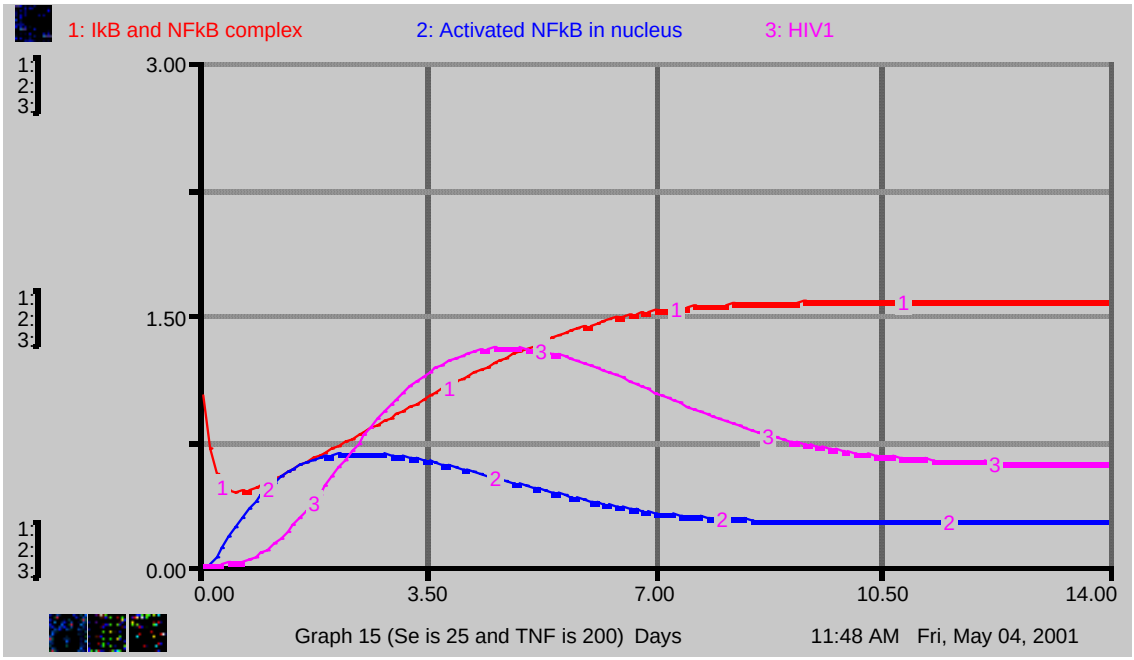
1: IkB and NFkB complex
2: Activated NFkB in nucleus
3: HIV1
3.00
1.50
0.00
0.00
3.50
7.00
10.50
14.00
Graph 15 (Se is 25 and TNF is 200) Days
11:48 AM Fri, May 04, 2001

Figure 5.7. Dynamic behavior of the system in the model during a 14-day period when Se is set at 25 and TNF-α is set at 200. The curves are color coded, matching with the number. **A.** (1) Amount of GPx in cytosol; (2) Amount of TR in cytosol; (3) Amount of reduced state Trx in cytosol; (4) Amount of reduced Trx in nucleus. **B.** (1) Amount of IκB/NF-κB complex in cytosol; (2) Amount of activated NF-κB in nucleus; (3) Amount of HIV-1 in the cell.

CHAPTER 6

CONCLUSIONS

Our results in all experiments strongly support the hypotheses tested. In summary, the key points are listed here. First, we demonstrate here that this HIV-1 encoded peptide, *pro-fs*, is a mimic of NF-κB and interacts with human cellular antioxidative protein Trx with high affinity in vitro, shown by both co-immunoprecipitation and GST-pull down assay. We were also able to show that *pro-fs* interacts with both wild type (Trx-wt) and the double Cys mutant (Trx-CS) of Trx, in which the two active center Cys residues were mutated to Ser. Therefore, our data suggest that this interaction is structural specific that involves more amino acid residues at the interactive surfaces. These results are in agreement with the modeling results of Taylor, et al. (unpublished data), which demonstrate that Trx binds *pro-fs* with a more favorable energy compared to Trx binding to its known ligand, the DNA binding loop of NF-κB, and that at least 8 amino acid residues are involved in the protein-protein interaction. The GST-pull down assay developed in this study can be further applied to the lysate of HIV-1 infected celsl. Combined with ^{75}Se labeling and 2-D electrophoresis, it could allow the detection of *pro-fs*. Second, when *pro-fs* was expressed in mammalian cells, including 293T, HeLa and MDCK cells, live cell imaging results showed that *pro-fs* localizes exclusively in the cell nucleus. Since *pro-fs* has sequence homology with the DNA-binding loop of NF-κB, we speculate that *pro-fs* may also bind to DNA, either to HIV LTR to activate HIV replication, or to host DNA to up-regulate important cellular genes that are usually regulated by NF-κB. FRET analysis using confocal microscopy revealed that *pro-fs* forms oligomer. Based on its sequence similarity with HIV-1 protease and NF-κB, both of which function as dimers, we think *pro-fs* dimerizes in cell nucleus. Third, our results from in vivo study demonstrate that *pro-fs* binds to both Trx-wt and Trx-CS in vivo, which is consistent with our in vitro data showing that the Trx-*pro-fs* binding is structural specific. Thus, *pro-fs* might have effects on many aspects of host-pathogen relationship that

involves Trx. Moreover, the in vivo experiment showed that nuclear translocation of Trx induced by PMA treatment is essential for *pro-fs* binding. Thus, it brings up the consideration that the regulation of important signal transduction in relation to intracellular compartmentalization needs to be further explored. The FRET method used in both Chapter 3 and 4 was successful. With essential negative controls and positive control, we are able to correctly analyze the energy transfer efficiency between different fluorescent-tagged proteins. In Chapter 3, we also described a novel method to measure and analyzed FRET efficiency using scanning fluorometry, which is much easier to use, more efficient and less expensive comparing to confocal microscopy.

At last, our kinetic model built using STELLA software on redox regulation of NF-κB activated HIV-1 gene transcription successfully demonstrates the effects of the ROS inducing agent (TNF-α) and antioxidant (selenium) on the activation of NF-κB and the resulted viral replication. The results strongly support that Se administration may provide beneficial effects in the treatment of HIV-infected individuals. We also suggest that dietary Se uptake may be used as an alternative way or in combination with current expensive drug therapy to inhibit HIV replication and thereby to prolong the latency period of the virus.